Investigations into the magnetic properties of rare earth compounds

H. D. Ellis

INVESTIGATIONS INTO THE MAGNETIC PROPERTIES OF RARE EARTH COMPOUNDS.

by

H. D. Ellis, B. Sc.

Presented in candidature for the degree of

Doctor of Philosophy.

December, 1967.

ABSTRACT.

Magnetic measurements have been carried out on compounds of the form $Gd_xY_{1-x}Co_2$, where x varies from 1 to 0. The measurements were carried out over a wide range of temperatures and applied magnetic fields on a vibrating sample magnetometer.

The results show that these compounds with high gadolinium content are strongly magnetic, and their Curie points range from 400°K in $GdCo_2$ down to near zero for $x \leq 0.1$. The compound YCo_2 is shown to be antiferromagnetic, with a Neel point of 190°K. The magnetisation versus temperature results show an anomaly in the form of a "kink" in the curves for those compounds with x greater than 0.33, and the presence of this kink is shown to be dependent on the strength of the applied magnetic field, a minimum, or critical field being required before the anomaly appears.

The model proposed to explain this behaviour is an adaptation of one proposed by Lotgering, for which an antiferromagnetic Gd-Co coupling, an antiferromagnetic Co-Co coupling, and a ferromagnetic Gd-Gd coupling are required. Given these conditions, it is shown that a triangular configurations of moments can exist, in which the Gd moments lie parallel to the applied magnetic field, and the cobalt moments lie antiparallel to the applied field, but tilted alternately right and left at an angle so as to form a triangle with the Gd moment. It is shown that such a condition can exist only below a certain critical temperature, and at

fields above a certain critical value. In all respects this model appears to fit the observed results well, but confirmation of the existence of such a configuration not only in these compounds, but probably in rare-earth - $(\text{cobalt})_2$ and rare-earth - $(\text{iron})_2$ compounds also, must await neutron diffraction measurements with a moderately high magnetic field applied to the specimens.

NOMENCLATURE

Other symbols are defined in the text. Occasionally symbols shown here are used with different meanings in the text; in such cases they are re-defined in the text.

H - Magnetic field

J - Total quantum number

L - Total orbital angular momentum

S - Total spin angular momentum

S_e - Total spin angular momentum of an electron

R - Rare earths

SWG - Standard wire gauge

E_f - Fermi energy

k_f - Fermi vector

k_B - Boltzmann's constant

Θ, T - Temperature

Θ_P - Paramagnetic Curie point

Θ_C - Curie temperature

Θ_N - Neel temperature

g_j - Gyromagnetic ratio

z - Charge

σ - Magnetisation

μ_B - Magnetic moment, Bohr magnetons

v_o - Atomic volume

LIST OF ILLUSTRATIONS.

CONTENTS

CHAPTER ONE

INTRODUCTION

CHAPTER ONE

1.1 Introduction

In the past ten years or so, interest in the properties of the series of elements known as the rare earths has increased enormously. In particular, research into their magnetic properties has grown at a remarkable pace, chiefly through a search for materials which might be used in solid state devices. So far as basic theory is concerned, the interactions which cause co-operative magnetic phenomena in the solid elements, compounds and alloys are proving to be of a complex nature. The work described in this thesis is an investigation into the magnetic properties of a series of compounds of the form $Gd_xY_{1-x}Co_2$, where X varies from 1 to 0, in an attempt to more fully understand the magnetic interactions which are present in the rare earths.

All the compounds investigated are of the same structure, the Laves phase cubic structure, of the $MgCu_2$ type. The interatomic distances change very little throughout the series.

1.2 The Rare-Earths

Though a large amount of information has accrued in the past 150 years on the rare earths, their commercial uses have, up to the present time, remained few. About 25% of the yearly production of rare earths is used in carbon arc lighting, another 25% is taken up by various metallurgical applications; for instance a 70% rare-earth-30% iron alloy is used in the production of lighter flints. Rare earths are also used to improve malleability, tensile strength, ductility and welding ability in ferrous

alloys, and the improvement of oxidation resistance in various chromium type stainless steels. They also improve some of the mechanical and metallurgical properties of many other metals, including aluminium, cobalt, magnesium, nickel, silver and titanium. Another 25% is used by the glass industry in polishing powders, decolorisers and colouring agents. The remaining 25% is divided among various applications such as use in vacuum tube getters, waterproofing agents, fungicides and catalysts.

The rare earths are very similar chemically, and separation techniques were far from satisfactory, until the discovery that the rare earths made excellent radiation shields and radiation absorbers led to great advances in separation techniques about 25 years ago. It was not until these advances had been made that considerable quantities of most of the rare earths in a relatively pure form became available. Many magnetic measurements depend on having a single crystal of the material available, for example in measuring anisotropy energies, and single crystals of the rare earths have only recently become available.

The name by which this series of elements is usually known is rather a misnomer, since the oxides of the elements occur naturally in large quantities in minerals such as monazite, xenotime and gadolinite. In fact, they are much more abundant than the platinum group metals. The word "earth" is also misleading, since, in the elemental form, all the rare earths are metals. They are heavy elements, occurring between atomic numbers 58 and 71, and are generally trivalent, though some elements may be divalent, others tetravalent. The valence shells of the series are the 6s and 5d shells, but it is in the 4f shell that the elements differ

electronically. This is also the shell which gives rise to the interesting magnetic properties of the rare earths, for the energy configurations are such that one 4f sub-shell (spin $\frac{1}{2}$ electrons) must be filled before the other (spin-$\frac{1}{2}$ electrons) may begin to be filled. The outer electron shells are identical in the series, i.e. the 4d, 5s, 5p and 6s shells are all filled, and in most elements there is one electron in the 5d shell. Table 1 shows the electronic structure of the complete lanthanide (rare earth) series.

1.3 The Magnetism of the Rare Earths

Hund's principle of maximum multiplicity (ref 1.1) shows that the unpaired 4f electrons which are responsible for paramagnetic behaviour should increase regularly in number from one with cerium to a maximum of seven with gadolinium, and then decrease to one with ytterbium. This suggests a maximum in permanent magnetic moment at gadolinium, whereas in fact two maxima occur: one peak near neodymium, and the larger peak at dysprosium and holmium. Fig 1.1 shows the variation of permanent magnetic moment with atomic number. The reason for the two maxima is given by Hund's rules, the third of which states that for a shell which is less than half-filled (in this case $n < 7$), the total quantum number, J, is given by $J = L - S$, and for a shell which is more than half-filled, $J = L + S$. L is the total orbital angular momentum of the shell formed by the addition of the angular momenta of the individual 4f electrons, and S is the total spin angular momentum of the shell formed in a like manner. The 4f electrons fill up the shell in a manner dictated by Hund's first two rules, which state that (i), the spin arrangement should have the

ELEMENT	ATOMIC NUMBER	SYMBOL	METALLIC STATE BONDING ELECTRONS			IONIC CONFIGURATIONS (4f ELECTRON NUMBER)		
			6s	5d	4f	M^{2+}	M^{3+}	M^{4+}
LANTHANUM	57	La	2	1	0	–	0	–
CERIUM	58	Ce	2	1	1	–	1	0
PRASEODYMIUM	59	Pr	2	1	2	–	2	1
NEODYMIUM	60	Nd	2	1	3	–	3	–
PROMETHIUM	61	Pm	2	1	4	–	4	–
SAMARIUM	62	Sm	2	1	5	6	5	–
EUROPIUM	63	Eu	2	0	7	7	6	–
GADOLINIUM	64	Gd	2	1	7	–	7	–
TERBIUM	65	Tb	2	1	8	–	8	7
DYSPROSIUM	66	Dy	2	1	9	–	9	–
HOLMIUM	67	Ho	2	1	10	–	10	–
ERBIUM	68	Er	2	1	11	–	11	–
THULIUM	69	Tm	2	1	12	–	12	–
YTTERBIUM	70	Yb	2	0	14	14	13	–
LUTETIUM	71	Lu	2	1	14	–	14	–

TABLE 1. ELECTRONIC STRUCTURE OF THE METALLIC AND IONIC STATES OF THE RARE EARTH.

THE CORE OF THE ELEMENTS IS IN ALL CASES $1s^2$, $2s^2$, $2p^6$, $3s^2$, $3p^6$, $3d^{10}$, $4s^2$, $4p^6$, $4d^{10}$, $5s^2$, $5p^6$.

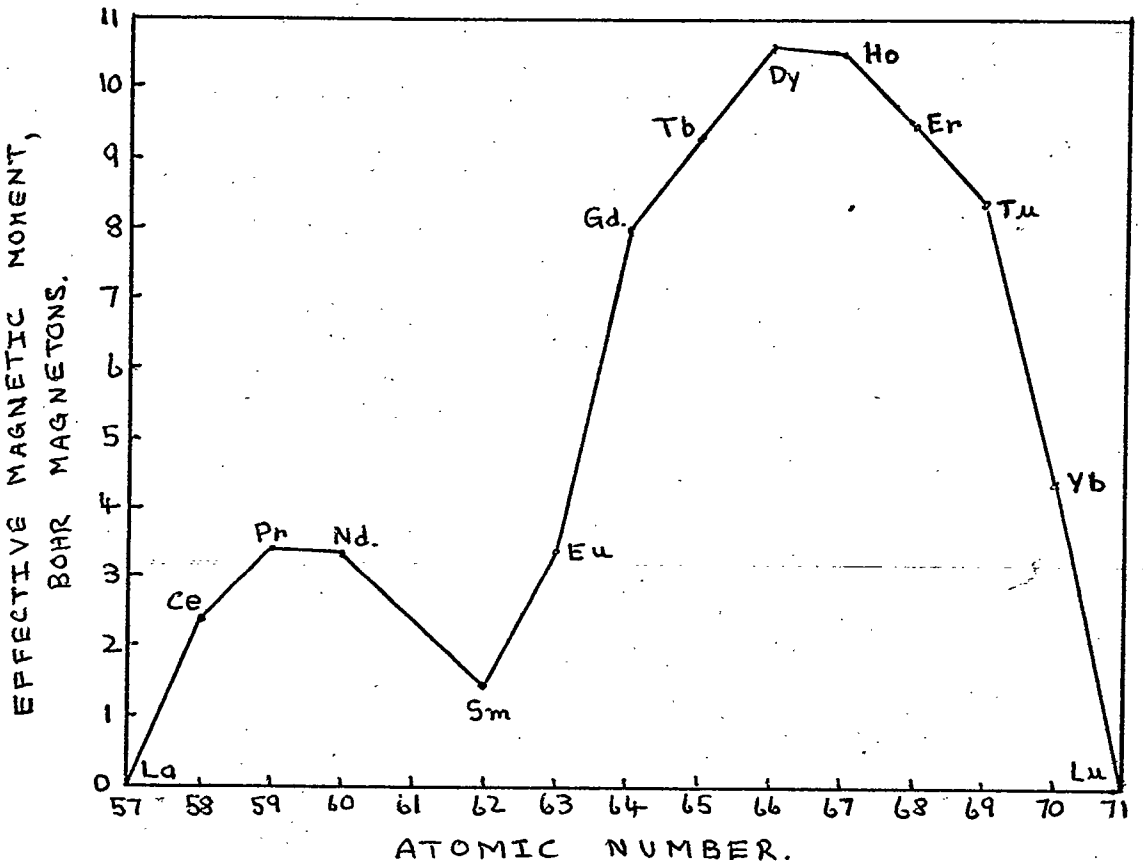
EFFECTIVE MAGNETIC MOMENT, BOHR MAGNETONS.
ATOMIC NUMBER.
0
1
2
3
4
5
6
7
8
9
10
11
57
58
59
60
61
62
63
64
65
66
67
68
69
70
71
La
Ce
Pr
Nd.
Sm
Eu
Gd.
Tb
Dy
Ho
Er
Tm
Yb
Lu

FIG. 1.1.

maximum total spin angular momentum, and (ii) the orbital arrangement should have the maximum orbital angular momentum within the restriction of rule (i) and of the Pauli exclusion principle. Thus the orbital angular momenta of the 4f electrons will be, in order, 3, 2, 1, 0, -1, -2, -3, 3, 2, 1, 0, -1, -2, -3; and the spin angular momenta of the individual electrons will be, in order, $\frac{1}{2}$ for the first seven electrons, and $-\frac{1}{2}$ for the last seven. So, for example, cerium has $\mathbf{L} = 3$ and $\mathbf{S} = \frac{1}{2}$, giving $J = 2\frac{1}{2}$; praseodymium has $L = 5$, $S = 1$, and $J = 4$, whereas gadolinium has $L = 3+2+1+0-1-2-3 = 0$, $S = 7/2$, and $J = +7/2$; terbium has $L = 3$, $S = 3$ and $J = +6$.

In order to calculate the magnetic moment of the atoms, J must be multiplied by g, the gyromagnetic ratio. The value of g is obtained by using the Lande formula

$$g = 1 + \frac{J(J+1) + S(S+1) - L(L+1)}{2J(J+1)}$$

and the appropriate values of J, L and S. The agreement between theoretical and experimental values is excellent, except for Eu^{3+} and Sm^{3+}. This discrepancy is interpreted in terms of the fact that the energy separation between the ground state and the first excited state is fairly small for these elements, and is comparable to the thermal energy, kT. Since such an excited state has a larger value of J than the ground state for the less than half-filled 4f shell, thermal excitation is expected to increase the magnetic moment above that calculated according to Hund's rules. Van Vleck and Frank (ref 1.2) have carried out this calculation for

europium and samarium, and agreement of these calculated results with experiment is excellent.

1.4 The 4f Shell in the Rare Earths

The rare earth series is distinctive in that the electronic shell giving rise to the strong magnetic properties of the series, the 4f shell, is deep lying and well screened from neighbouring atoms. The radius of this shell is only about 10% of the interatomic distance in the metals, and about 30% of the atomic radius, which ranges from 2.04Å for europium to 1.61Å for beta-phase scandium. This gives rise to the 4f shell experiencing a very high effective nuclear charge. The 4f electrons do not form a band, since they are very deeply buried in the atom. This deeply buried character of the 4f shell means that it does not take any part in chemical bonding, which in turn means that the elements are chemically very similar. This accounts for the great difficulty experienced in developing effective techniques for separating one rare earth from another. One further consequence of the chemically similar nature of the rare earths is that they usually form solid solutions with each other quite easily, and generally they may substitute for one another in any given compound. The limit to this behaviour is set by size, so that alloying and substitution only occur readily if the atomic radii do not differ by more than 15%.

1.5 Exchange Interactions in the Rare Earth Metals - RKKY Theory

The 4f electrons of a rare earth atom in the metallic form can not perform an exchange interaction directly with the 4f electrons of a

neighbouring atom, because of their deep lying position, shielded by the 5s and 5p shells. Strong magnetic coupling does exist in the metals, however, and the theory of indirect interaction between atoms, due to Ruderman, Kittel, Kasuya and Yosida, known as the RKKY theory (ref 1.3) has been developed to explain the observed magnetic phenomena.

1.5.1 Qualitative s-f Interaction

The interaction between conduction electrons and ion spins in the rare earths may be described by a scalar coupling between spins of the form

$$H_{1kk'} = -\Gamma_{kk'}\, S.S_e \quad ----- \quad (1)$$

where H_1 is the dominant interaction, k and k^1 are two orbital states of the conduction electron, and Se is the spin of this electron. It is usually sufficient to replace $\Gamma_{kk'}$ by a unique constant Γ. The effects of a scalar interaction of the type shown in equation (1) have been discussed by Yosida (ref 1.4) for Cu-Mn alloys, and by Kasuya (ref 1.5) for gadolinium.

The exchange constant Γ, arises from three effects:

a) The 4f shell produces a coulomb potential and an exchange potential which act on the conduction, or S, electrons. The coulomb potential is non-spherically symmetric, since the 4f shell is not spherical, and it depends on the orientation of the orbital moment L of the ion. The most important term is given by the interaction between the charge of the conduction

electron and the 4f shell quadrupole. It is, however, very small, because of the small radius of the 4f shell.

b) The exchange term depends on the relative orientation of conduction electron spin and the rare earth spin S. It may be represented approximately by an interaction of the form of equation (1).

c) Effect of virtual bound 4f levels. A conduction electron may be absorbed by the 4f shell (in which it occupies a metastable level), then emitted again. If the metastable level is quite near the Fermi level, a scattering resonance is obtained. The virtual levels thus obtained may also be described by a scalar interaction of the form shown in equation (1). Here the constant Γ is only an exchange integral; it is not necessarily either positive or constant in the series.

De Gennes (ref 1.6) has shown that if the Anderson mechanism (ref. 1.7) is applied to these virtual bound levels, an antiferromagnetic Γ may be produced.

1.5.2 Polarisation of Spin Near Rare Earth Ions

The interaction described by equation (1) leads to the conduction electron spins being polarised in the neighbourhood of a rare earth ion. If the direction of the spin S of the ion does not change, the polarisation P(R) may be calculated by assuming that the conduction electrons instantly adopt the equilibrium configuration in the presence of the ion spin S (adiabatic approximation). By Yosida's approximation (ref 1.4)

$$P(R) \equiv \langle \sum_{\ell} S_{\ell}\, \delta(R_{\ell} - R) \rangle$$

$$= \frac{9\pi z^2}{4 v_0^2} \cdot \frac{\Gamma}{E_F} \cdot S\left(\frac{-\rho\cos\rho + \sin\rho}{\rho^4} \right)$$

$$= \frac{9\pi z^2}{4 v_0^2} \cdot \frac{\Gamma}{E_F} \cdot S \cdot F(\rho) \quad - - - (2)$$

In this formula $\rho = 2k_F \cdot R$, R being the distance from the rare earth ion being observed. The polarisation P(R) has a fairly large spatial range and alternates in sign. These two properties, which are to a great extent independent of the detailed mechanism of the s-f interaction, are fundamental in the understanding of the magnetism of the rare earth metals.

1.5.3 Indirect Interaction between Two Ions

Consider two ions S_1 and S_2 a distance R_{12} apart in the metal. The first ion causes spin polarisation $P_1(R-R_1)$ in the surrounding conduction electrons, which reacts on the second ion. In the absence of spin-orbit coupling, the resultant indirect interaction becomes

$$-\Gamma S_2 \cdot P_1(R_2 - R_1) = -\frac{9\pi z^2}{4 v_0^2} \cdot \frac{\Gamma^2}{E_F} S_1 \cdot S_2 F(2k_F R_{12}) \quad - - (3)$$

The principal problem in applying this interaction to the rare earths is to correctly include the effect of the spin-orbit coup ling on the spins S_1 and S_2. It turns out that, for $k_B T \ll U_{LS}$ where U_{LS} is the spin

orbit coupling energy, S_1 may be replaced by $(g_j-1)J$ in equation (3).

1.6 Consequences of the RKKY Theory

The long-range oscillatory nature of the indirect interaction described by the RKKY theory allows the unusual magnetic phenomena of the rare earths to be explained, including the existence of metamagnetism (the phenomenon where a transition takes place from ferromagnetism to antiferromagnetism and vice versa, the transition being induced by the application of a strong field or by a change in temperature). The ferromagnetic to antiferromagnetic transitions observed in, for example, Tb, Dy, Ho, Er and Tm are a direct result of the existence of helical spin structures in the heavy rare earths. In turn, the helical spin structures may be accounted for [redacted] on the basis of the RKKY theory of indirect exchange. This configuration was first propounded by Yoshimori (ref 1.8) to explain the properties of the antiferromagnetic compound MnO_2, by Villain (ref 1.9) for $MnAu_2$, and by Kaplan (ref 1.10). In this type of structure, the spin magnetic moments in a given plane (say the xy plane), are all aligned parallel to one another, while the next plane along the z axis has spin moments which again are all aligned parallel, but point in a different direction to those in the neighbouring xy planes. It has been shown that for such a structure to be stable, the interaction between nearest-neighbour planes must be of opposite sign to that between next nearest-neighbour planes. Such a situation can arise with an indirect exchange interaction which is long range and oscillatory in sign. If J_1 and J_2 are the exchange integrals for the interactions between one atom and all atoms in the first and second neighbour planes, respectively,

($J_1 > 0$ and $J_2 < 0$), then the necessary condition for a helical spin configuration is $|J_2| > J_1/4$.

The helical spin configurations of the heavy rare earths have been explained by Miwa and Yosida (ref 1.11) in terms of a helical spin structure modified by the presence of a magneto-crystalline anisotropy.

The RKKY theory may also be applied to the parmagnetic Curie points, θ_p, of the rare earths. In fact θ_p is simply proportional to the mean of the interactions between an ion and its neighbours.

If direct coupling between f shells is negligible, then using Yosida's model (ref 1.4) it follows that

$$k_B \theta_p = +\frac{3\pi z^2}{4} \Gamma^2 (g_J - 1)^2 J(J+1) \sum_{j \neq i} F(2 k_F R_{ij})$$

For a given structure, the quantities $k_F R_{ij}$ are unique functions of the number of valence electrons per atom z.

It should be noted, with regard to the RKKY theory, that

a) the model is based on a free electron model of the solids,

b) it assumes the potential distribution at the ion is a δ function,

c) the use of the RKKY theory in the rare earths is justified by

(i) in the heavy rare earths, a plot of θ_p against $J(J+1)\ (g_J-1)^2$, assuming that $\sum F(2k_F R_{ij})$ remains constant, provides a straight line (ref 1.6)

(ii) the model gives good agreement with experimental data for spin resistivity (ref 1.12)

(iii) the model gives fairly good agreement with experimental results for the angle of turn in helical spin configurations in the rare earths (ref 1.10)

1.7 Developments of the RKKY Theory

Freeman and Watson (ref 1.14) have included the effect of the distribution of spins in the 4f shell, i.e. making the potential well not a δ function. This modifies the form of the polarisation P(R) considerably, though it is still long range and oscillatory in nature.

Overhauser, Wolf and others (ref 1.15) provide a further refinement by including a more correct usage of the Pauli exclusion principle as applied to the free electrons (conduction electrons), thus modifying the function $F(2k_F R_{ij})$ in equation (3). Again, the polarisation remains long-range and oscillatory.

Yosida and Watabe (ref 1.16) used a model based on the RKKY theory in an attempt to predict the turn angle in the heavy rare earth helical configurations, and obtained a value of 48°, which agrees very well with the values found experimentally in H_o, Er and Tm, but bears little relation to the values found in Gd, Tb and Dy. De Gennes and St James (ref 1.17) carried out a development of this work by attempting to include the effect of spin disorder resistivity on the electron mean free path. They obtained turn angle values ranging from 0° in Gd to 53° in Tm, in fair agreement with experiment.

For a given metal, as the temperature is lowered and the amount of order increases, the mean free paths associated with the spin disorder will increase, which would lead one to expect an increase in turn angle as the temperature is decreased. In fact, experiment shows that turn angles decrease with decreasing temperature. One mechanism which might be expected to explain this discrepancy has been proposed by Overhauser (ref 1.18), Mackintosh (ref 1.19), Miwa (ref 1.20) and Elliott and Wedgwood (ref 1.21). The development of magnetic ordering over many lattice spacings as the temperature is decreased introduces a periodic structure in the scattering potential which creates new planes of energy discontinuity in the Brillouin zone structure. When the energy gaps appear in the conduction band, the effective number of conduction electrons is reduced and the electrical resistivity increases. Elliott and Wedgwood (ref 1.21) carried out calculations using this model, and obtained results which were in good agreement with empirical values for the elements Tm, Er and Ho, which have small gap widths and spin quantum numbers, but agreement was very bad for Tb and Dy, due presumably to the effects of spin disorder resistivity mentioned earlier.

Miwa (ref 1.22) has recently attempted a unified theory which includes both the band gap and disorder scattering effects, but achieves only moderate success.

Darby and Taylor (ref 1.23) have attempted an explanation of the widely varying paramagnetic Curie temperatures and some reported Neel temperatures of the RX compounds, where R is Gd, Tb, Dy, Ho, Tm or Yb and X is N, P, As, Sb or Bi, in terms of the variations in lattice spacings

of the compounds, using the free electron indirect exchange theory of RKKY. Their results indicate that if the effective number of conduction electrons per rare earth ion is taken to be 1.42 for all the compounds, then the values of the Fermi vector k_f and the widely varying paramagnetic Curie points of these compounds can be accounted for entirely by changes in lattice spacing.

In conclusion, we may say that the RKKY theory provides a very fair physical picture of the magnetic properties of the rare earths. It provides a basis for predicting the magnetism of the rare earths, at least in their elemental form. Quantitative agreement between the theory, in its refined form, and experiment is quite good. When we move from the elemental form of the rare earths, and take a look at rare earth alloys and compounds, the picture is not so well ordered.

1.8 Rare Earth Alloys and Compounds

Before attempting to understand the magnetic properties of rare earth compounds as a generic group, it may be instructive to recall why these properties are of interest, and why they are not easily predictable. In all the rare earths, the outer electronic configuration is identical, i.e. the 4d, 5s, 5p and 6s shells are all filled, and there is one electron in the 5d level in most cases. The 6s and 5d electrons are easily stripped off, making the ion, as a rule, tripositive. As the 4f shell is filled, the nuclear charge also increases, and since the inner electron shells do not completely shield the 4f and higher shells from this increased charge, the 4f and valence shells are both more firmly bound to the atom, and contract in diameter, as the atomic number increases. This

effect, known as the lanthanide contraction, is one of the causes of the variations in the chemical properties of the elements, and also complicates the magnetic properties of the compounds. Elementary quantum theory states that half and completely filled levels are stable states, and this principle, when applied to the 4f shell of the rare earths, means that, for example, the tetravalent state may in some circumstances be more energetically favourable than the trivalent state, in the case of terbium. Cerium and praseodymium may also act as tetravalent ions, and samarium, europium and ytterbium have divalent states as well as the normal trivalent ones. In other words, for a substantial part of the rare earth series, the electron configuration can not be predicted with certainty.

The basic point of interest in the magnetic properties of compounds and alloys of the rare earths is that here we have available a series of elements, chemically very similar, with strong magnetic properties. It is possible with these elements to make up a series of magnetically active alloys or compounds with another element in which a minimum of parameters change through the series. A magnetic study of such a series might be expected to provide a set of data which can be easily interpreted in terms of the differences in composition of the specimens, which in turn can be expected to demonstrate readily the parameters which are important to the magnetic interactions in the series. Such knowledge must throw light on the nature of the magnetic interactions, together with an [redacted] understanding of how such an interaction works. Such an understanding can only lead to advances in the theory of magnetism, and to the

ability to tailor a material to carry out a specific task in a magnetic device.

Previous work on rare-earth alloys and compounds may be found in a condensed form in the books by Gschneidner (ref 1.24) published in 1961, and by Spedding and Daane (ref 1.25); also in a paper by Bozorth (ref. 1.26), given at the Twelfth Annual Conference on Magnetism and Magnetic Materials, November 1966.

1.8.1 Rare Earth Alloys

The magnetic properties of R-R alloys have by now been fairly thoroughly investigated, and it has been shown (ref 1.27) that the Néel temperature may generally be expressed as follows:- $\theta_N = 4\upsilon\, \bar{G}^{\frac{2}{3}}$, where $\bar{G} = c_1G_1 + c_2G_2$, and $G = (g-1)^2 J(J+1)$, G being the de Gennes factor (ref 1.28), and c_1 and c_2 the atomic concentrations of the constituents of the alloy. The Curie points of the alloys, in contrast, show some ordering with changes in composition, but are much more dependent on the actual elements in the alloys than in the case of the Néel temperatures. The anomalies are thought to be due to transformations which occur in the direction vectors of the individual magnetic moments of the constituent atoms when the average population of the 4f level exceeds a certain number. For example, in the Ho-Er alloys, at a composition corresponding to about ten 4f electrons per atom, a minimum occurs in the Curie temperature against number of 4f electrons curve (ref 1.32), this is thought to correspond to a change in the direction vector of the Ho and Er moments. In fact, the anomalies which arise in the Curie temperatures of the alloys of the heavy rare earths are basically due to the spiral spin structure of some of the

elements. The R-R alloys, in short, are becoming generally well understood, though there are some problems still to be solved.

1.8.2 Rare Earth Compounds

Compounds of the rare earths with other elements are multitudinous and they display a large variety of types of magnetic behaviour. Wilkinson et al (ref 1.29) have studied the magnetic properties of rare earth compounds containing V (b) elements such as N, P, As, and Sb. Their results show that TbN, DyN, HoN and ErN are ferromagnetic, with Curie points of 42°, 26°, 18° and 5°K, respectively. HoP is ferromagnetic below 5°K, but others, such as TbP, TbAs, TbSb, HoSb, ErP and EnSb are antiferromagnetic with Neel points below 15°K.

Pauthenet (ref 1.30) determined the saturation magnetic moments of the rare earth oxide garnets, and found that the orbital moments of the rare earth elements in these compounds seem to be partially quenched at temperatures below about 100°K. The strong ferromagnetism of EuO below 77°K was investigated by Matthias, Bozorth and Van Vleck (ref 1.31). The saturation magnetisation at low temperatures has the very high value of 1917 gauss, comparable with iron, gadolinium, or Fe-Co alloy.

1.8.3 Rare Earth - Transition Metal Compounds

Nesbitt et al (ref 1.33) have carried out measurements on RCo_5, RFe_4 and RNi_5. They find that, for RCo_5, an antiferromagnetic coupling takes place, with five cobalt moments opposed to the single rare earth moment. When the rare earth is Sm, Nd or Pr, however, they conclude that the compound has a ferromagnetic structure. Using such a model, the

experimental results are in good agreement with calculated values, except for Sm, Ce, Nd and Pr. The authors maintain that these discrepancies cannot be explained by a failure of the compounds to reach saturation, since, for example, if the data for $NdCo_5$ is extrapolated to infinite field, the value obtained still lies 10% below the calculated value. They explain the anomalous behaviour of the Sm, Nd and Pr compounds by suggesting that the rare earth spin moments couple antiferromagnetically with those of the cobalt while the orbital moments couple ferromagnetically. The $CeCo_5$ anomaly is ascribed to a sharp charge in the lattice parameter for this compound as compared with the others, which they state indicates the loss of a 4f electron to the conduction band. It is quite possible, however, that the Sm, Nd and Pr compound results may be explained by a mechanism due to a crystal field effect which quenches the moment, such as has been proposed by Bleaney (ref 1.34) for RNi_2 and RNi_5 compounds, and which will be discussed later. Nesbitt's results show that for the compounds $DyCo_5$ and $TbCo_5$, where the agreement between experiment and theory for the magnetic moments (assuming antiferromagnetic alignment) is very good, a minimum occurs in the magnetic moment at a temperature of $147^{\circ}K$ for $DyCo_5$ and $120^{\circ}K$ for $TbCo_5$. These minima have been demonstrated to be compensation points, and the substitution of one copper atom for one cobalt atom per formula unit increases the temperature of the compensation point by $93^{\circ}K$ in the dysprosium compound, and by $150^{\circ}K$ in the terbium compound.

Compensation points are also observed in RFe_4 compounds by Nesbitt et al for holmium, dysprosium and erbium, which strongly suggests that

these compounds have antiferromagnetic coupling. The saturation values of magnetic moment obtained tend to bear this out, though there are considerable discrepancies between experimental and theoretical values. The authors do not offer an explanation.

In the case of the RNi_5 compounds, the authors could discover no antiferromagnetic coupling or compensation points, though some of the compounds are ferromagnetic at low temperatures. The authors observe that the compounds behaviour indicates that nickel carries a zero moment. They explain their behaviour by suggesting that the nickel 3d band is filled by rare earth valence electrons. They also observe that, for example in $GdNi_5$, the observed moment is $6.1\mu_B$, whereas if the nickel took no p art in the magnetism of the compound, a value of $7\mu_B$ should be observed. As has already been stated, Bleaney (ref 1.34) explains the results by calculating the orbital moment quenching due to the effects of the crystal field, assuming nickel to be in the $3d^{10}$ state, though this cannot account for the anomalous $GdNi_5$ result, since gadolinium has no orbital moment.

Abrahams et al (ref 1.35) have carried out a series of measurements on the magnetic properties of RNi compounds. They compare their measurements with theoretical values calculated on the assumption that the moment is due entirely to free R^{3+} ions and obtain excellent agreement. As in the case of the RNi_5 compounds investigated by Nesbitt et al, and of RNi_2 compounds investigated by Skrabek and Wallace (ref 1.36), the nickel again appears to carry no moment, and can be regarded as neutral with configuration $3d^{10}$. The measured magnetic moments of the compounds are consistent with a ferromagnetic exchange interaction between the spin moments of the

rare earth components. There is also some evidence to indicate an antiferromagnetic coupling between the orbital moments of the rare earth ions, though this is not confirmed.

Bozorth et al (ref 1.37) have measured the Curie points and saturation moments for RIr_2, ROs_2 and RRu_2 compounds. They find that the Curie point (ie the strength of the exchange interaction) is at its highest for the gadolinium compounds, and falls away as the number of 4f electrons is either increased or decreased. The saturation moments of the compounds lie below the values which might be expected if the ferromagnetic exchange interaction were between the total moments of the rare earth ions, but are above the values predicted by a model assuming coupling between spin moments only. This discrepancy is interpreted in terms of partial quenching of the orbital moments caused by the strong crystal field found in these compounds.

1.8.4 RB_2 Compounds

All the rare-earth-transition metal compounds of the RB_2 type have the cubic Laves phase ($MgCu_2$) structure. Figure 1.2 shows a representation of this type of structure, with rare earth atoms represented by black balls, and transition metal atoms by white balls. There are eight rare earth atoms and sixteen transition metal atoms per unit cell.

Ross and Crangle (ref 1.38) have investigated the magnetic properties of RB_2 compounds, where B is Fe, Co, Ni, Rh and Pt. Their magnetisation versus temperature results for the iron and cobalt compounds (ref. fig. 1.3) show anomalies in the form of "kinks" in the curves, which they say

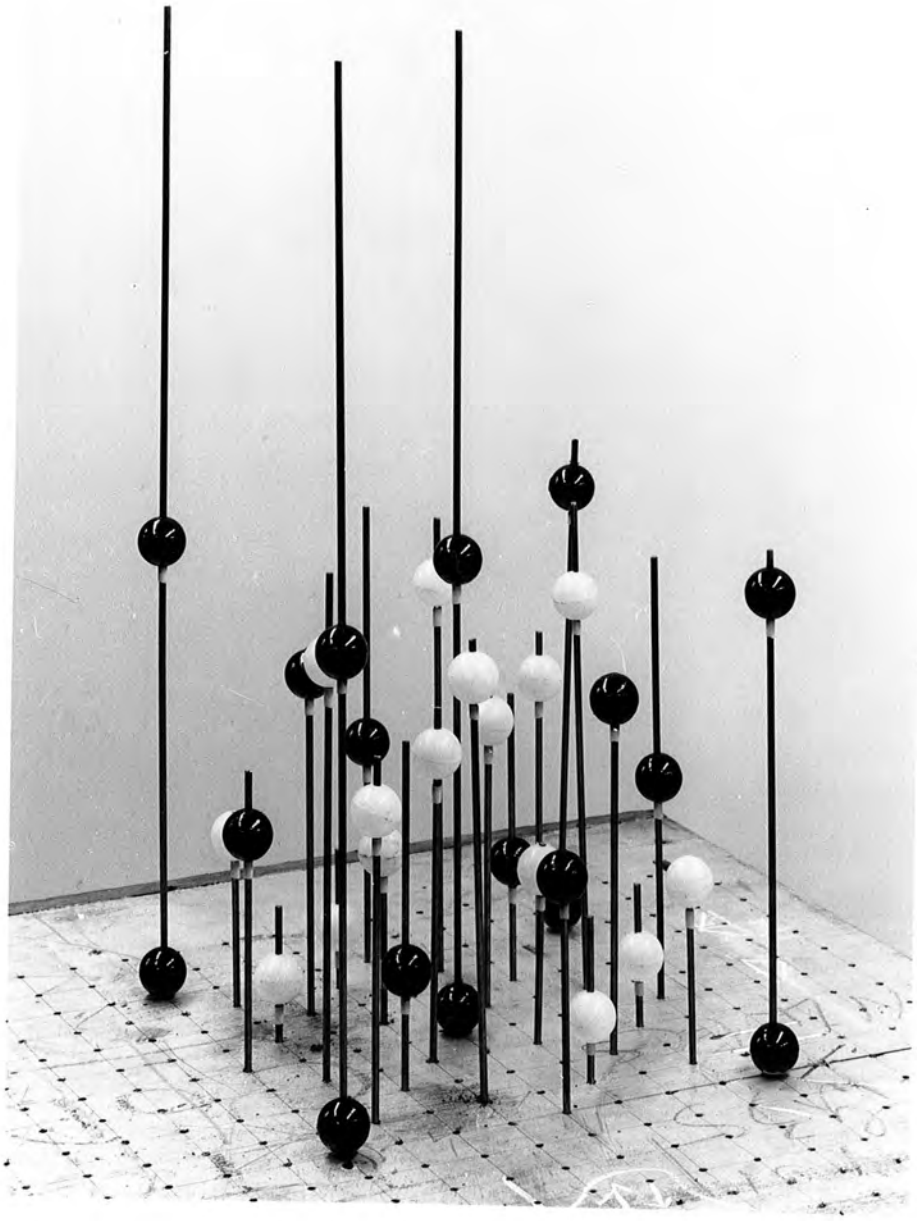

Fig. 1.2. CUBIC LAVES PHASE ($MgCu_2$) STRUCTURE.

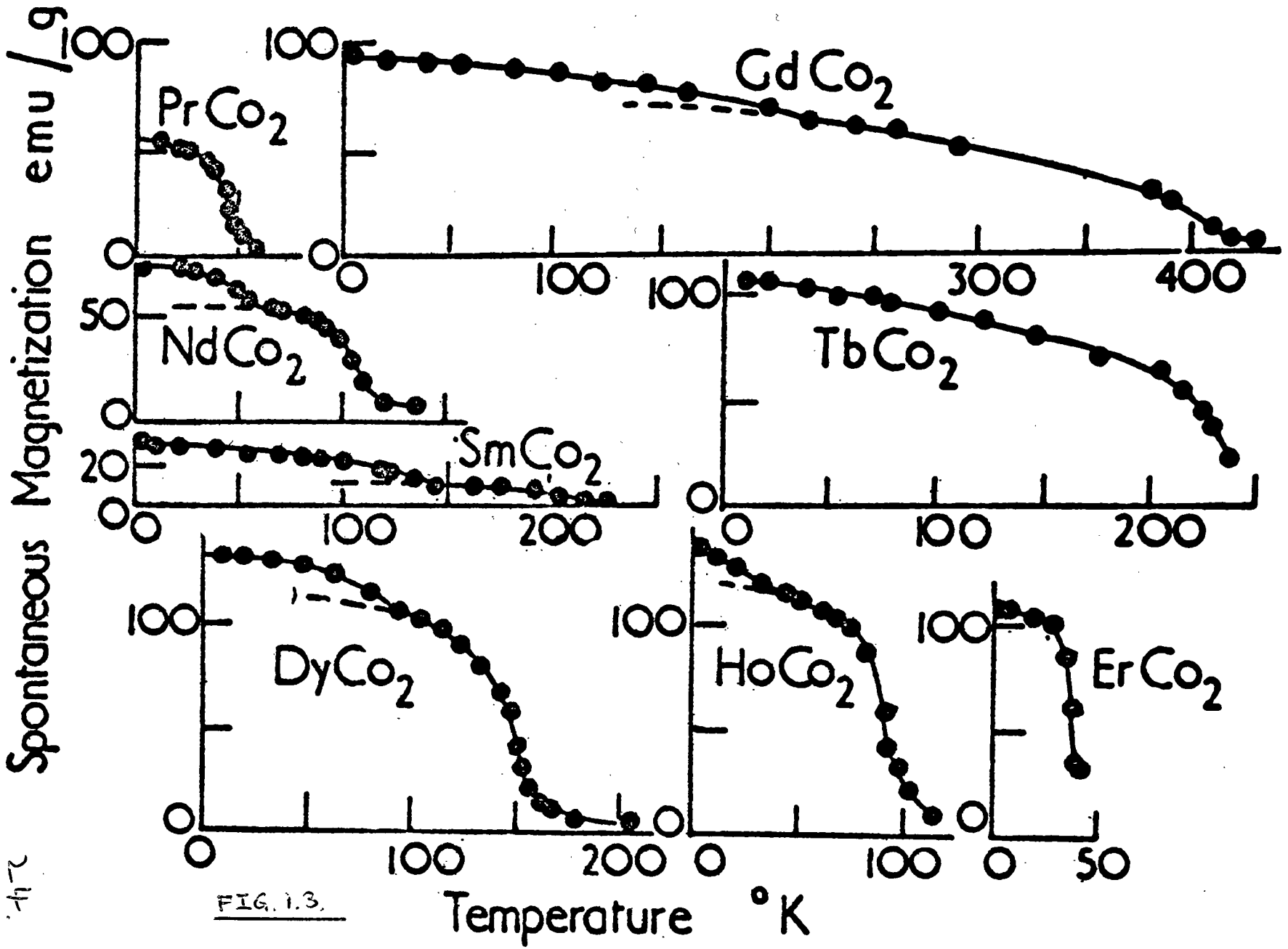
Spontaneous Magnetization emu/g
PrCo2
GdCo2
NdCo2
SmCo2
TbCo2
DyCo2
HoCo2
ErCo2
Temperature °K

FIG. 1.3.

seem to be associated with the presence of localised moments on both kinds of atoms present in the compounds. They speculate that these kinks, which are also observed by Wallace and Skrabek (ref 1.36), Farrell and Wallace (ref 1.39) and also appear in this thesis, may be due to some kind of triangular arrangement of spins as discussed by Lotgering (ref 1.40). The results of Ross and Crangle are consistent with an indirect exchange interaction being the dominant mechanism. They conclude that crystal field effects, in all compounds except those of gadolinium, reduce the orbital moments of the rare earth ions. For gadolinium, they propose that the slight discrepancy between the observed results and the full gadolinium moment may be explained by a net negative magnetisation of the polarised conduction electrons in the vicinity of the rare earth ions. This implies an antiferromagnetic coupling between the localised 4f shell of the gadolinium and the nearby conduction electrons. They also state that the reduced transition metal moments in the iron and cobalt compounds align antiparallel to the rare earth for the heavy rare earths, and parallel to the rare earth moment for the light rare earths. Thus, in all cases where the transition metal has a moment, it aligns antiparallel to the spin moment of the rare earth.

Wallace and Skrabek (ref 1.41) have also investigated the magnetic properties of RNi_2 and RCo_2 compounds. As has been previously stated, their magnetisation versus temperature results for some of the RCo_2 compounds have a characteristic shape which is very like the anomalous results shown in this thesis for $Gd_xY_{1-x}Co_2$ compounds, the results obtained by

Crangle and Ross for RCo_2 and RFe_2 and the results obtained by Farrell and Wallace for RCo_2. Bleaney (ref 1.42) explains the results of Wallace and Skrabek in terms of quenching of the rare earth orbital moment due to the effects of electrostatic fields set up within the crystal.

The work of Farrell and Wallace (ref 1.39) on RNi_2 and RCo_2 compounds largely discounts the possibility of crystal field quenching being the dominant cause of the low magnetic moments. This paper, in relation to the crystal field quenching theory, will be discussed in detail in Chapter Four.

We may summarise this brief review of some of the more interesting magnetic properties of the rare earth alloys and compounds by saying that the magnetic situation in a material containing rare earths is often of a complex nature. The two major factors which make it difficult to predict the magnetic behaviour of rare earth compounds are firstly, the tendency of some of the rare earths to interact with a spin-only moment when a high crystal field is present in the material, the orbital moment being quenched; and secondly, the tendency of the rare earths to lose some of their valence electrons, and occasionally some 4f electrons, in an unpredictable manner such that the electron configurations of the rare earth and of the other element in the compound are not known with any certainty; nor is the number of electrons which have been promoted into the conduction band.

1.9 $Gd_xY_{1-x}Co_2$ Compounds

The present work is an investigation of compounds of the type $Gd_xY_{1-x}Co_2$, where yttrium acts simply as a non-magnetic substitute for

gadolinium. It was at first thought that these compounds would exhibit simple ferromagnetism, with a compensation point somewhere near the middle of the range where the moment due to the concentration of gadolinium would balance the moment due to the cobalt. It was thought that the results obtained would throw light on the type of interactions involved, and to a good quantitative knowledge of the coupling constants. The results, as will be seen later, proved to be qualitatively and quantitatively completely remote from our predictions.

CHAPTER TWO

EXPERIMENTAL APPARATUS

CHAPTER TWO

2. EXPERIMENTAL APPARATUS

2.1 Introduction

In order to make magnetisation and susceptibility measurements on a large number of magnetic materials, an instrument was required with a wide range of sensitivity and capable of making measurements over a wide range of field and temperature. The instrument constructed was based on the vibrating sample magnetometer first developed by Foner (Ref 2.1). This instrument was chosen because of its essential versatility and built-in error elimination. In principle the Foner magnetometer is very simple. A long, thin, light rod is attached to a vibrating source (originally a loudspeaker diaphragm), which causes the rod to vibrate vertically along its own axis at a fixed frequency. The sample under investigation is mounted at the bottom of the rod, in an external magnetic field. A reference specimen, which is either a small permanent magnet or a small coil carrying a DC current, is mounted at the top of the rod. Both specimens have multi-turn pick-up coils mounted near them, in which emf's are induced by the dipole radiation from the vibrating sample. One of these two signals is phase-shifted to be 180° out of phase with the other, the two signals are mixed, and the resultant is put through a high-gain tuned amplifier. The resultant is zeroed by either attenuating one signal or altering the current through the DC reference coil if this is used.

In developing the instrument, it was found that the instability of the power supply driving the magnetic field was the biggest obstacle to achieving high sensitivity. This gave rise to a very large amount of noise in a normal pick-up coil system used with a magnet, so that the instrument's sensitivity was very small indeed. In an attempt to overcome this difficulty, a pair of circular pick-up coils were used in conjunction with a solenoid. These were mounted with their axes colinear, with a small separation between them. The two coils were matched and connected in series opposition, with their axes along the line of vibration of the specimen, which rests between the two coils. With this arrangement, fluctuations in the external magnetic field theoretically induce equal and opposite emf's in the two coils, while the vibrating sample induces equal and like emf's. In practice, it was found that the amount of noise in the output of the coils was drastically reduced.

The noise level was still such as to make it impossible to mix the sample and reference signals satisfactorily, so in the final form, the signals are switched alternately into the system and their magnitudes compared.

The final form of the magnetometer is shown in Fig 2.1. It consists of two pairs of pick-up coils, one pair each for the sample and reference. Either of these two coil systems may be switched into the system, either directly or through a variable attenuator in the form of a helipot. The signal is amplified by a high gain amplifier, tuned to 70 cps. An AC output from the amplifier is supplied to a phase sensitive

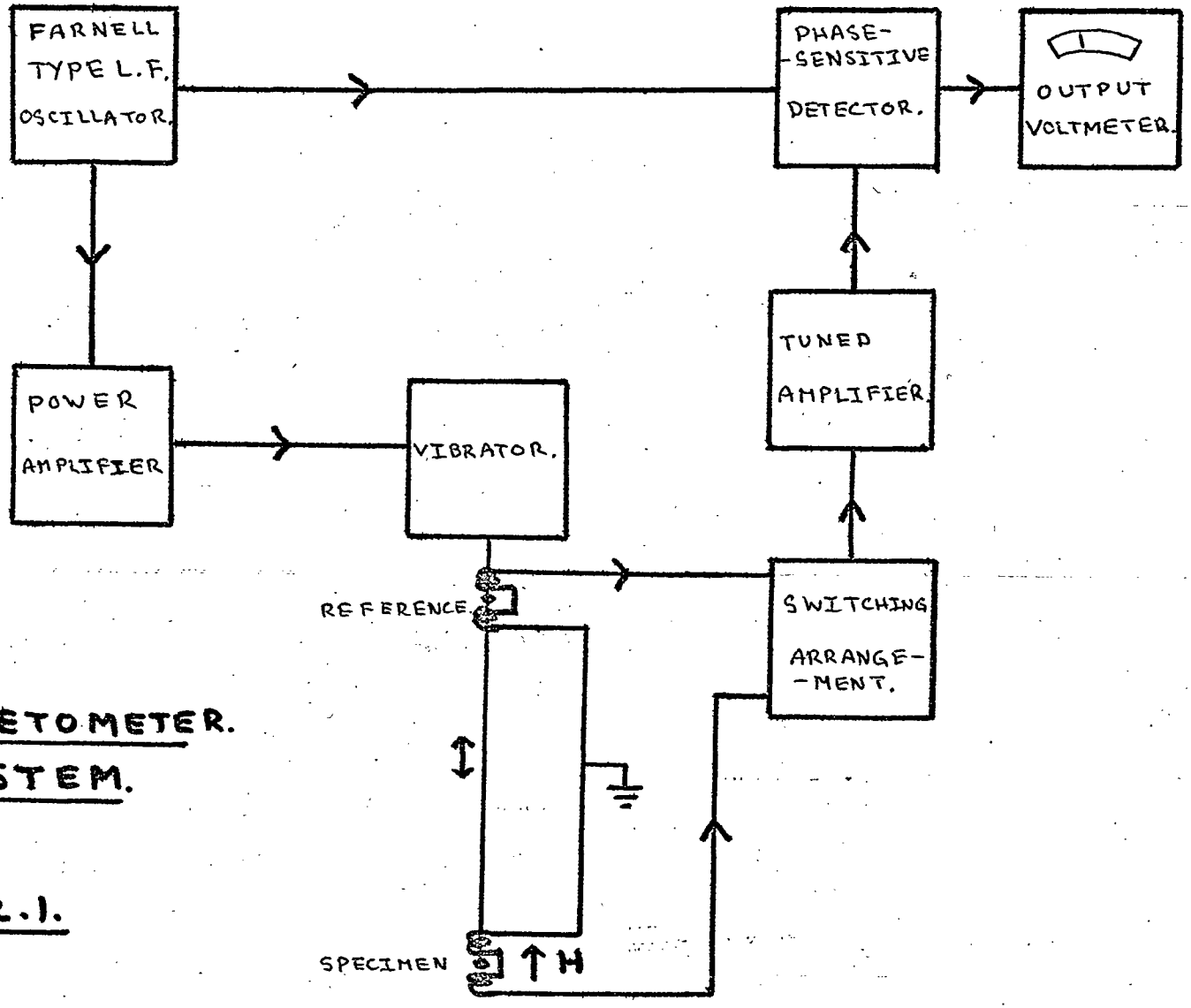

MAGNETOMETER.
SYSTEM.

FIG. 2.1.

detector, which is supplied with a reference direct from the oscillator driving the vibrating rod. The DC voltage output from the phase-sensitive detector, which is proportional to the input signal voltage, is read on an Avometer. Fig 2.2 shows a signal input/output graph for the system.

In this form the magnetometer still retains many of the advantages of the Foner magnetometer, but lacks one of its main features, namely that it is not a null-output instrument. It is also sensitive to rapid, short period changes in vibration amplitude, and to a lesser extent vibration frequency. In practice it is found that any changes of frequency or amplitude are both small and slow, and are therefore a negligible source of error.

2.2 Power Supply and Solenoid

2.2.1 Power Supply

The power supply for the solenoid is a Westinghouse 0-200 volts DC 50 KW Rectifier, with a continuously variable output control. The DC voltage output has 5% 600 cps and 0.5% 100 cps ripple at all levels. There are also irregular fluctuations in the output, of up to 5% change in voltage level, and of varying rate of change.

2.2.2 The Solenoid

The solenoid used was originally constructed by Hutchinson for work on the magnetostriction of nickel and gadolinium (1958) (ref 2.2). Basically, the solenoid consists of flat coils of copper strip in the shape of pancakes. Several of these coils are stacked one on top of the

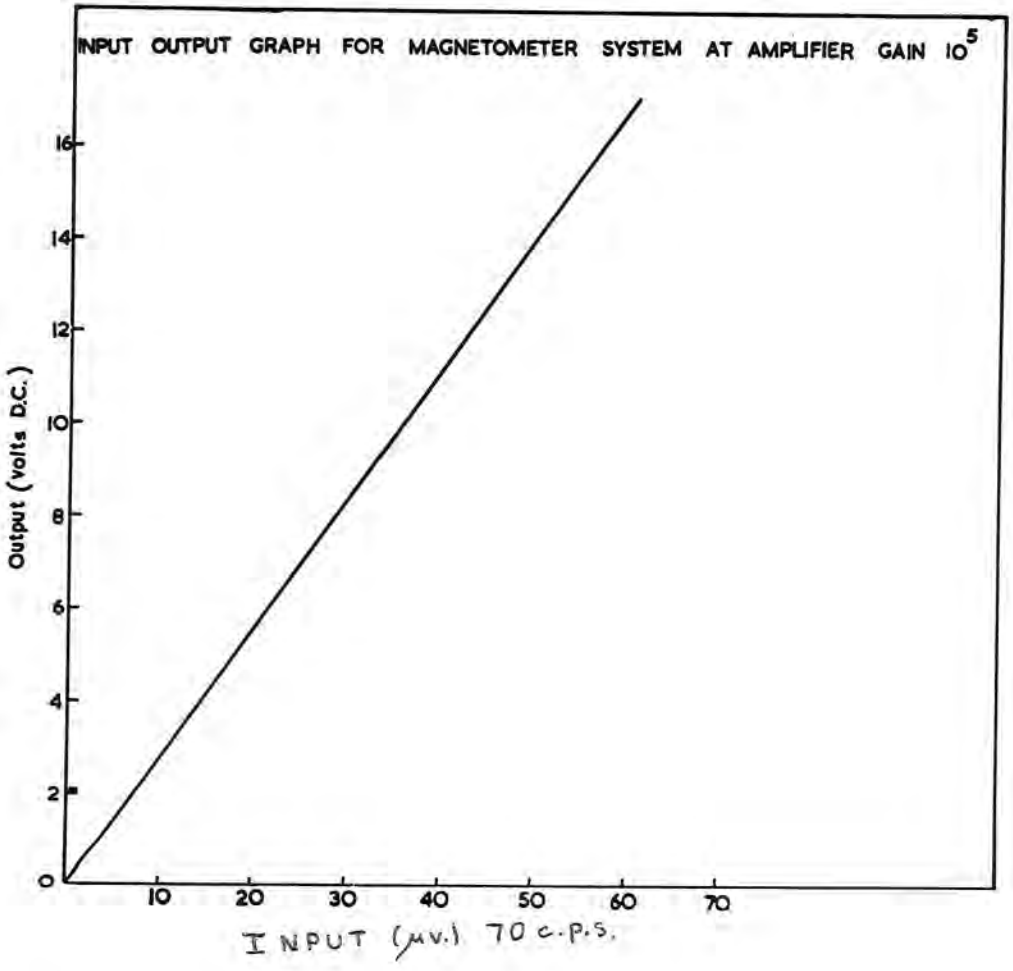
INPUT OUTPUT GRAPH FOR MAGNETOMETER SYSTEM AT AMPLIFIER GAIN 10^5
Output (volts D.C.)
0
2
4
6
8
10
12
14
16
10
20
30
40
50
60
70
INPUT (μv.) 70 c.p.s.

FIG. 2.2.(A).

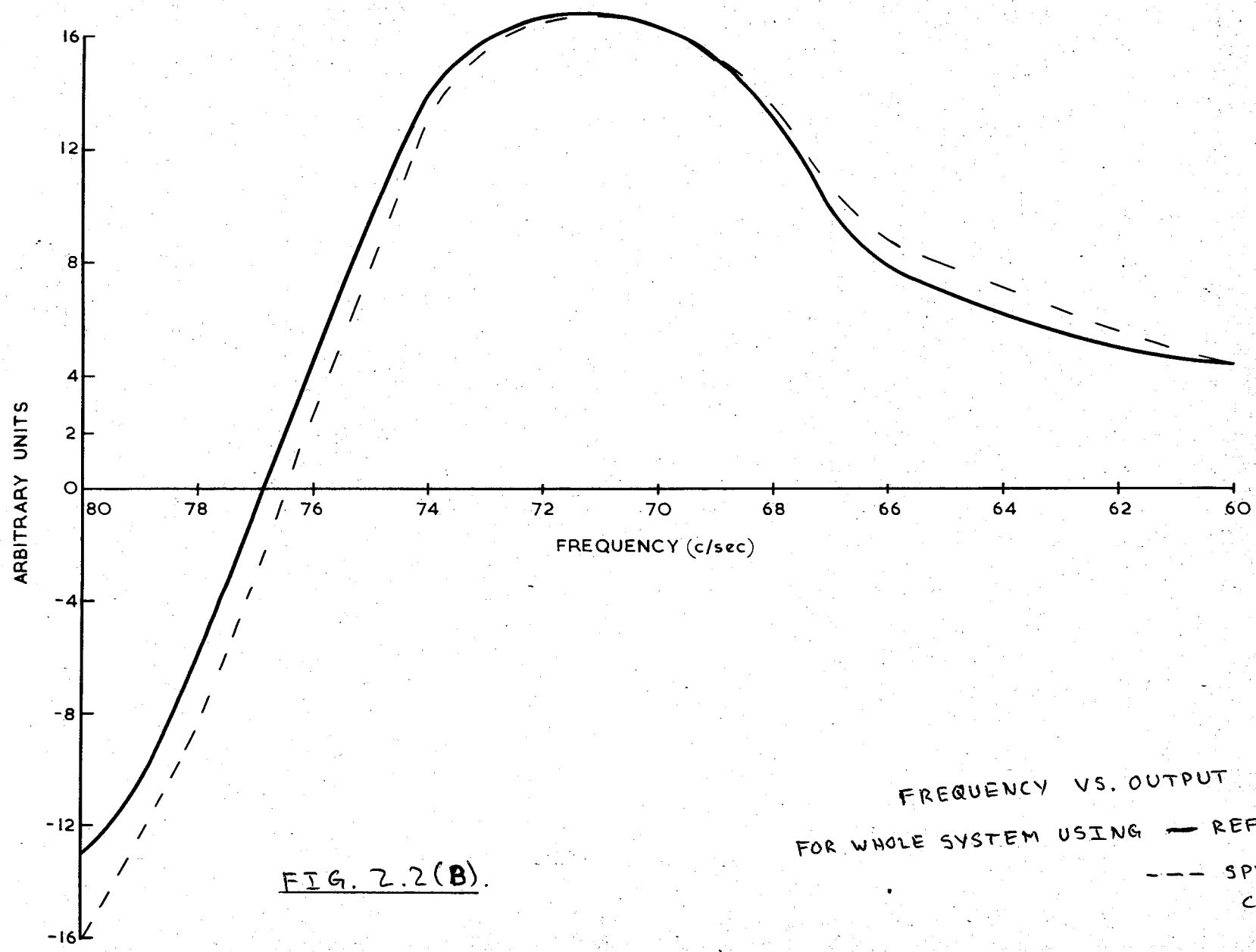

FIG. 2.2(B).

FREQUENCY VS. OUTPUT

FOR WHOLE SYSTEM USING — REF. COILS

--- SPECIMEN COILS.

other, with insulating spacers between them. The coils are electrically connected, and mounted on a central tube. An outer waterproof jacket allows water to be circulated through the coils to act as a coolant. The de-ionised coolant water is circulated continuously through the solenoid by means of a pump, and also passes through a heat exchanger. In its original form, the inner tube of the solenoid was of brass, but this was changed to one of araldite-coated tufnol, because of difficulty in preventing shorting between the pancakes and the central tube.

The solenoid gives a maximum field of 10,500 oersteds at a peak current of 250 amps. The field produced is linear with current, giving 42 oersteds per ampere at the centre of the solenoid. There is a 0.3% difference in field between the centre of the solenoid and a distance of 1 cm along its axis from the centre. There is also a radial field distortion of 0.05% in the central 2 cms of the solenoid.

The solenoid is bolted to a lifting platform which may be wheeled into position and located on the floor by two screw down feet, the solenoid then being raised into position. This minimises vibration of the solenoid due to turbulence of the cooling water, consequently minimising vibration of the dewars, which are located inside the solenoid by means of spacers. This in turn cuts down movement of the specimen pick-up coils relative to the specimen, since the pick-up coils are mechanically linked to the dewars, while the specimen is not. The solenoid is supported in its final position by two spacing bars, which prevent the platform sinking because of leakage in the hydraulic lifting piston. Fig 2.3 shows the lifting platform and solenoid in position.

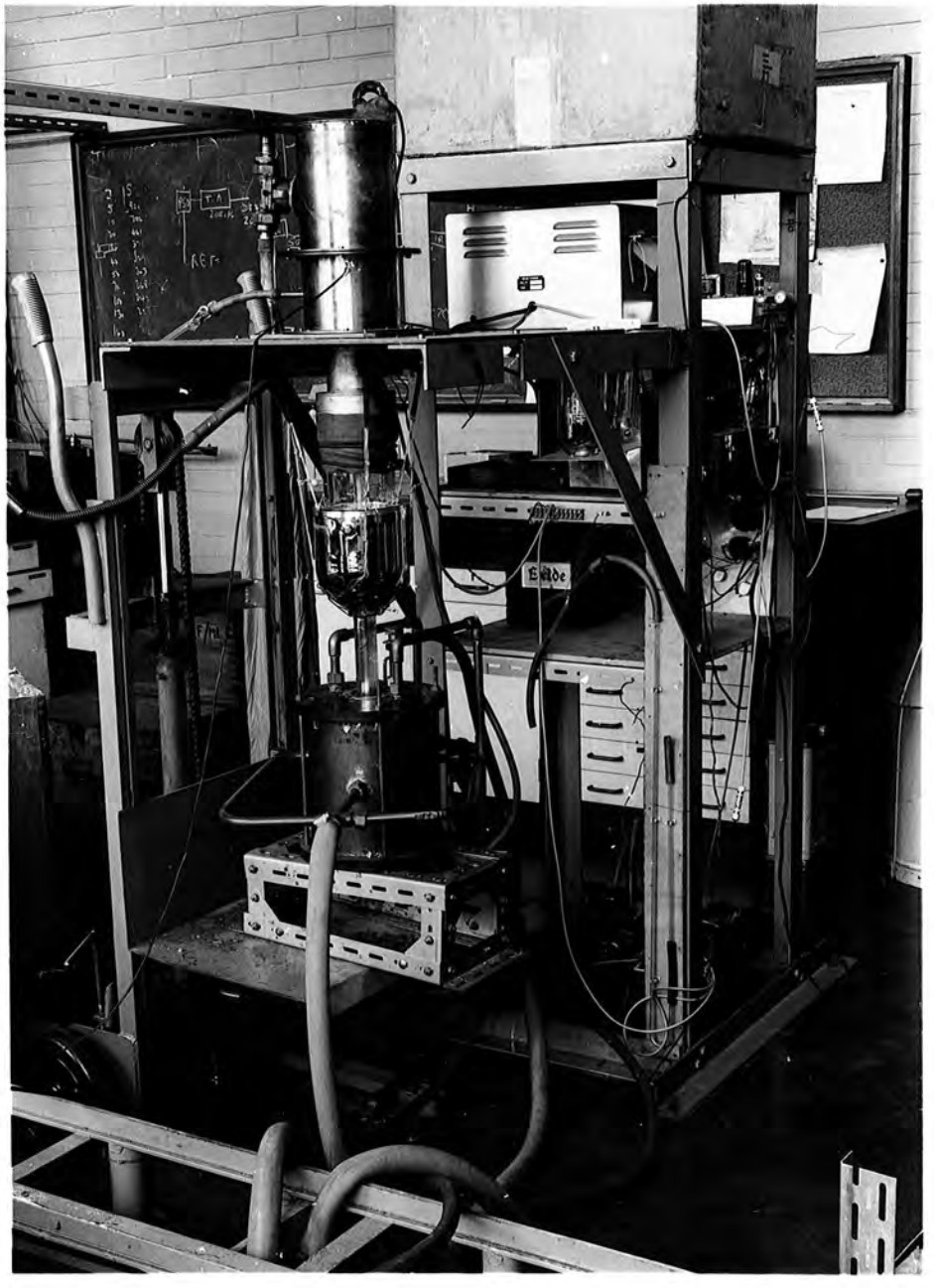

FIG. 2.3.

2.3 Mechanical Construction

In order to further reduce mechanical vibration, the magnetometer and dewars were mounted on a platform attached to a rigidly constructed tower, as shown in Fig 2.3.

The vibrator, an Advance Type Vl Vibrator is mounted on four brass pillars so that it may be adjusted to give a vertical mounting. The vibrator is enclosed in a vacuum chamber, which is removed in two parts. The lower part has hermetic seals fitted to allow electrical access to the interior. This makes two-part demounting necessary.

The vibrating rod is enclosed by a fused silica tube which is mounted in a vacuum seal on the underside of the supporting platform. Fused silica is used because of the high temperatures which the tube must withstand to enable measurements to be made on the specimen at elevated temperatures. (Ref para 2.7)

Since the reference pick-up coils are mounted on the supporting platform directly below the vibrator, a large amount of unwanted signal is generated by induction in the pick-up coils direct from the vibrator. In order to reduce this, a mu-metal screen is introduced between the two.

The cryostat head is attached to the underside of the main platform, concentric with the inner glass tube.

2.4 Dewars

The two Pyrex dewars, one nitrogen and one helium, were made to specification by James A. Jobling Ltd, of Sunderland.

The helium dewar is held firmly in the cryostat head by four springs

supporting a cradle which fits around the bottom of the dewar. A neoprene gasket provides a certain amount of cushioning between the dewar and the cryostat head. The interior of the dewar is made vacuum tight by a piece of rubber tube which fits tightly over the top of the dewar and the lower part of the cryostat head. Since the interior of the dewar is often subjected to vacuum pumping to dry it out and to achieve lower temperatures, an arrangement of O-rings is employed to prevent the rubber tube being sucked into the cryostat head.

The springs supporting the dewar are just tight enough to hold the dewar firmly in its seating when filled with liquid, while allowing any build up of pressure inside the dewar due to rapid boil off of liquid to force the dewar down and escape to the atmosphere.

The inner tube surrounding the vibrating rod is located inside the helium dewar with PTFE spacers.

The nitrogen dewar is also suspended by a cradle and four springs, so that when it is empty it is not in contact with the helium dewar. Spacers are used to locate the helium dewar inside the nitrogen dewar, and to locate the nitrogen dewar centrally in the solenoid.

2.5 Coil Systems

2.5.1 DC Coil (Reference specimen)

The reference coil consists of 750 turns of 38 SWG enamelled copper wire wound on a cylindrical perspex former, which is also the lower of two mechanical connectors between the vibrator and the main part of the vibrating rod. The coil has a turns-area of 5,300 cm^2 and has a magnetic

moment of 0.53 gauss cm^3 per milliamp coil current. It is located at the centre of the reference pick-up coil system, and takes a maximum current of 30 milliamps before heating becomes appreciable. A 6 volt 80 ampere-hour accumulator is used to provide current for the DC coil, as mains operated DC supplies were found to give rise to a noisy output from the reference pick-up coils.

2.5.2 Reference Pick-Up Coils

The reference pick-up system consists of two matched coils, each of 2620 turns of 38 SWG enamelled copper wire wound on a tufnol former. Each coil has a turns-area of 1.03×10^5 cm^2 and they are separated by a $\frac{3}{8}$" gap. The coils are connected in series opposition to reduce unwanted pick-up arising mainly from the vibrator. A bucking-out coil to eliminate remaining pick-up is connected in parallel with the pick-up coils, and is mounted on the outside of the vacuum chamber using modelling clay, to allow easy adjustment.

2.5.3 Sample Pick-Up Coils

The sample pick-up coil former is made from PTFE rod. The two matched coils wound on this former both consist of 400 turns of 46 SWG enamelled copper wire, with a turns area of 1020 cm^2 each. The coils are separated by a 6 mms gap, and again are connected in series opposition to reduce noise arising from variations in the magnet power supply.

The coils are potted in araldite to prevent shorting between windings at high temperatures. The sample, at the end of the vibrating rod, is located at the centre of the gap between the coils. The former for these coils is machined to be a push fit on the silica tube enclosing

the vibrating rod. This allows the position of the coil with respect to the sample to be adjusted for optimum output.

2.6 Vibrating Rod

A long drinking straw of 4 mm diameter was found to be satisfactory as a vibrating rod, being light, thin, and longitudinally rigid. To withstand the high temperatures produced in that region, the bottom six inches of the rod are of fused silica tube, the specimen being attached to the lower end with high temperature cement. Each specimen is mounted on a separate length of silica tube, to facilitate the changing of specimens. The straw and silica tube are connected by slipping the two over a short length of bored out perspex rod, the joint being sellotaped together. This arrangement proved satisfactory, the joint withstanding the temperature experienced in that region without losing longitudinal rigidity.

2.7 Temperature Variation

2.7.1 Method of Obtaining High and Low Temperatures

To enable measurements to be taken at elevated temperatures, two small heater windings were wound on the silica tube, one above and one below the sample pick-up coil. These two coils, dissipating up to 25 watts, enabled readings to be taken at sample temperatures up to 300°C. Electrical leads to the sample pick-up coils and heater windings are taken through the cryostat head by hermetic seals. A 24 volt DC supply used with a rheostat provides variable power for the heater.

Low temperature measurements are made using liquid nitrogen and liquid helium by employing standard techniques. Normally, low temperature measurements are taken during the warm up period. In order to check that

appreciable thermal gradients do not exist in the specimen during these warm up observations, preliminary magnetisation measurements were made on nickel, cobalt and gadolinium, and compared with published results (ref. 2.3). It was found that, to within 5%, these results were in agreement, showing that the rate of temperature rise is sufficiently low for thermal equilibrium in the specimen to be obtained. Above room temperature, the rate of temperature rise or fall can be controlled by altering the current through the heating coil.

2.7.2 Temperature Measurement

Measurement of the specimen temperature is carried out by using a copper constantan thermocouple threaded down the inside of the vibrating rod. One junction is held on the specimen, the other junction being kept at $0^{\circ}C$. The thermal emf is measured with a Pye Portable Potentiometer and is converted to temperature values using a graph prepared from the data given in the book by Kaye and Laby (ref 2.4).

2.8 Vacuum System

The helium dewar interspace and the interior of the vacuum chamber and tube enclosing the vibrating rod may be evacuated either together or separately using a Speedivac 2-stage high vacuum pump. The pressure is measured with a mercury manometer to ensure that a satisfactory vacuum, ie. not more than 1 mm of mercury is maintained. To avoid freezing out of the remaining gases in the innermost tube, this was flushed with helium gas before final evacuation.

2.9 Electronics

2.9.1 Driving Oscillator

A 12-volt sinusoidal output from a Farnell Type LF Solid State oscillator drives a single stage power amplifier, which is inductively coupled to the Advance vibrator which drives the vibrating rod.

2.9.2 Tuned Amplifier

The tuned amplifier is a Grubb-Parsons Type TA high-gain tuned amplifier, and it incorporates a special low-noise first stage, which is followed by two conventional triode amplifier stages which include a gain control. Stages four and five use high-slope pentodes operating with separate tuned twin-T negative feedback loops. These are band stop filters originally tuned to 10 cycles per second, but were modified for our purposes to have their stop band at 70 cps. This frequency was chosen as being well away from the fundamental and harmonics of the mains supply voltage. The twin-T filters allow voltages at all frequencies except the tuned frequency to feed back to the input of the pentode immediately preceding the filter. The feed-back signal is also phase-changed by 180° by the filter, so that the effect is that of a strong negative feed-back at all frequencies excepting the tuned frequency, thus reducing the gain at all other frequencies. The amplifier normally gives a DC voltage output, but since a phase-sensitive detector is necessary to give noise discrimination, an AC output is taken from the amplifier after the stage just preceding the rectifying circuit. Circuit details are shown in Fig 2.4.

2.9.3 Phase-Sensitive Detector

The phase-sensitive detector used is similar to one described by

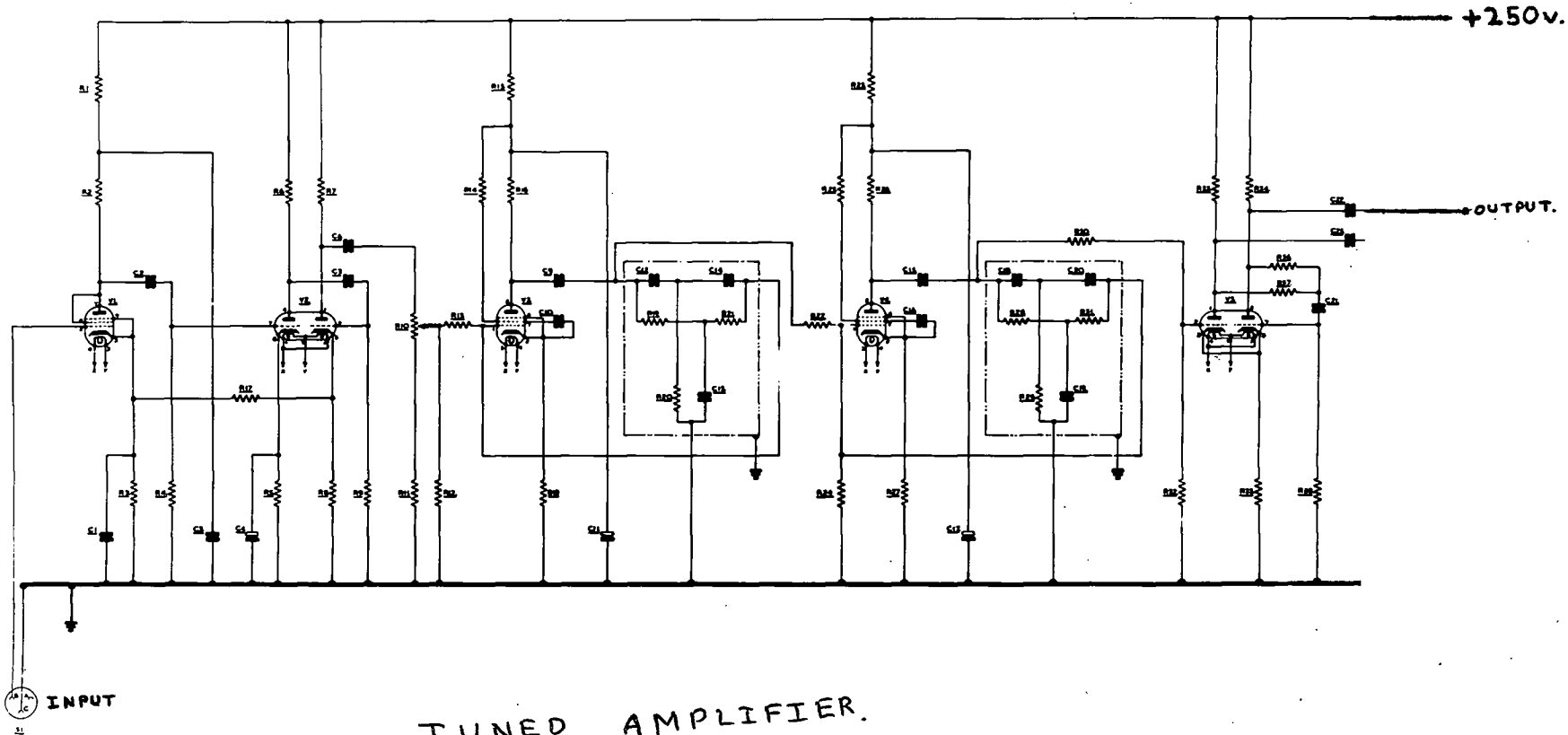

TUNED AMPLIFIER.

FIG. 2.4.

Schuster (ref 2.5). The circuit used is shown in fig 2.5. The phase-sensitive detector acts as a noise discriminator, a voltage difference appearing between the anodes of the twin triodes due to any signal supplied to the cathodes which is of the same frequency as the reference voltage. Any signal of a different frequency from the reference appears as an alternating voltage across the anodes, and as such, can be much reduced by connecting a condenser between the anodes, and reading the DC voltage across the condenser.

The phase-sensitive detector is normally used to measure phase, since the output is related to the phase difference between the signal and references voltages. If the phase difference is kept constant, however, the output is related to the amplitude of the supplied signal.

Very good noise discrimination is achieved for random noise due to mechanical vibration, mains pick-up, noise from the solenoid power supply etc, but zero errors due to pick-up at the operating frequency from the oscillator, vibrator etc, are eliminated elsewhere. Unwanted coherent pick-up in the reference pick-up coils is balanced out by altering the position of the bucking-out coil already mentioned.

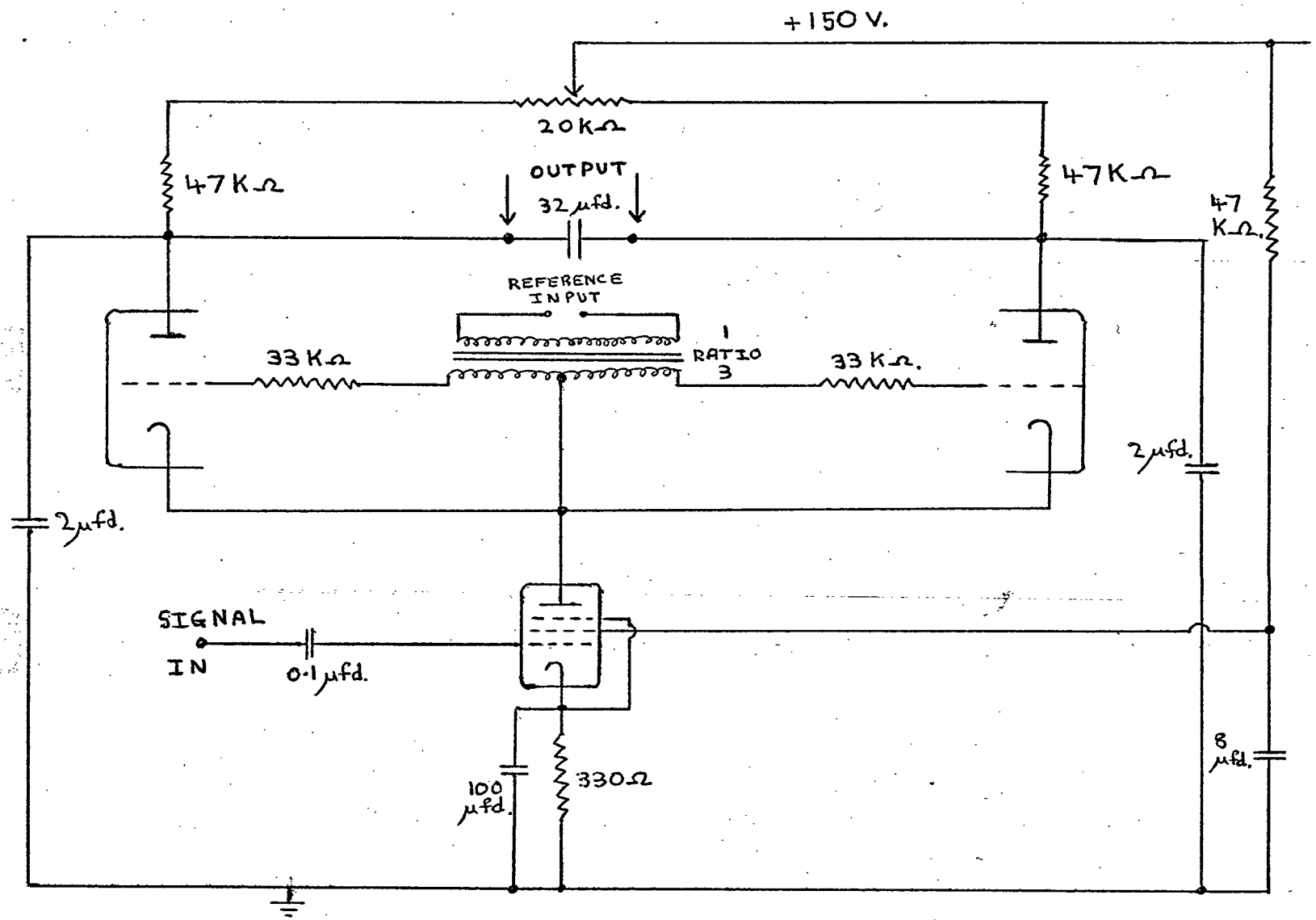

FIG.2.5. PHASE-SENSITIVE DETECTOR.

CHAPTER 3

EXPERIMENTAL

CHAPTER THREE

3. EXPERIMENTAL

3.1 Specimen Production

The cobalt, yttrium, and gadolinium metals used in the production of the specimens were obtained in ingot form from the Koch Light Chemical Company with purities of 4N, 3N and 3N respectively. Before weighing, the metals were cleaned with a file, a separate file being used for each element to avoid cross contamination. The cobalt metal was then chemically cleaned using a standard etching fluid. A variety of etches were tried on the gadolinium and yttrium metals, however none of these proved completely reliable, consequently it was decided not to etch these metals.

Stoichiometric amounts of the metals for each compound Gdx Y1-x CO_2 were weighed for x = 1;0.8;0.6;0.5;0.4;0.33;0.2;0.1;0. The total weight for each specimen was about 2 gms. The specimens were then made by melting the constituents together in an argon arc furnace at Sheffield University Physics Department made available to us by Dr J. Crangle of that department.

Each specimen was turned and remelted at least three times to ensure homogeneity. Specimens for x = 0.6 and 0 were prepared a second time because it was suspected that the first attempts to make these compounds had resulted in an inhomogeneous mixture of compounds. The second attempt proved to be more successful. Difficulty was experienced in making the $Gd_{0.5}Y_{0.5}CO_2$ compound, fragments tending to fly off the specimen, due to the high stresses set up in the material because of rapid

cooling. A second attempt at remelting the main lump and the fragments together was more successful. Reweighing the specimens after melting showed that the maximum weight loss was 0.02 gms.

Debye-Scherrer X-ray photographs were taken of each specimen and were found to be identical, the total change in lattice parameter between pure $GdCo_2$ and pure YCo_2 being too small to detect. The structure was found to be of the cubic Laves phase ($MgCu_2$) type with a lattice parameter of $7.26 \pm 0.05\text{Å}$, in good agreement with the value obtained for $GdCo_2$ by Ross and Crangle (ref 1.30) and Wernick and Geller (ref 3.1). Powder lines for Gd, Y, Co, and gadolinium-cobalt compounds other than $GdCo_2$ were specifically searched for as being possible imperfections, and slight traces of Gd and Co were found. It was assumed that yttrium-cobalt would yield approximately the same lines as gadolinium-cobalt compounds (ref. section 1.4). In addition, preliminary measurements showed that the magnetisation versus temperature curve for $GdCo_2$ gave very good quantitative agreement with the results obtained by Ross and Crangle. It was concluded that the specimens made were of the type $Gd_xY_{1-x}Co_2$.

All the specimens made were quite brittle and tended to crumble easily, more particularly those with a low gadolinium content. In order to obtain low demagnetising factors, attempts were made to make thin disc-shaped specimens, by crushing some of the material to a powder and compressing it in a steel press. A fine powder was easily obtained using a pestle and mortar, there being no fear of decomposition since the compounds seem to be very stable. The compounds are very hard, however, and attempts to make a well compacted disc were unsuccessful. Consequently, pieces of

the compound were chosen which were approximately rod-shaped, of 3 mms or less in length. These were weighed and mounted in specimen tubes as described in section 2.6.

3.2 Calibration of the Magnetometer

Iron and cobalt were chosen as calibrating specimens. Preliminary experiments were carried out using rods of iron of different lengths, to establish the importance of specimen size. This showed that the apparent value of magnetisation obtained began to drop for a specimen length in excess of 4.5 mms. It was assumed that the specimen width would not be important. Consequently, the final specimens were of length not greater than 3 mms, and of variable cross-section. The silica tube bearing the pure annealed iron specimen was mounted on the end of the vibrating tube, with the thermocouple in contact with the specimen. The enclosing tube (ref. section 2.3) bearing the lower pick-up coils was put in position, and the specimen space was evacuated. The solenoid was wheeled in position and was lifted until the top of the solenoid was just below the pick-up coils. A low current was passed through the solenoid, and the position of the pick-up coils was adjusted until the output from the magnetometer due to the magnetised vibrating iron specimen was a maximum. The solenoid was then removed, and the inner and outer dewars were put in position. The solenoid was then put into its operating position, where the specimen is within 2 mms of the centre of the solenoid tube, and is thus in the region of maximum field homogeneity. The specimen was demagnetised, and then a magnetisation versus field run at room temperature was carried out. To do this, the applied field was raised in intervals of 420 oersteds.

At each interval, the specimen signal being very strong, the reference coils were first switched into the magnetometer direct, and the output voltage for a fixed reference coil current was noted, the reference pick-up coils and phase-sensitive detector having been zeroed at the commencement of the experiment. The specimen coils were then switched into the magnetometer via the helipot input control, and the helipot was adjusted until the same output voltage was obtained as for the reference coils. The magnetisation (in emu. per gram) at each point is given by

$$\sigma = \frac{1000.I}{H.W} \cdot \frac{1}{S}$$

where I is the current through the reference coil in milliamps, H is the helipot reading, W is the mass of the specimen in grams and $\frac{1}{S}$ is a conversion factor. In the calibration runs, $\frac{1000.I}{H.W}$ was plotted against field, and the saturation value of $\frac{1000.I}{H.W}$ was obtained. By dividing this by the value of saturation magnetisation for iron given by Bozorth (ref 2.3), the conversion factor S was obtained.

Another field run was carried out at -193°C on the iron specimen, by pouring liquid nitrogen into the inner dewar and allowing sufficient time to elapse for the temperature to achieve equilibrium.

A similar procedure was carried out with the cobalt specimen. Both specimens gave the same value 112, for the factor S. Results are shown in figs 3.1 and 3.2.

At intervals during the experimental work, a check calibration run was carried out using the iron specimen. This was in order to detect any deterioration in the pick-up coils specifically, the system in general,

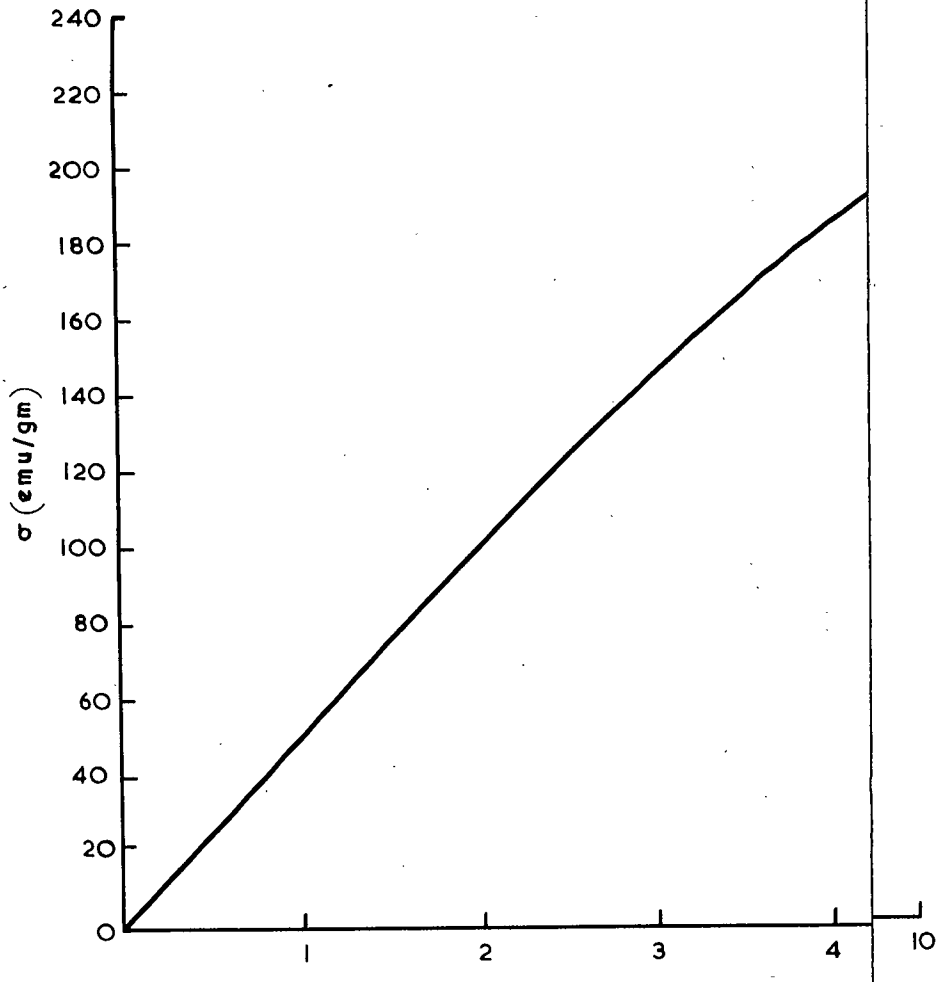

FIG. 3.1.

...EN-IRON θ = 290°K

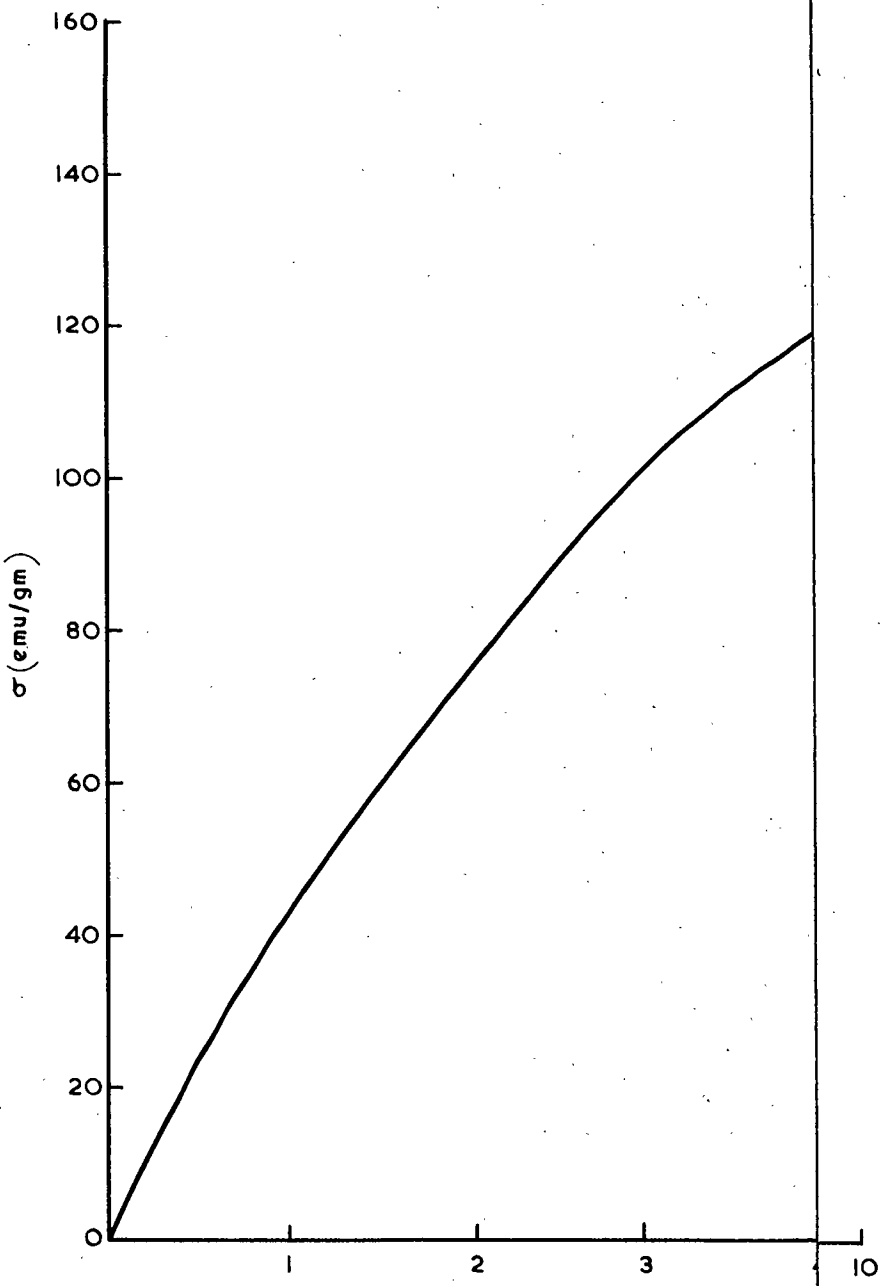

FIG. 3.2.

IMEN - COBALT θ = 290°K

and to provide a repeatability check. Throughout the experimental work, the calibration factor S stayed constant at 112, with a spread of 2%. It is felt that the 2% repeatability error arose mainly from the re-positioning of the pick-up coils for each specimen, since the output was quite sensitive to their position. It was relatively simple to re-position the pick-up coils accurately for specimens which are magnetically strong at room temperature, but for specimens which are weakly paramagnetic at room temperature, coil re-positioning was carried out by shifting the centre of the pick-up coils to the centre of the specimen position, since this was found to be the position for maximum output for strongly magnetic specimens. While there was a region of 1 mm. coil position in which the output remained constant and at a maximum output signal, there were found to be errors of $\pm$ 5% in repeatability trials on weakly magnetic specimens.

A temperature versus magnetisation run was carried out at H applied = 8.4 koe. on the iron specimen, in order to detect any temperature dependence of the calibration constant, due to factors such as change in impedance of the specimen pick-up coil. The magnetisation curve obtained was comp ared with the absolute data of Weiss and Forrer (ref 3.2). Within the limits of experimental error, S was found to be temperature independent.

3.3 Magnetic Measurements

In making magnetic measurements on the specimens, the same setting up procedure was followed as in the calibration runs.

Magnetisation versus temperature measurements were carried out on all the specimens at various applied magnetic fields, the temperature being raised slowly from 4.2°K to approximately 580°K over a period of approxi-

mately two hours, and magnetisation versus external magnetic field measurements were made on all specimens at various constant temperatures, such as 4.2 K, 80 K, 288 K and elevated temperatures. Checks of reproducibility were made by repeating measurements on some of the materials at intervals of up to two months.

In two cases (for X = 0.6 and 0.2), two separate specimens were taken from different parts of the original lumps of metal. In both cases, the two specimens were quite different in length, shape and weight. In both cases, the results corresponded to within the total experimental error, ±7%.

In cases where the specimen signal was less than the reference signal, the specimen signal output was first read direct through the system. The reference signal was then switched in via the helipot, which was adjusted to give an output reading equal to that due to the specimen. When taking readings in this manner, the conversion factor was adjusted accordingly.

In all cases, before taking a reading, the outputs due to the specimen and reference are checked twice to ensure that they correspond. The interval between taking the two readings is approximately two seconds. Reference coil zero and phase sensitive detector zero were checked frequently during each run to ensure that no zero shift had occurred in the system.

3.4 Results

The results obtained on the compounds studied are shown graphically in the following pages.

Figures 3.3 to 3.15 show the variation of magnetisation with temperature for each specimen at various fixed external fields. These results are given in order of decreasing gadolinium content, and for any one specimen, are given in order of decreasing field.

Figures 3.16 to 3.26 show the variation of magnetisation with applied magnetic field strength for each specimen at various fixed temperatures. Again, the results are given in order of decreasing gadolinium content, and for any one specimen, in order of decreasing temperature.

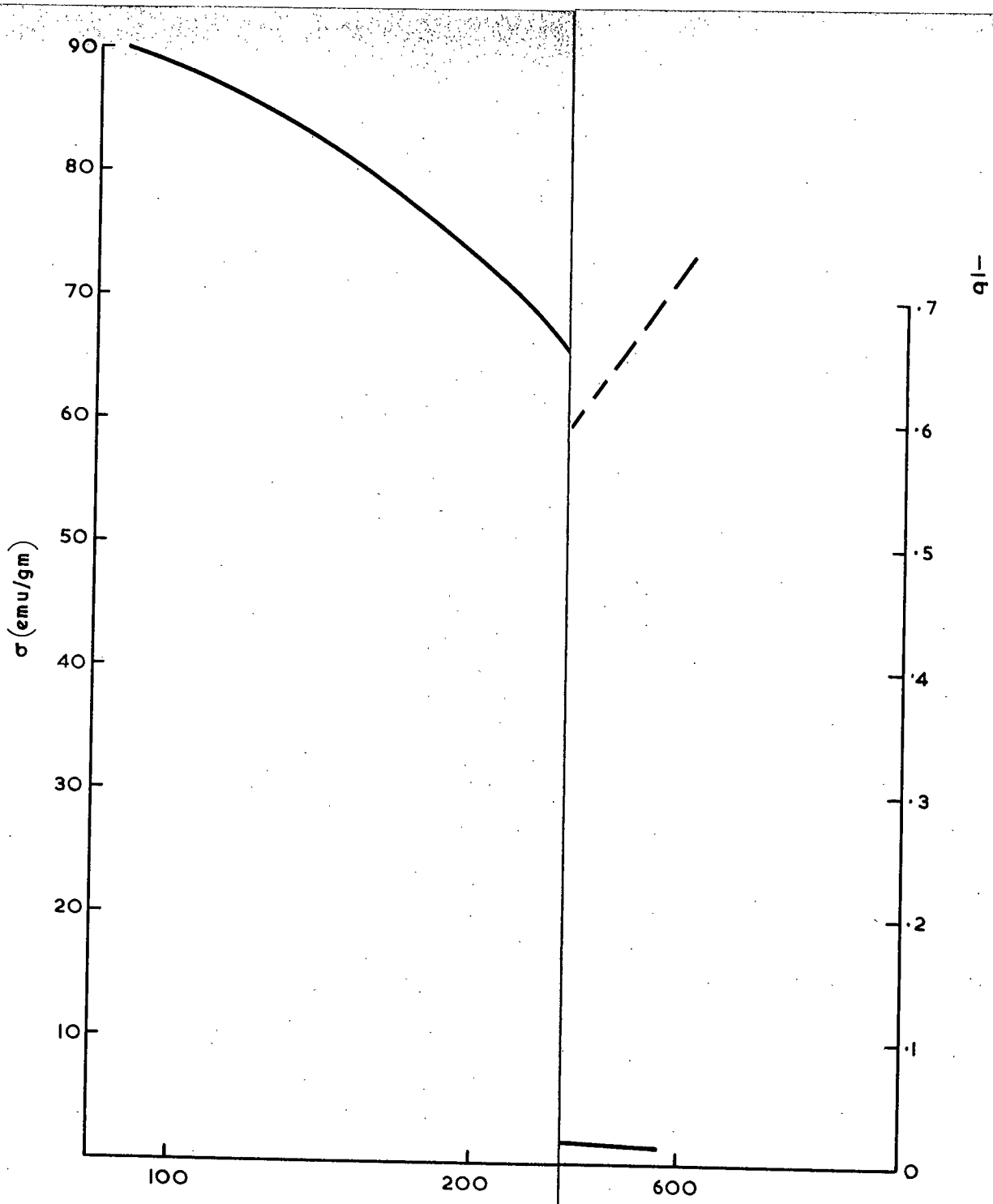

FIG. 3.3.

H = 8·4koe

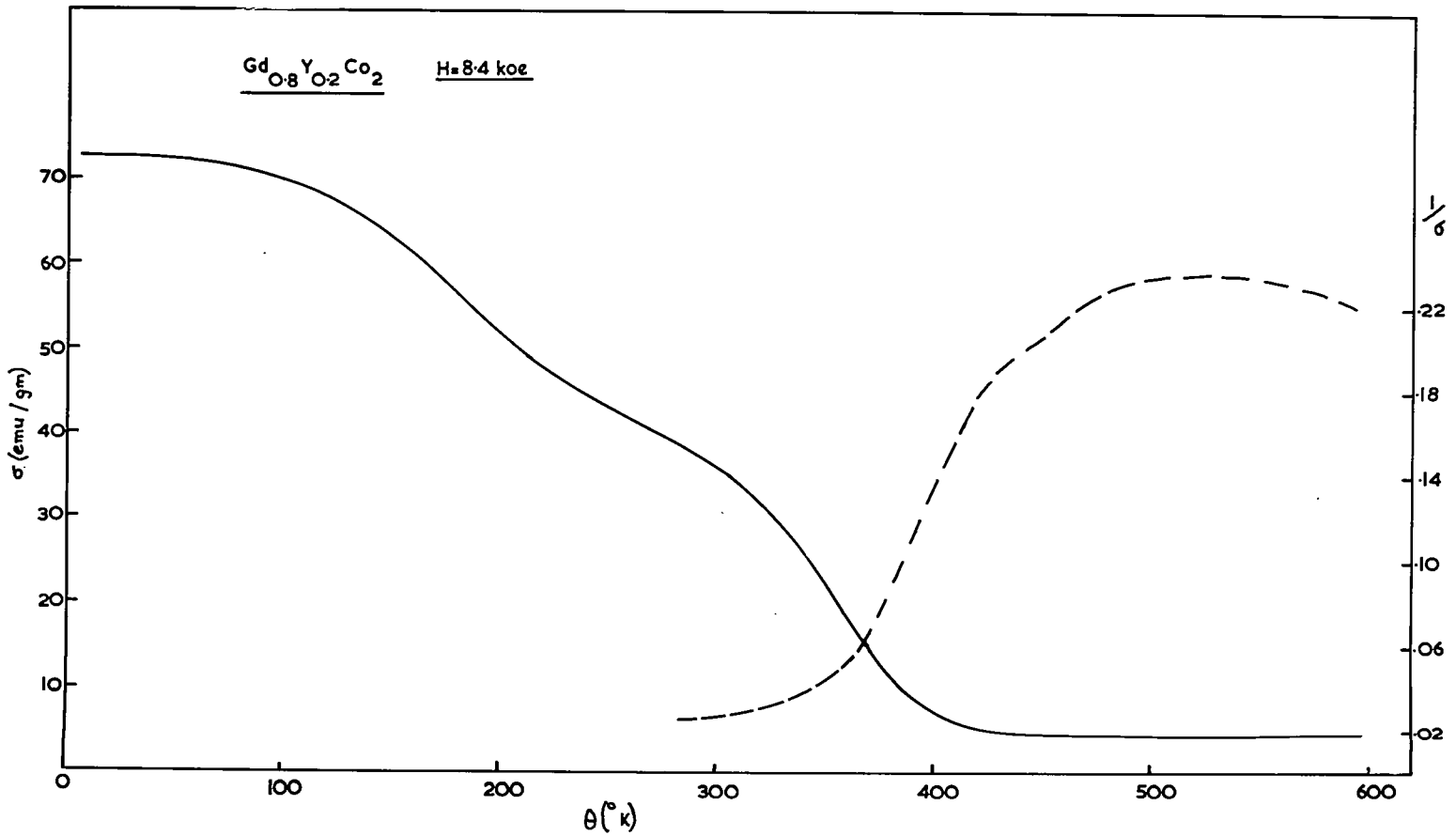
$Gd_{0.8}Y_{0.2}Co_2$
H=8·4 koe
σ (emu / gm)
70
60
50
40
30
20
10
0
100
200
300
400
500
600
θ(°K)
1/σ
·22
·18
·14
·10
·06
·02

FIG. 3.4.

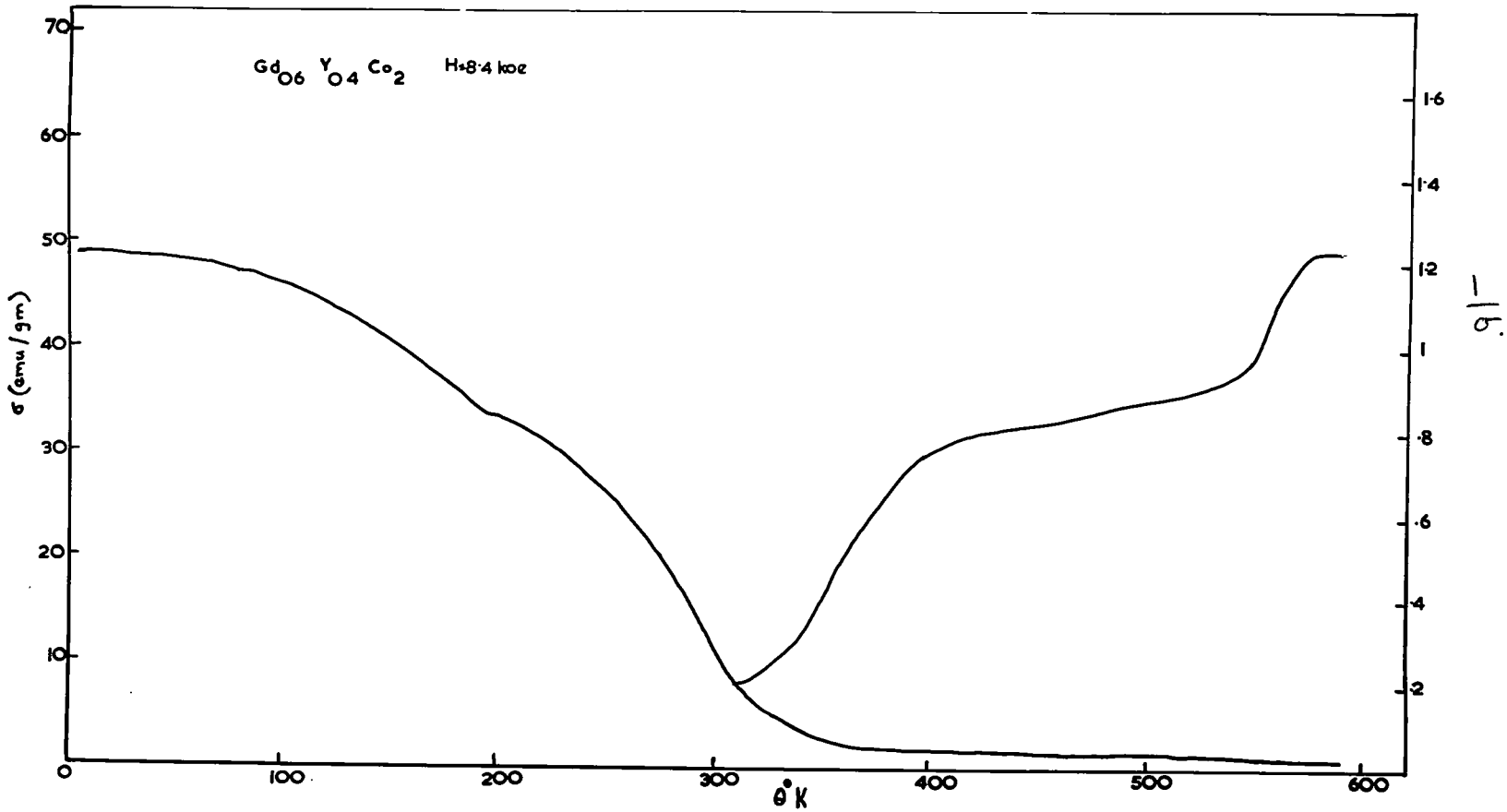
$Gd_{0.6}\ Y_{0.4}\ Co_2$ H=8·4 koe
σ (emu/gm)
θ°K
1/σ
70
60
50
40
30
20
10
0
100
200
300
400
500
600
1·6
1·4
1·2
1
·8
·6
·4
·2

FIG. 3.5.

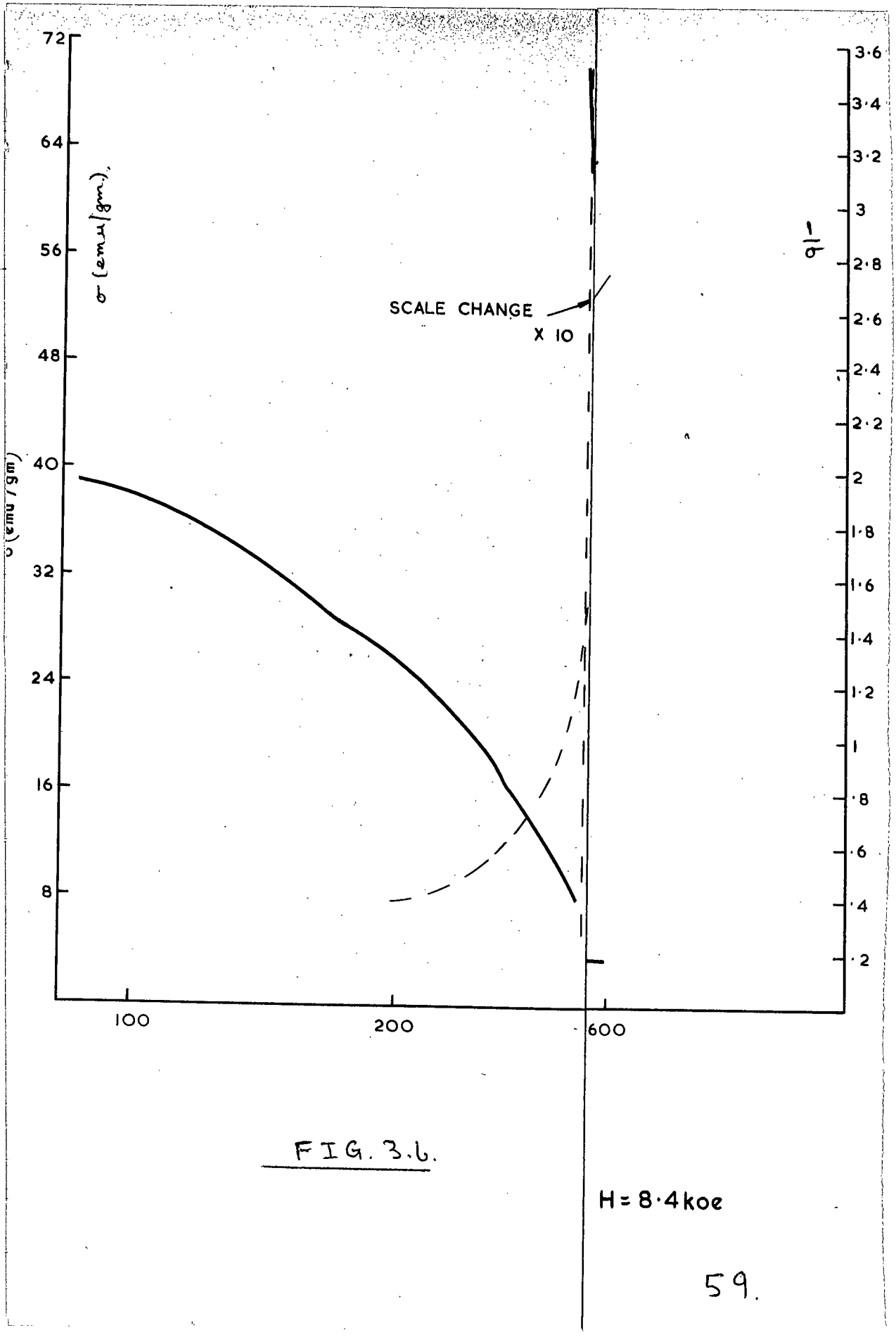
72
64
56
48
40
32
24
16
8
σ (emu/gm).
σ (emu / gm)
SCALE CHANGE
X 10
3·6
3·4
3·2
3
2·8
2·6
2·4
2·2
2
1·8
1·6
1·4
1·2
1
·8
·6
·4
·2
1/σ
100
200
600
H = 8·4 koe

FIG. 3.6.

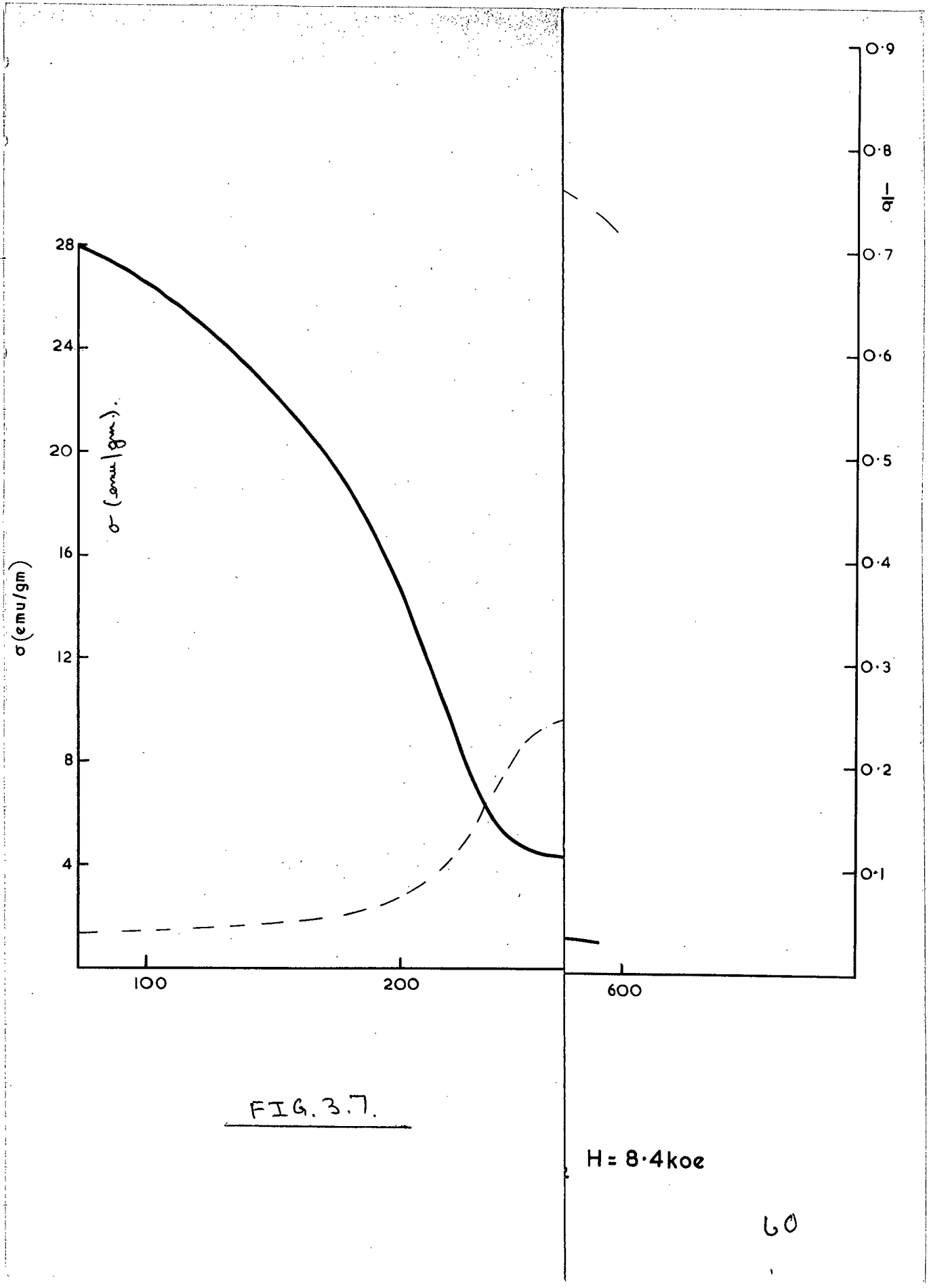
σ (emu/gm).
σ(emu/gm)
28
24
20
16
12
8
4
100
200
600
0·9
0·8
1/σ
0·7
0·6
0·5
0·4
0·3
0·2
0·1
H = 8·4koe

FIG. 3.7.

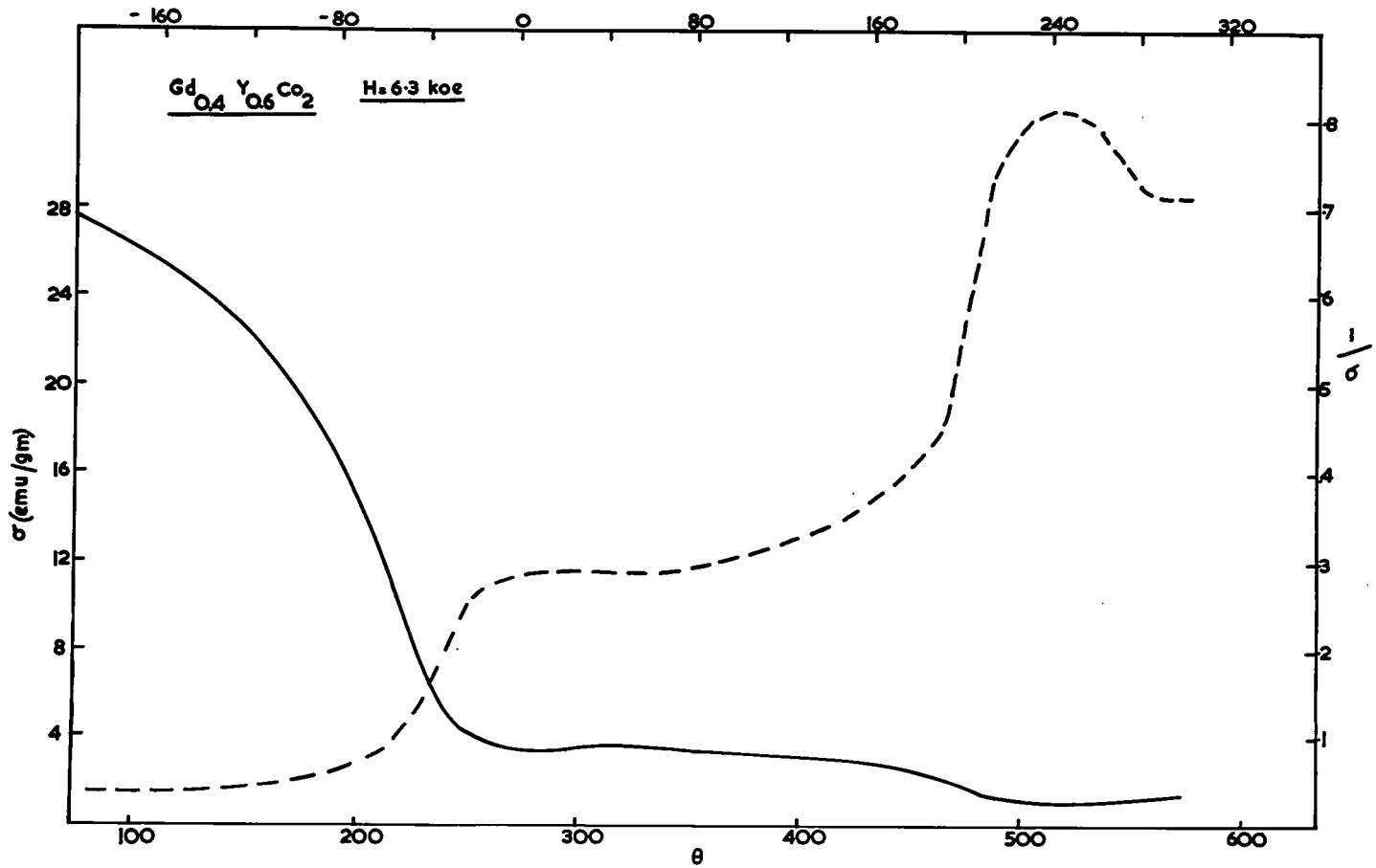
$Gd_{0.4}Y_{0.6}Co_2$
H = 6·3 koe
σ (emu/gm)
1/σ
θ
- 160
-80
0
80
160
240
320
28
24
20
16
12
8
4
8
7
6
5
4
3
2
1
100
200
300
400
500
600

FIG. 3.8.

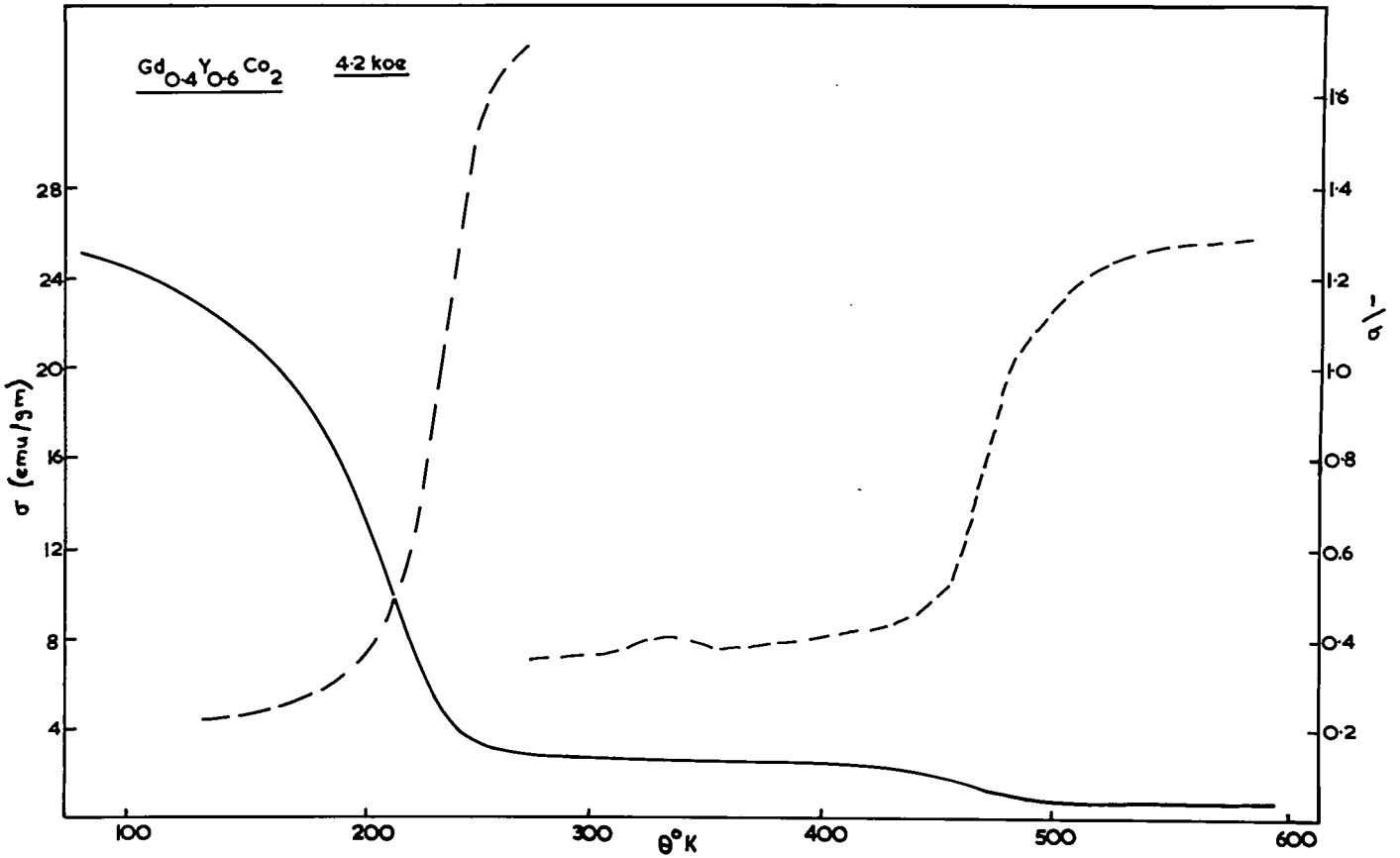
$Gd_{0.4}Y_{0.6}Co_2$
4·2 koe
σ (emu/gm)
28
24
20
16
12
8
4
100
200
300
θ°K
400
500
600
1·6
1·4
1·2
1·0
0·8
0·6
0·4
0·2
1/σ

FIG. 3.9.

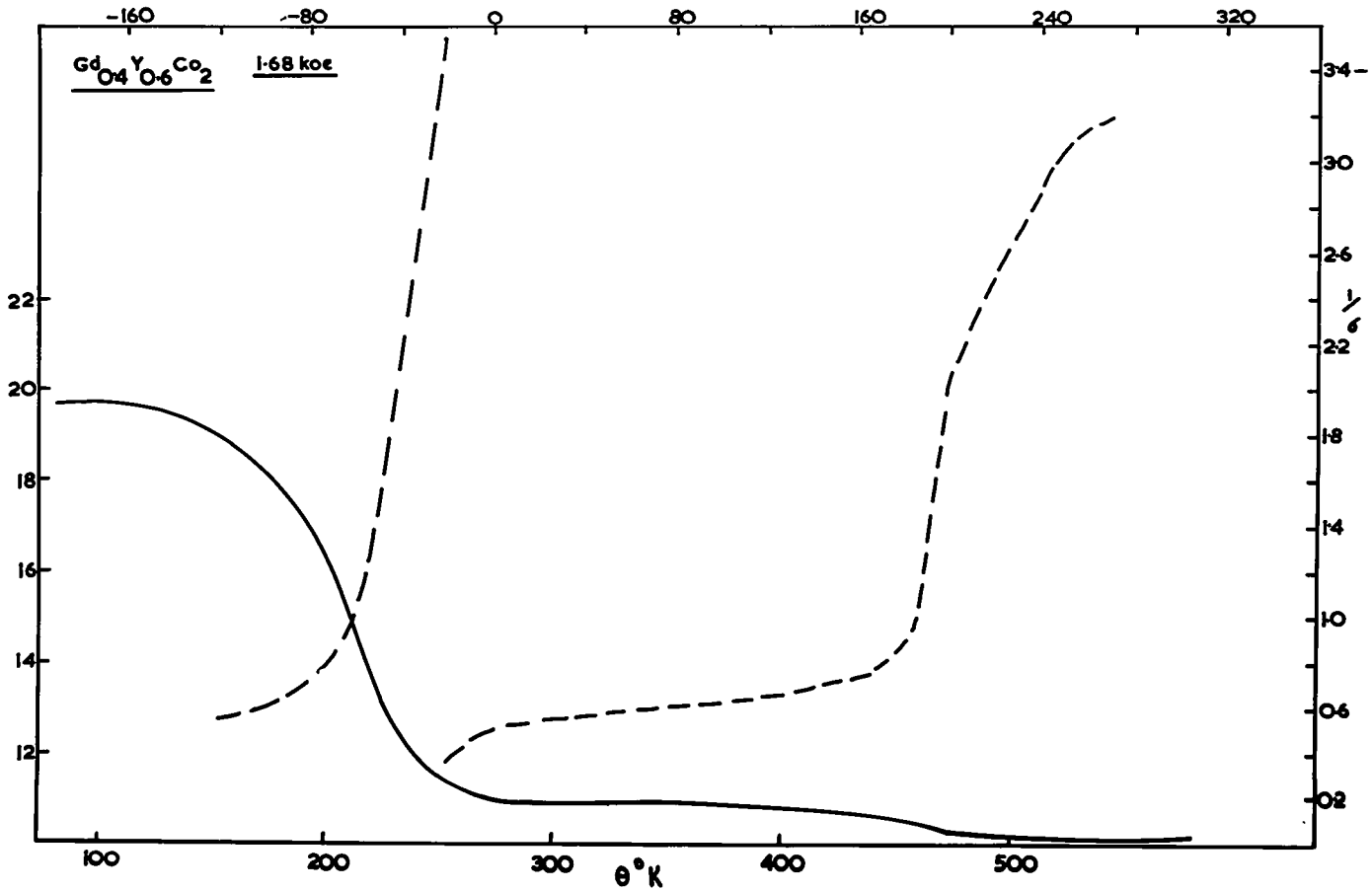
Gd0·4Y0·6Co2
1·68 koe
-160
-80
0
80
160
240
320
22
20
18
16
14
12
100
200
300
θ°K
400
500
3·4
3·0
2·6
1/6
2·2
1·8
1·4
1·0
0·6
0·2

FIG. 3.10.

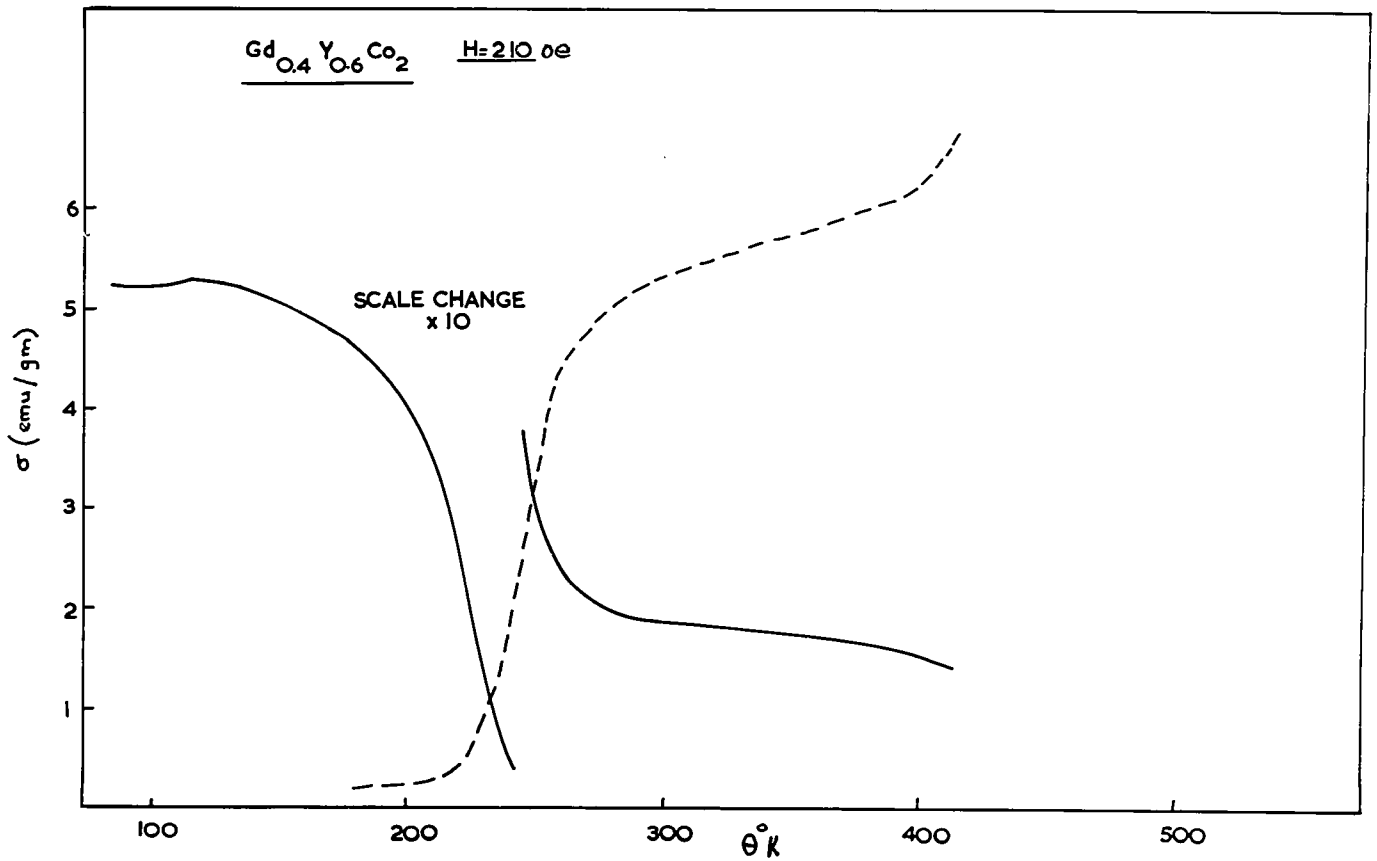
$Gd_{0.4}Y_{0.6}Co_2$ H=210 oe
SCALE CHANGE
x 10
σ (emu/gm)
6
5
4
3
2
1
100
200
300
400
500
θ°K

FIG. 3.11.

GF

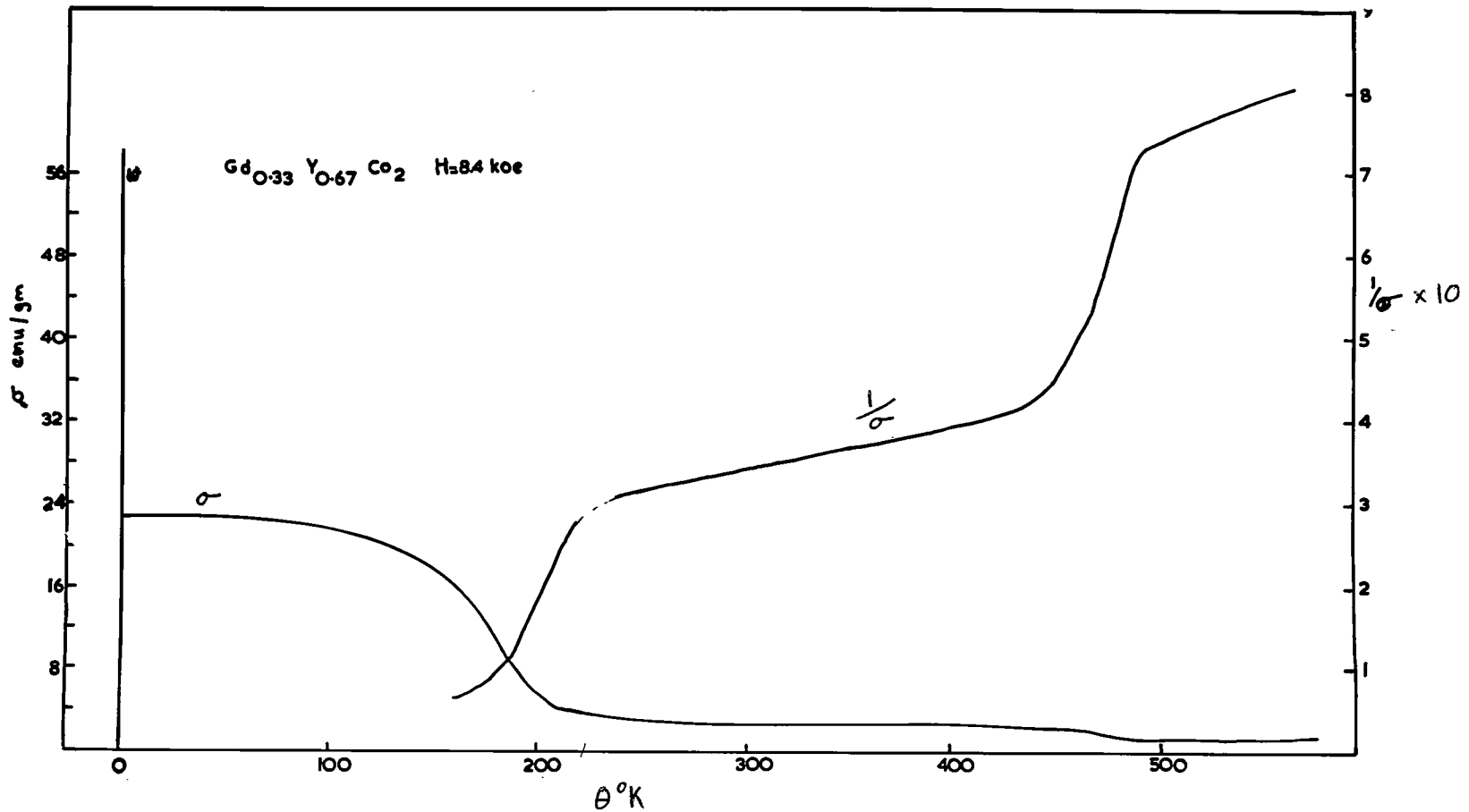
$Gd_{0.33}\ Y_{0.67}\ Co_2$ H=8.4 koe
σ emu/gm
56
48
40
32
24
16
8
σ
1/σ
1/σ x 10
8
7
6
5
4
3
2
1
0
100
200
300
400
500
θ°K

FIG. 3. 12.

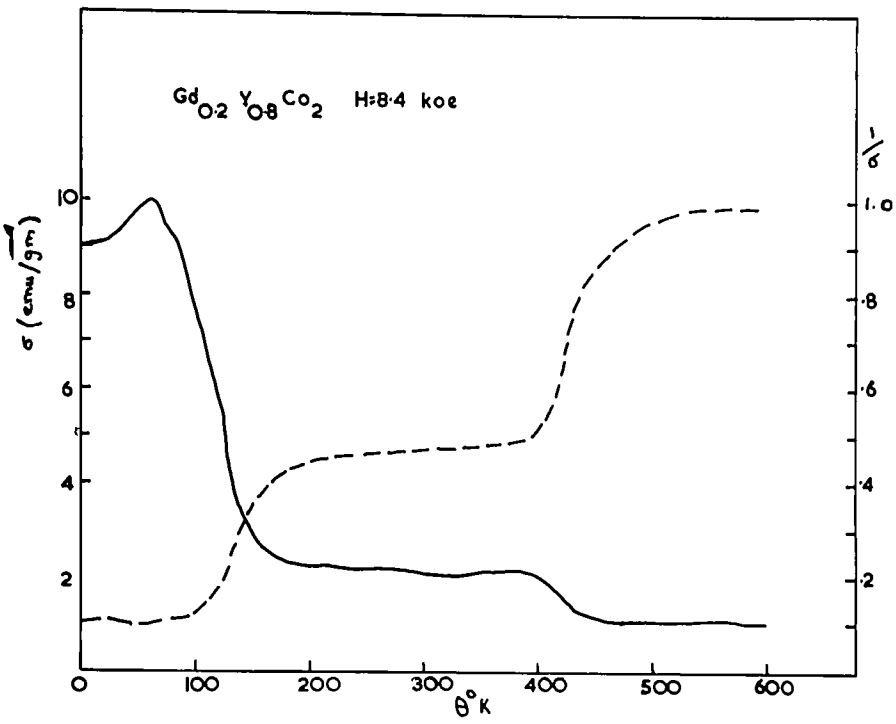
$Gd_{0.2}Y_{0.8}Co_2$ H=8·4 koe
σ (emu/gm)
1/σ
10
8
6
4
2
1.0
·8
·6
·4
·2
0
100
200
300
400
500
600
θ°K

FIG. 3.13.

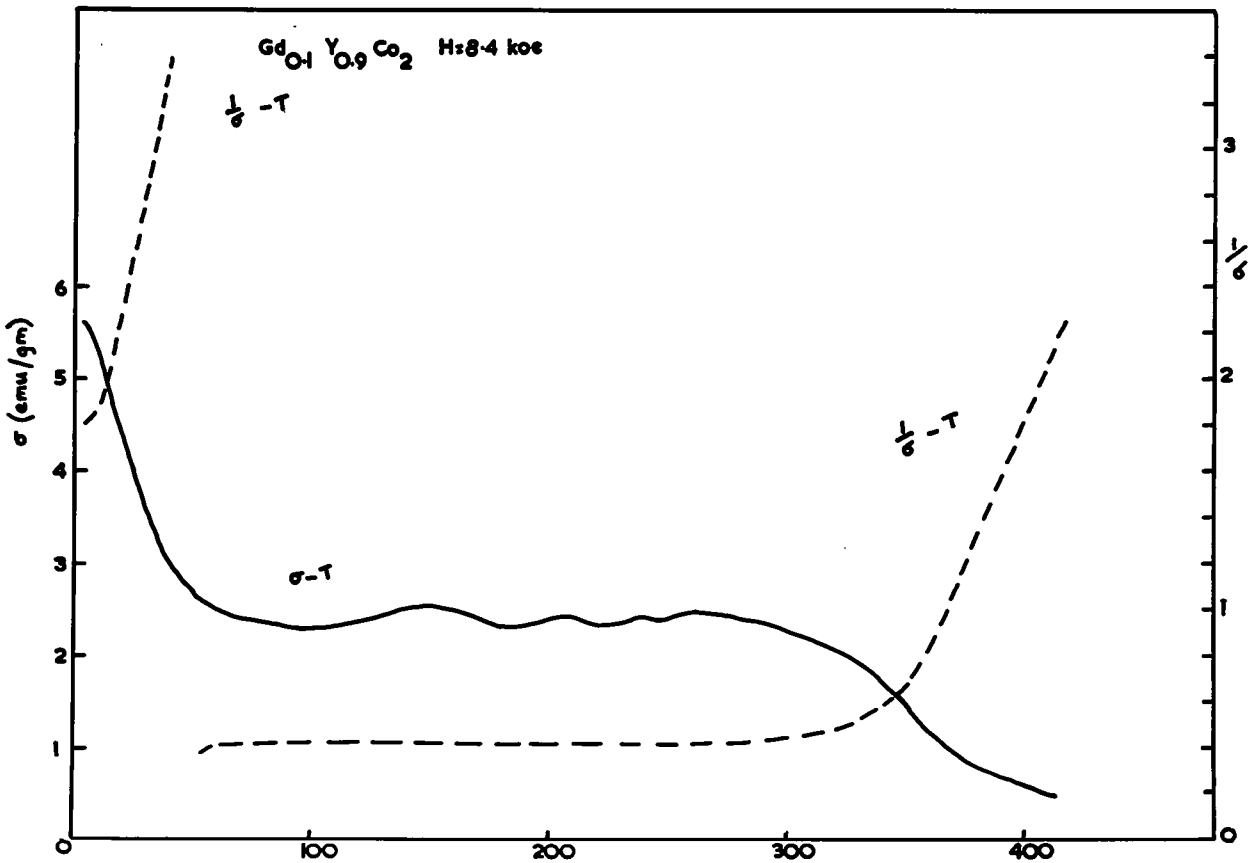
$Gd_{0.1}\ Y_{0.9}\ Co_2$ H=8·4 koe
$\frac{1}{\sigma}$ -T
σ (emu/gm)
σ-T
$\frac{1}{\sigma}$ -T
$\frac{1}{\sigma}$
0
1
2
3
4
5
6
100
200
300
400

FIG. 3.14.

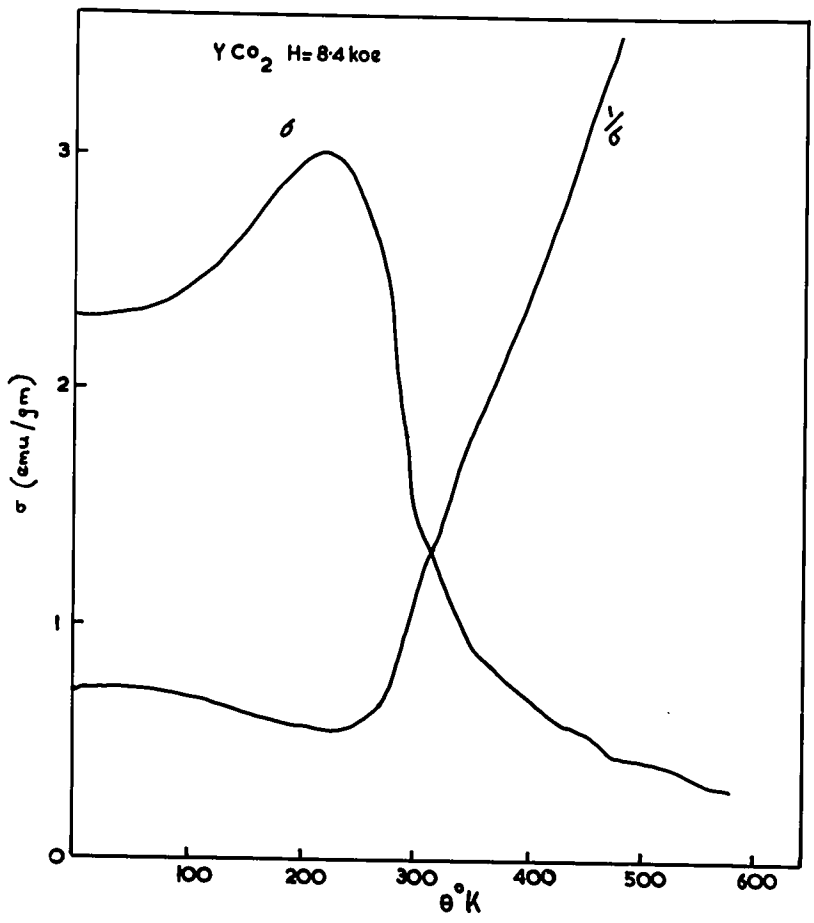

FIG. 3.15.

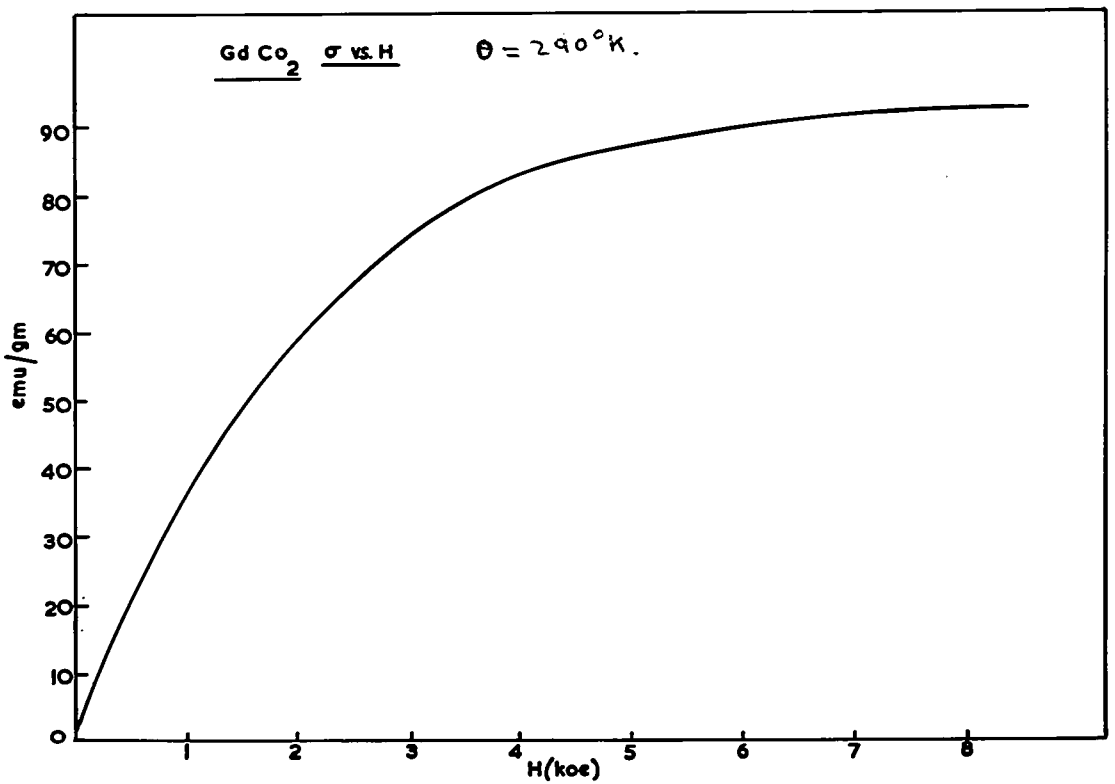
Gd Co2 σ vs. H
θ = 290°K.
emu/gm
0
10
20
30
40
50
60
70
80
90
1
2
3
4
5
6
7
8
H(koe)

FIG. 3.16.

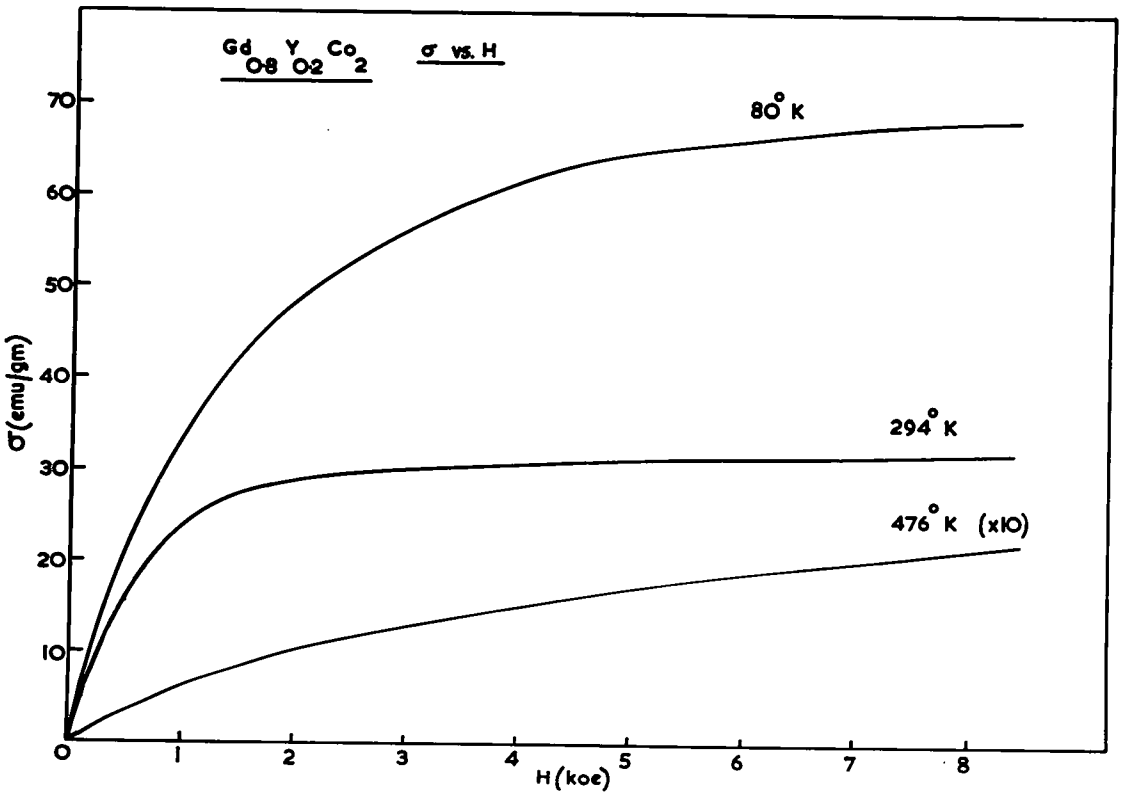
Gd 0.8 Y 0.2 Co 2
σ vs. H
80° K
294° K
476° K (x10)
σ (emu/gm)
H (koe)
0
10
20
30
40
50
60
70
1
2
3
4
5
6
7
8

FIG. 3.17.

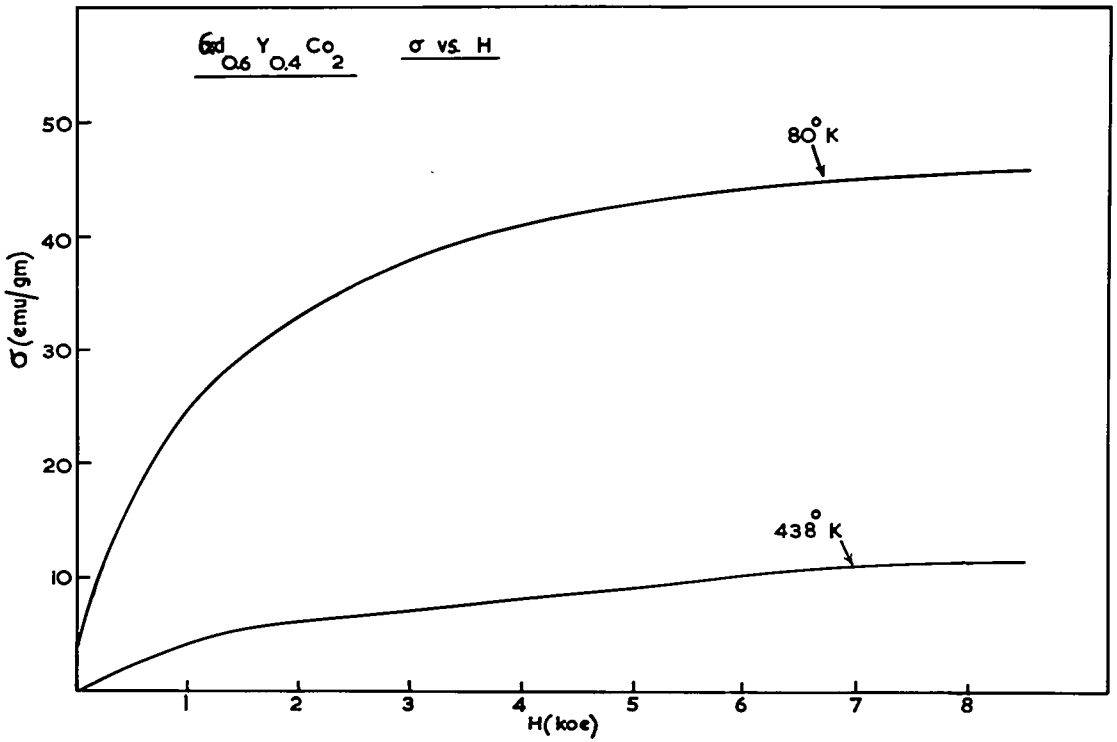

FIG. 3.18.

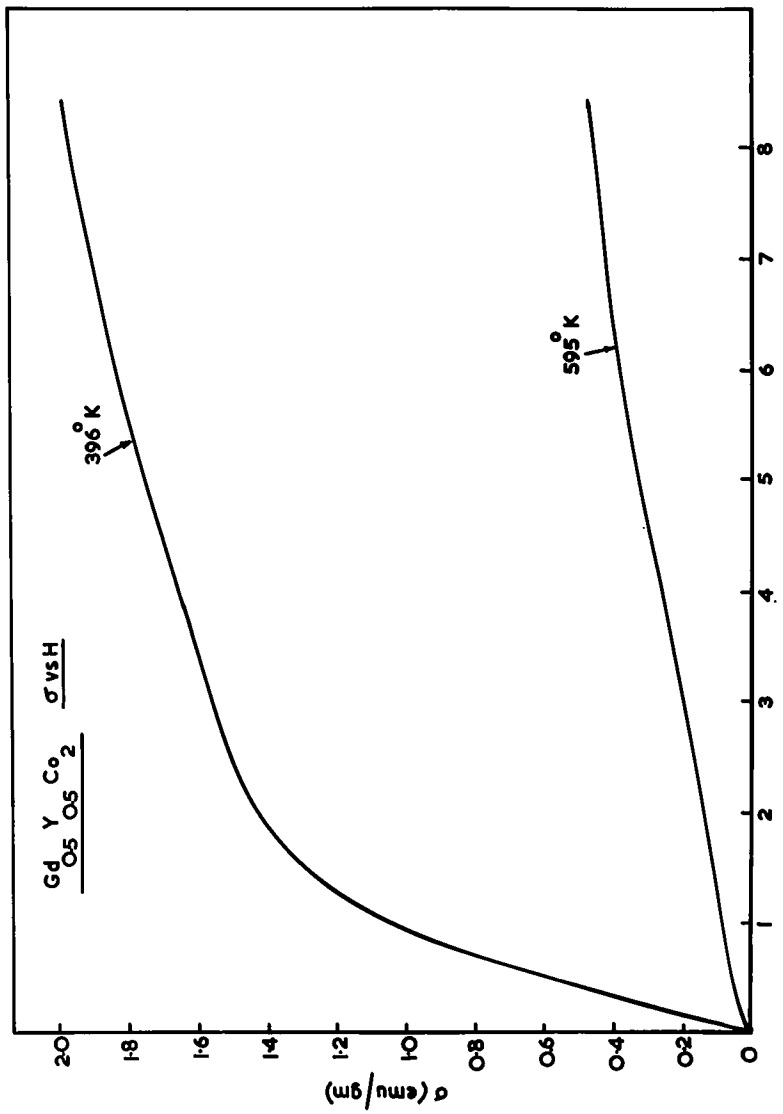
$Gd_{0.5}Y_{0.5}Co_2$ σ vs H
396° K
595° K
σ (emu/gm)
0
0·2
0·4
0·6
0·8
1·0
1·2
1·4
1·6
1·8
2·0
1
2
3
4
5
6
7
8

FIG. 3.19.

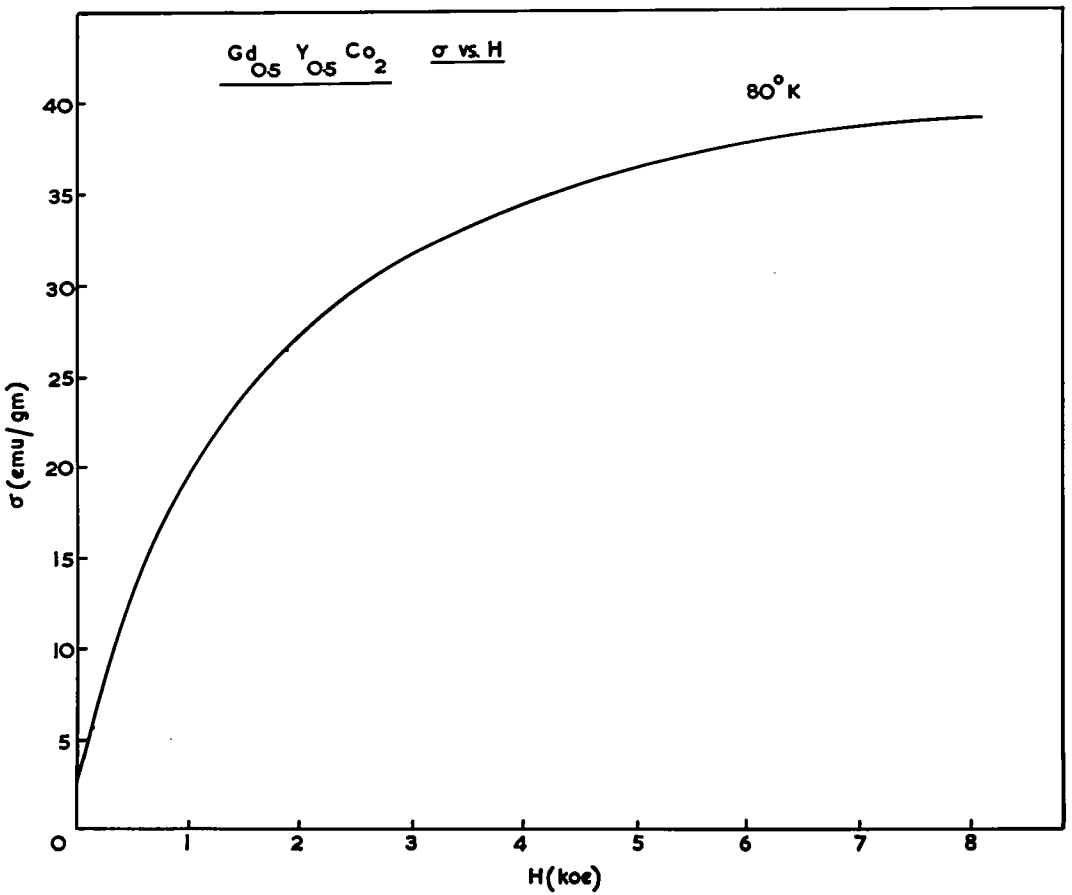
$Gd_{0.5}Y_{0.5}Co_2$ σ vs. H
80°K
σ (emu/gm)
H(koe)
0
5
10
15
20
25
30
35
40
1
2
3
4
5
6
7
8

FIG. 3.20.

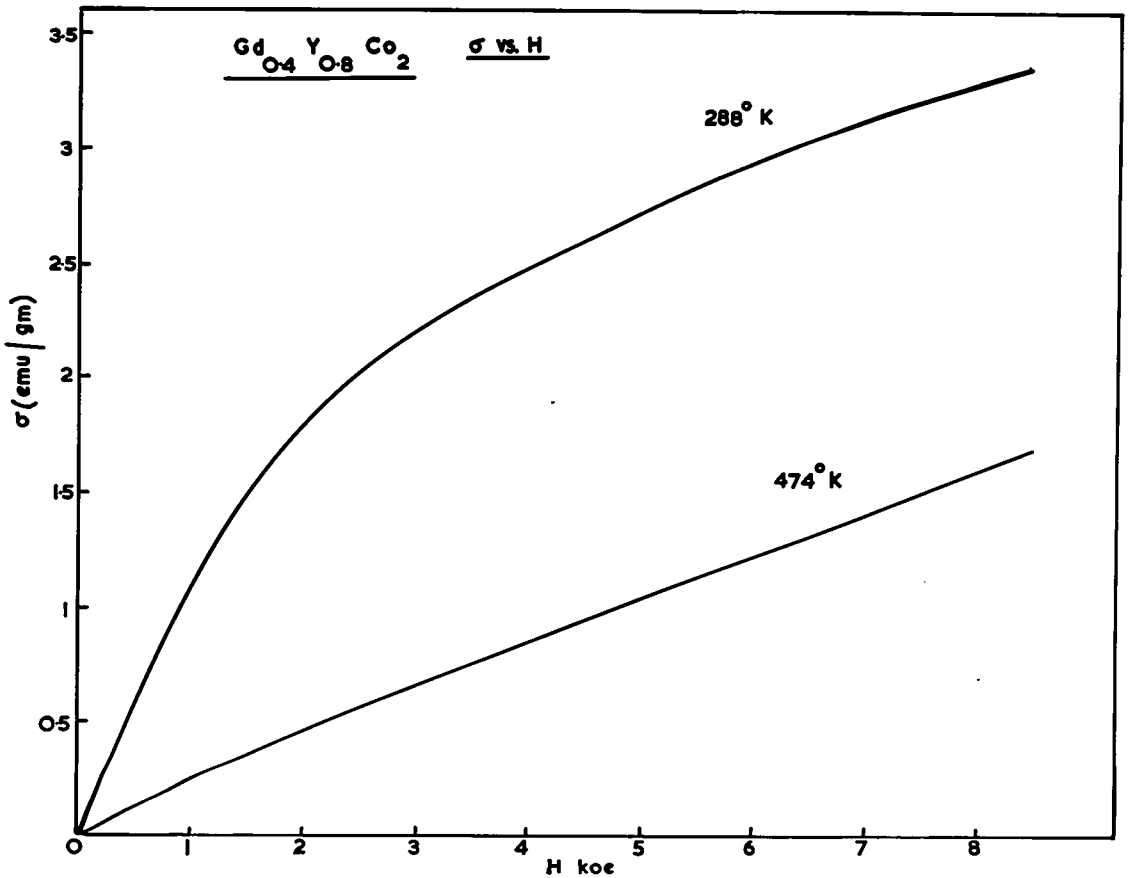
Gd0·4 Y0·8 Co2
σ vs. H
288° K
474° K
σ (emu / gm)
H koe
0
0·5
1
1·5
2
2·5
3
3·5
1
2
3
4
5
6
7
8

FIG. 3.21.

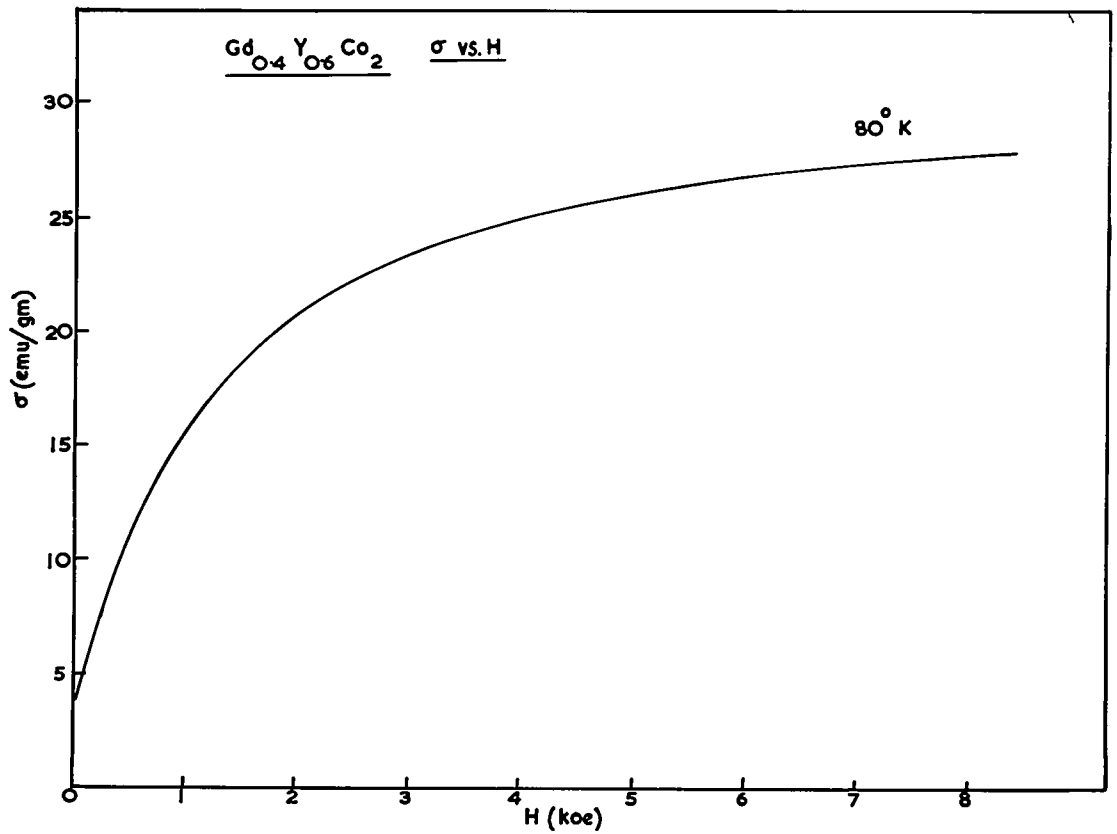

FIG. 3.22.

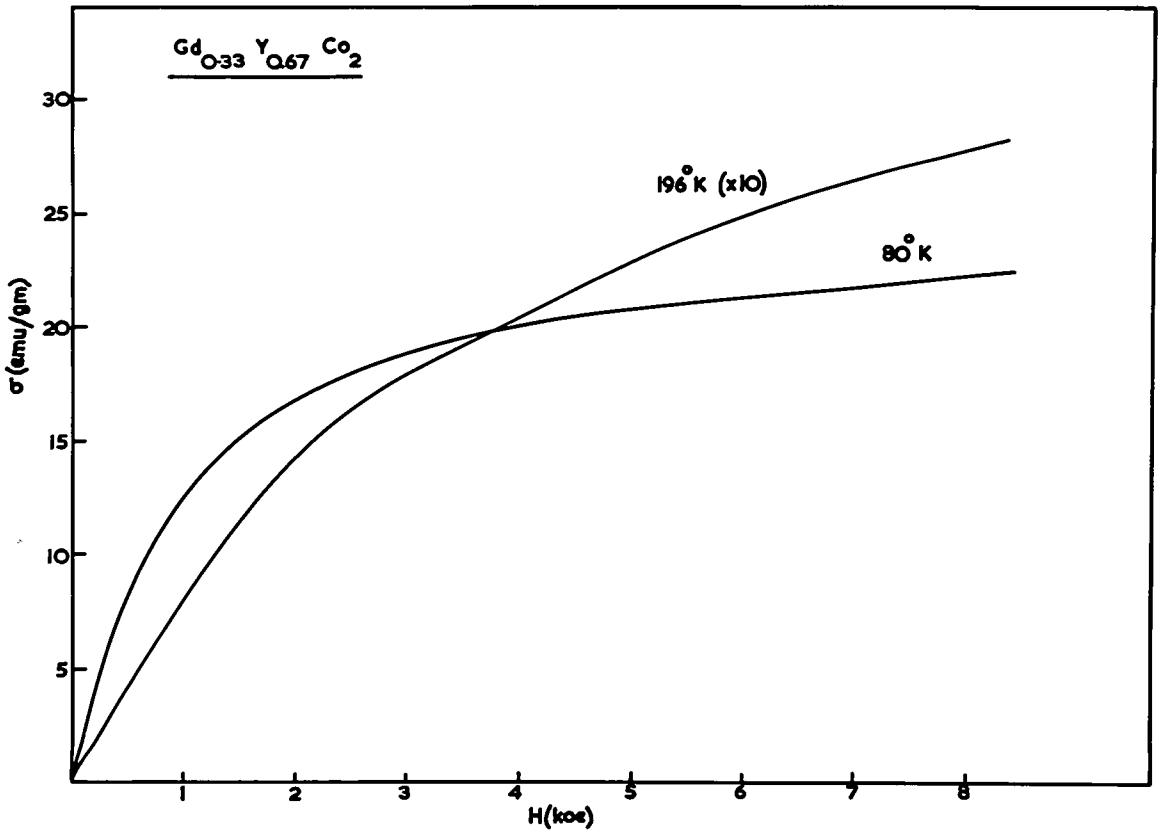
$Gd_{0.33}\ Y_{0.67}\ Co_2$
196°K (x10)
80°K
σ(emu/gm)
30
25
20
15
10
5
1
2
3
4
5
6
7
8
H(koe)

FIG. 3.23.

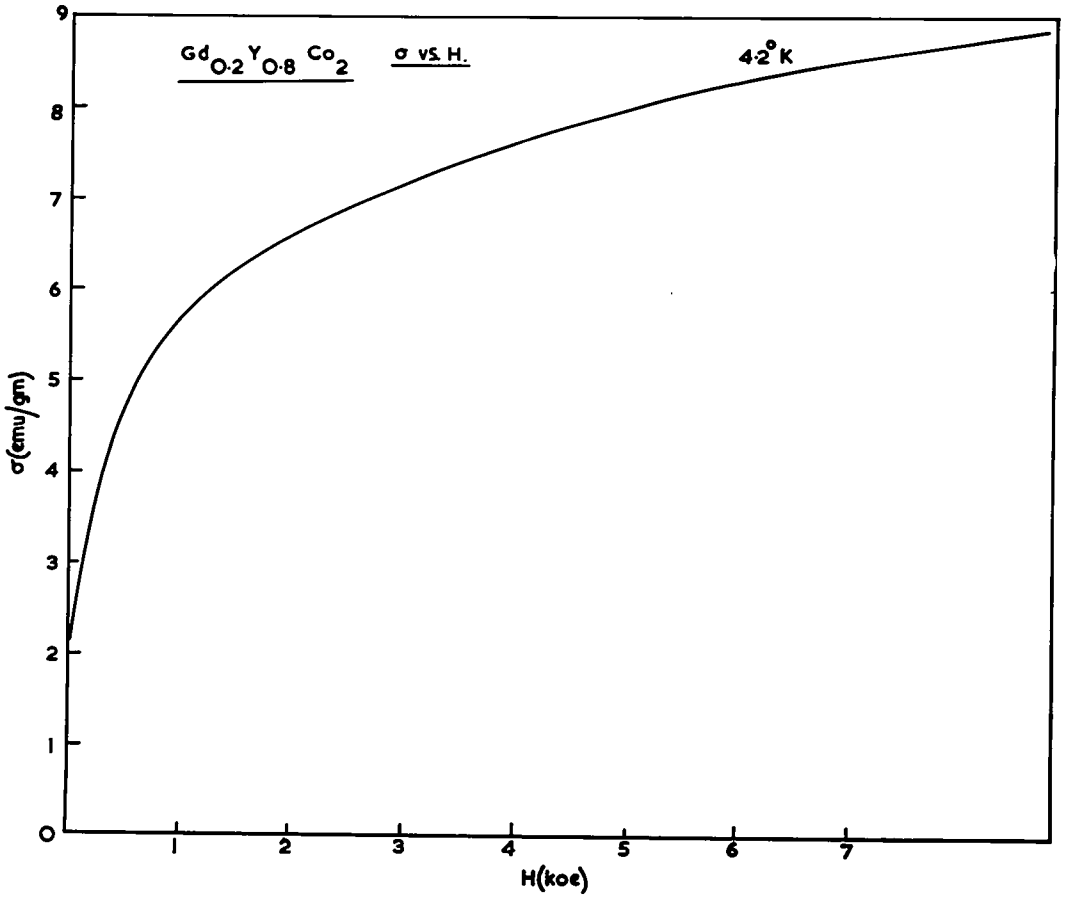

FIG. 3.24

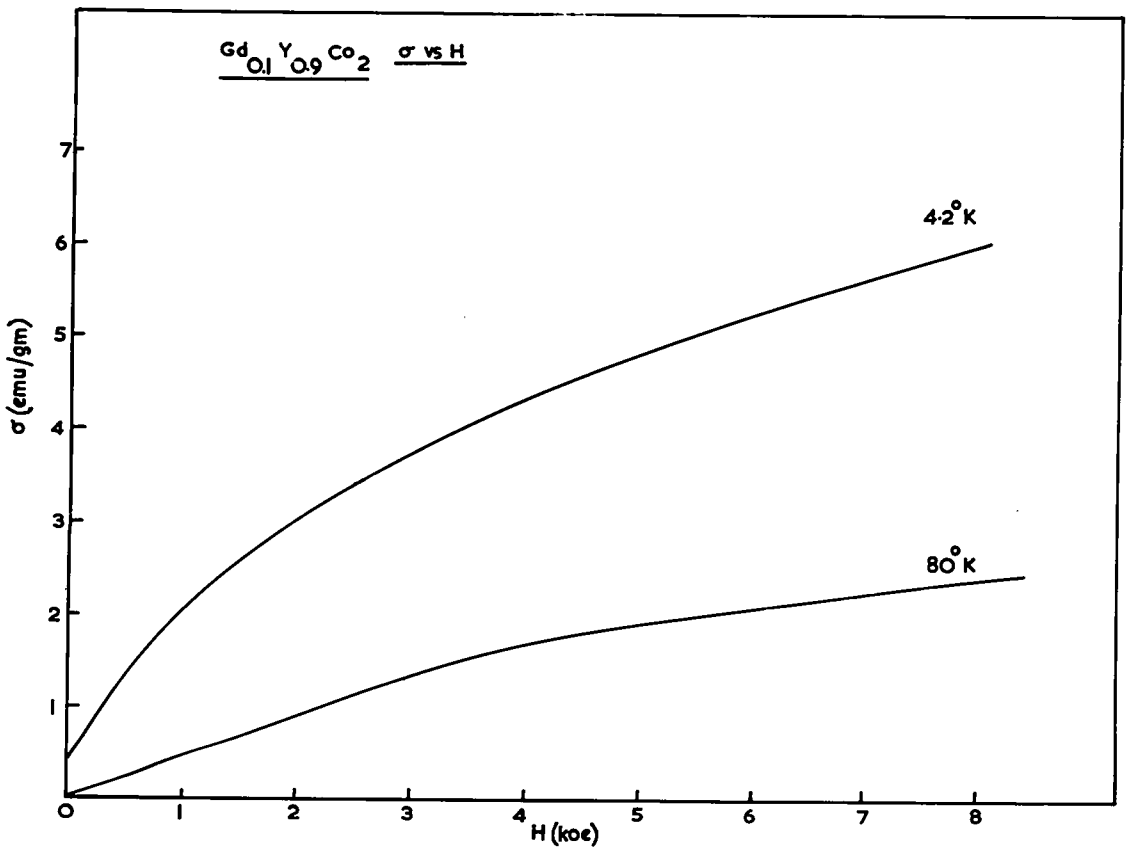

FIG. 3.25.

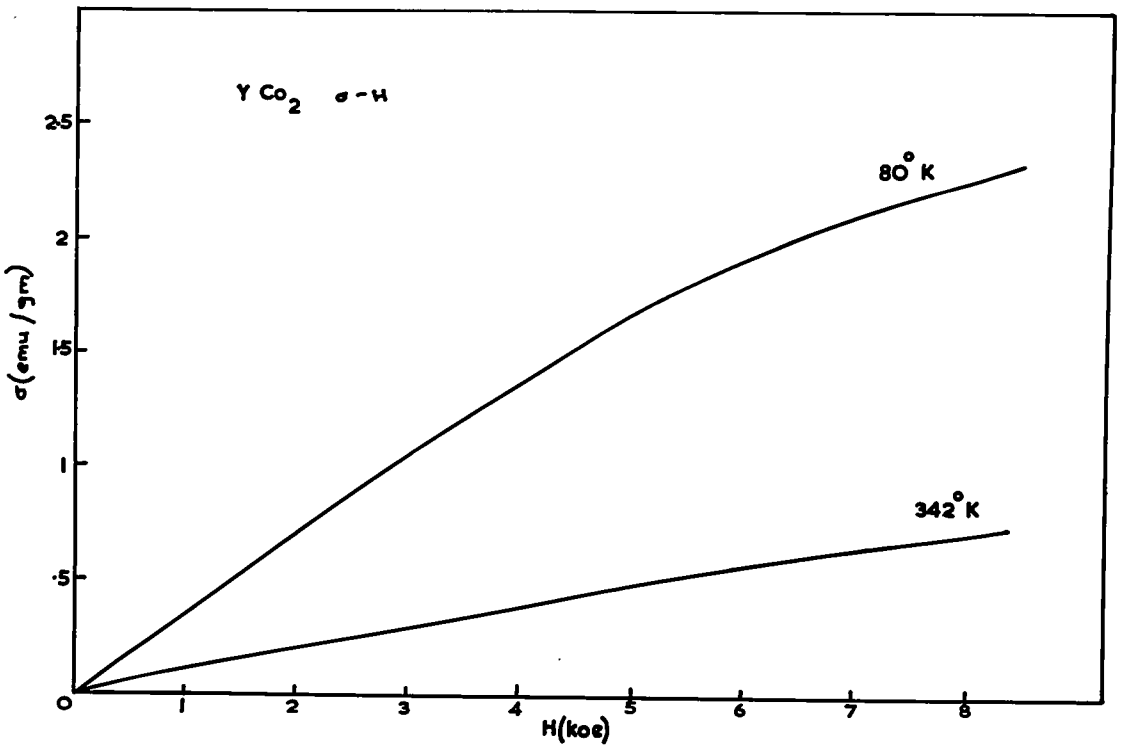

FIG. 3.26.

CHAPTER FOUR

DISCUSSION

CHAPTER 4

DISCUSSION

4.1 Introduction

When this work began, it was thought that in keeping with the early work of Wallace (ref 1.36) and Nesbitt et al (ref 1.33), the magnetic behaviour of these substituted compounds could be understood using a model in which the magnetisation vectors of the gadolinium/yttrium sublattice, and the cobalt sublattice, would be aligned antiparallel, the dominant sublattice being parallel to the applied magnetic field provided that the magnetocrystalline anisotropy is small. It was expected that by diluting the gadolinium sublattice with yttrium, which is a non-magnetic ion, the saturation moment per molecule at absolute zero would vary with yttrium concentration and would pass through a minimum at a composition where the magnetisations of the two sublattices were of equal magnitude. In this way, provided that the individual moments did not change with yttrium concentration, and that the moment on the gadolinium ion could be taken as its free ion value of $7\mu_B$, then the moment on the cobalt ion could be obtained, thus resolving some of the problems raised in Chapter One. Unfortunately, as may readily be seen from figure 4.1 no such minimum is observed, and this rather elementary approach must be drastically modified, if not totally abandoned. In figure 4.1, σ_1 is the observed magnetisation in emu/gm. at an applied field value of 8.4 koe and a temperature of $4.2^{\circ}K$. This value was used in preference to values obtained by extrapolating the linear high field parts of the magnetisation versus field

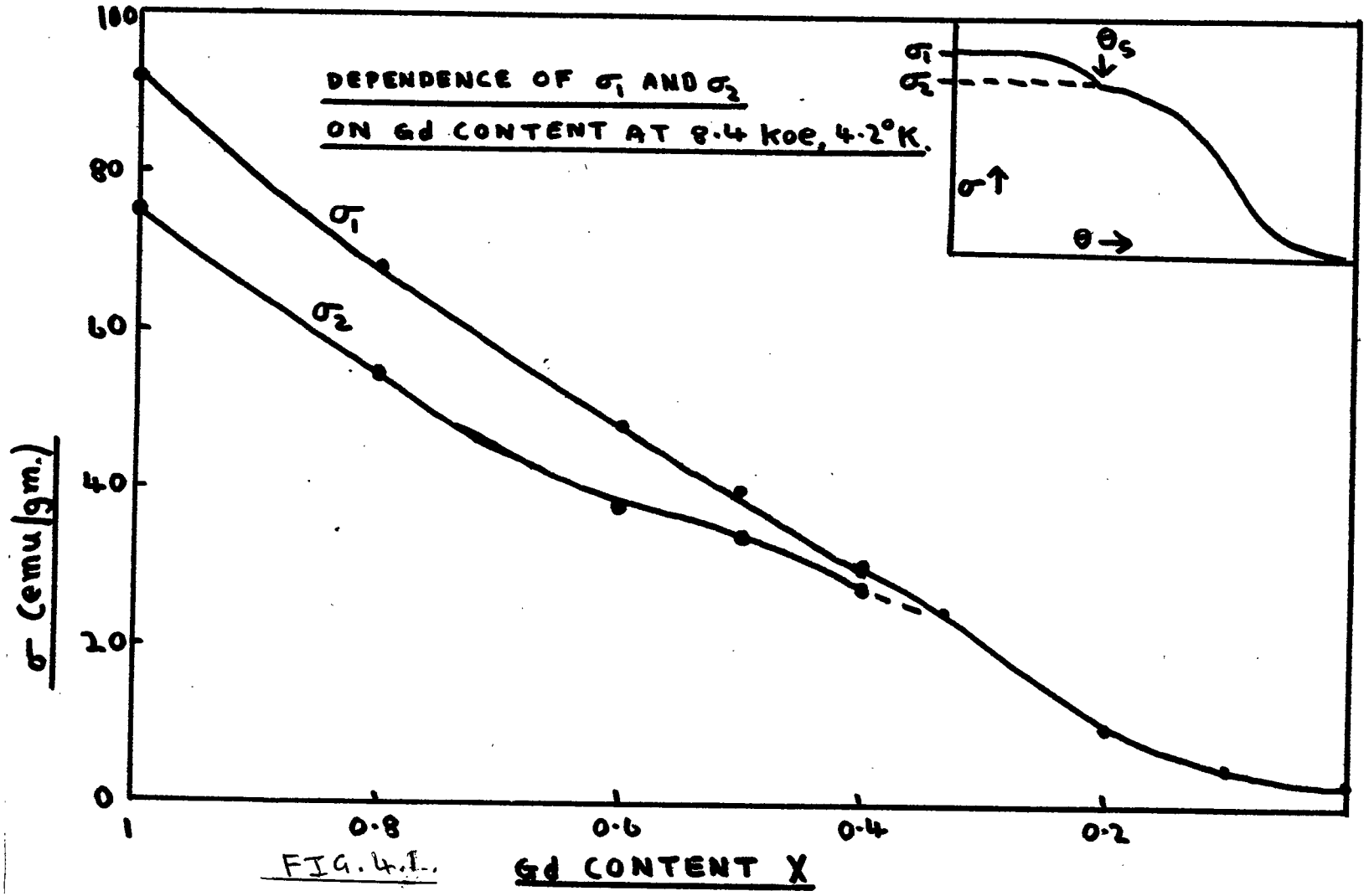
DEPENDENCE OF σ_1 AND σ_2
ON Gd CONTENT AT 8.4 koe, 4.2°K.
σ_1
σ_2
θ_s
$\sigma\uparrow$
$\theta\rightarrow$
100
80
60
40
20
0
σ (emu/gm.)
1
0·8
0·6
0·4
0·2
Gd CONTENT X

FIG. 4.1.

curves at 4.2°K back to H=0, since it was felt that the applied field was not high enough for the curves to approach saturation sufficiently for this method to be used with accuracy. σ_2 is an estimate of the magnetisation which would be observed at 8.4 Koe and 4.2°K if the anomaly did not occur, and is obtained by extrapolating the high temperature portion of the magnetisation versus temperature curves at 8.4 Koe applied field back to θ = 4.2°K. It will be realised, therefore, that values for σ_2 are rather approximate, and have an estimated error of ± 5% on top of the total experimental error on the results as a whole.

We must now look at the results in more detail, so as to identify the questions which must be answered by any model chosen to account for the magnetic behaviour of these compounds.

4.2 Observed Magnetic Behaviour

The temperature variation of magnetisation for those compounds with $X > 0.33$ (ref figs 3.3 to 3.7) is characteristic of the behaviour of RCo_2 and RFe_2 compounds, as was mentioned in Chapter One. The important features of this behaviour are

a) The temperature dependence of the magnetisation is complex, the magnetisation decreasing in two distinct steps as the temperature is raised. The temperature at which the anomalous, low temperature step occurs (θ_s), shown in figure 4.2 as a function of X, appears to be characteristic of the compound involved, as also, of course, is the high temperature step, which represents the vicinity of a Curie point.

FIG. 4.2.

θ_s VS. X DEPENDANCE

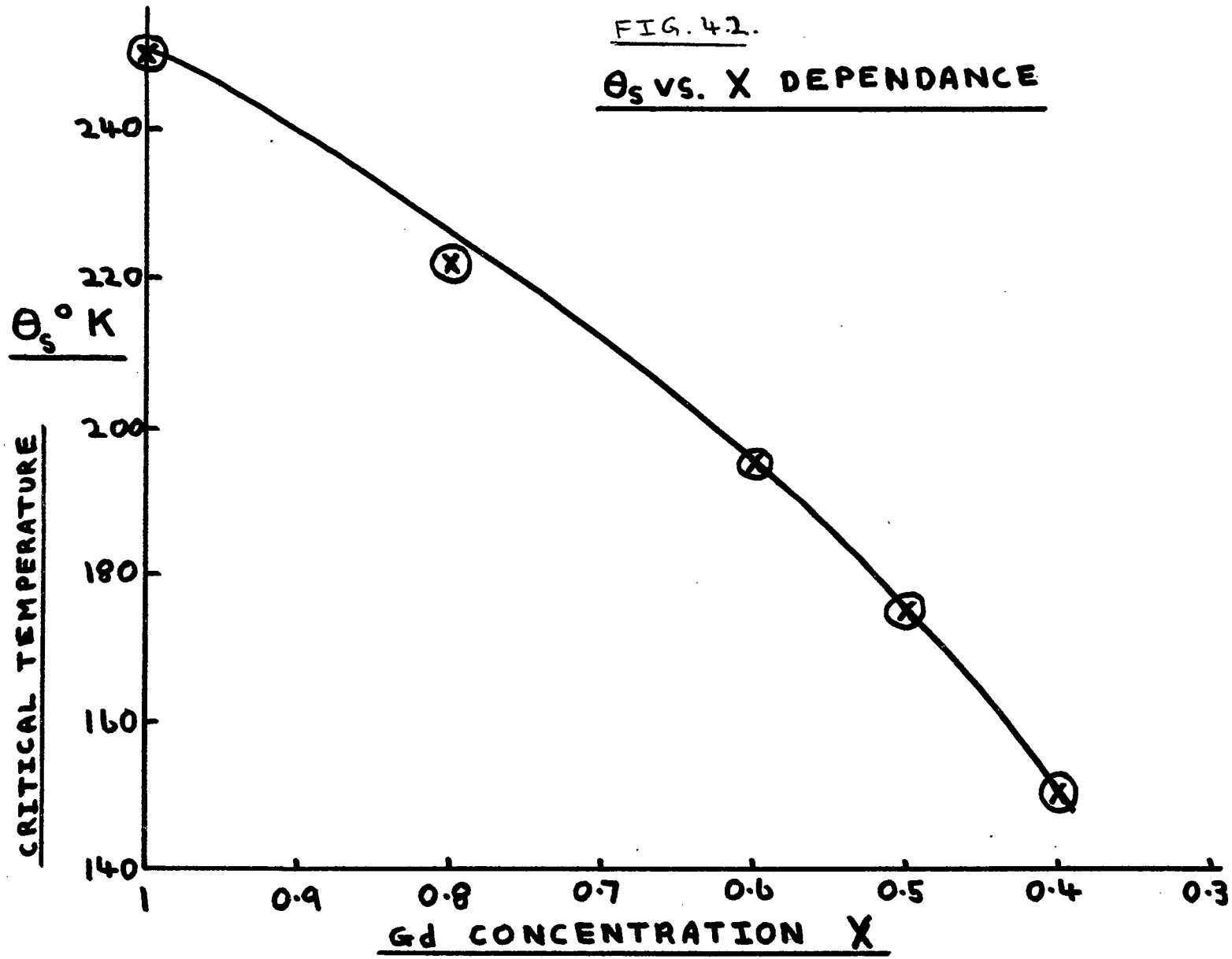

Specimens for which $X < 0.4$ do not show the first of these characteristics, however, and in some cases it is difficult to establish an accurate value for the Curie temperature. For the special case when $X = 0$ (ie YCo_2), the saturation magnetisation is extremely low, and as figure 3.15 shows there is evidence for a Neel point at a temperature of $190^{\circ}K$. It is important at this stage to note that this is in complete contrast to the previously mentioned results of Wallace and Skrabek, who find that YCo_2 is ferromagnetic, with a Curie temperature of $296^{\circ}K$; and of Farrell and Wallace, who find a Curie temperature of $320^{\circ}K$. Figure 4.3 shows the results obtained by the present author for the variation of the paramagnetic Curie points, obtained by extrapolating the high temperature linear portion of the inverse susceptibility versus temperature curve on to the temperature axis, (and the Neel point, in the case of YCo_2), as a function of gadolinium concentration, X.

b) The observation of a low temperature saturation moment whose value is such that it may evidently be taken as evidence for the antiparallel alignment of the two magnetic sublattices.

In attempting to understand the unexpected results it is necessary and convenient at this point to examine in some detail the models proposed

FIG. 4.2

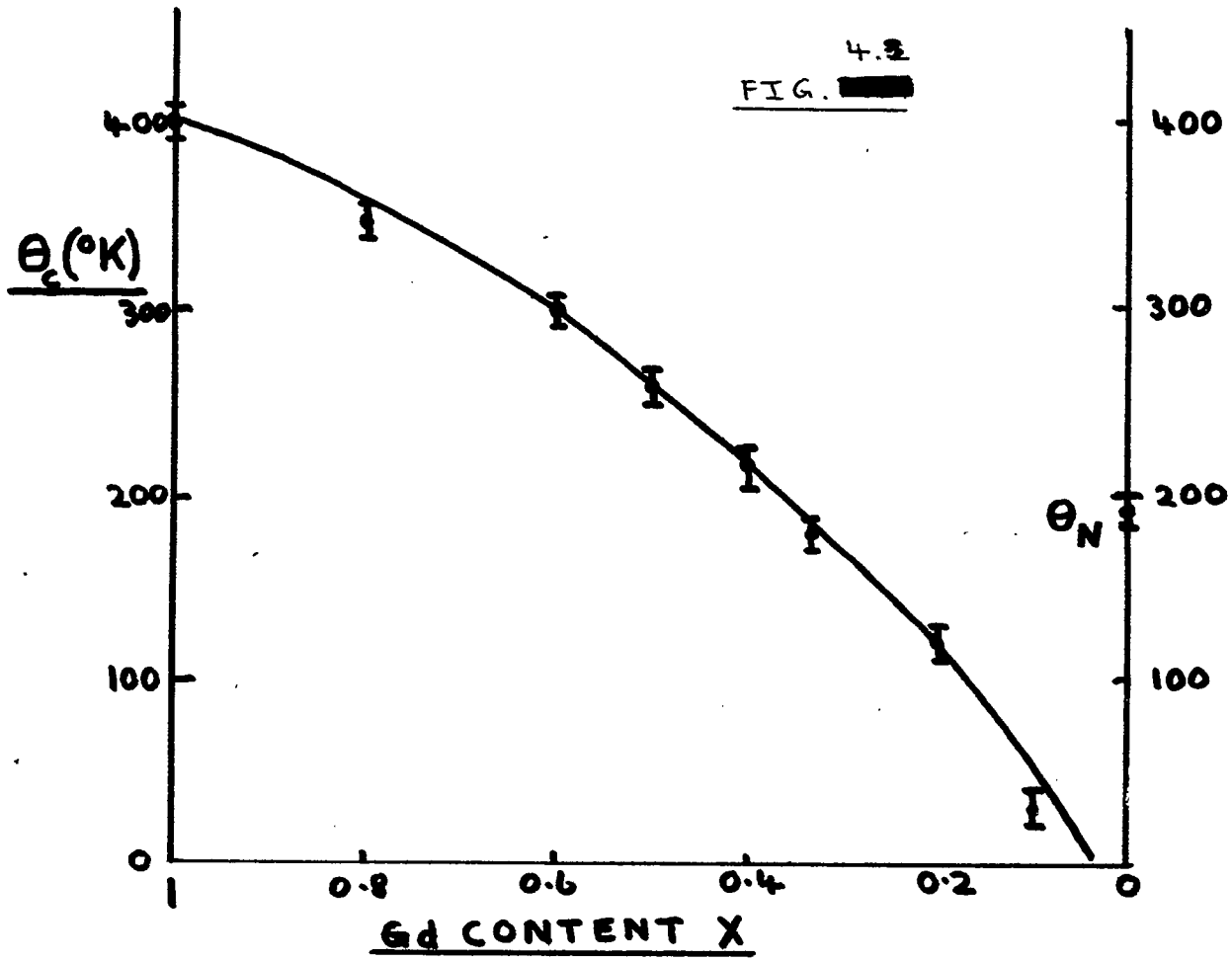

CURIE TEMPERATURE vs. GADOLINIUM CONTENT

in the earlier work with unsubstituted compounds.

4.3 Spin Alignment

From the saturation moment at absolute zero results obtained by the earlier workers for the unsubstituted RCo_2 and RFe_2 compounds, namely Wallace and Skrabek, Crangle and Ross, and Farrell and Wallace, it is clear that the resultant magnetisation of the iron or cobalt sublattice is parallel/antiparallel to the resultant sublattice magnetisation of the light/heavy rare earths respectively. Bearing Hund's rules in mind, it is clear that this simply means that the transition metal magnetisation is always antiparallel to the net spin-only moment of the rare-earth sublattice.

Qualitative confirmation of this model has come from the neutron diffraction studies carried out by Moon et al (ref 4.1) on a few RCo_2 compounds. The electron spin resonance work by Peter (ref 4.2), Jaccarino et al (ref 4.3) involving Gd and $GdAl_2$ has shown that the conduction electrons at the gadolinium ion site have a net spin opposed to the spin vector of the Gd ion. Similar evidence is not available for other lanthanides, but it is usually assumed that their behaviour is similar. This negative polarisation of the conduction electrons has been shown to extend as far as the aluminium site in $GdAl_2$ (ref 4.4). Farrell pointed out that if one assumes that the same situation applies in the RCo_2 compounds, and that the interaction between the conduction electrons and the cobalt moment is ferromagnetic, then the coupling between the cobalt and rare earth will be ferromagnetic in the light rare earths and antiferromagnetic in the heavy rare earths. This is borne out experimentally, so it appears

that a very reasonable qualitative explanation of the magnetic behaviour of the unsubstituted RCo_2 and RFe_2 compounds may be advanced on the basis of an indirect polarisation interaction occurring between the rare earth and transition metal ions. We must now, however, take into account the magnitudes of the moments measured experimentally.

4.4 Values of Magnetic Moment

As was mentioned in Chapter One, considerable doubt exists about the moments carried by both the rare earth and cobalt (or iron) ions in the unsubstituted RCo_2 and RFe_2 compounds. In general, previous views have been that firstly, the moment on the rare earth ion is less than that for the free tripositive lanthanon ion, an effect attributed by Skrabek and Wallace to partial quenching of the moment by the crystal field; secondly, the transition metal moment as was mentioned in Chapter One is appreciably reduced, being zero for all RNi_2, RNi_5 and RNi compounds, varying from approximately Zero in YCo_2 to about $1\mu_B$ in $DyCo_2$, and having a value of about $1.5\mu_B$ in the RFe_2 compounds. Many of these values have been obtained by extrapolating the lanthanon ion moment from its RNi_2 value to either the RCo_2 or RFe_2 compounds, thus allowing an estimate to be made of the magnitude of the transition metal ion moment. The behaviour of the cobalt moment has been attributed by Bleaney (ref 1:34 and 1.42) to the presence of an induced moment proportional to $(g_J-1)\langle J_z\rangle = (g_J-1).\frac{1}{g_J}M_s^1$, where as is discussed below M_s^1 is the maximum moment allowed for the lanthanan ion in a cubic crystal field.

Bleaney examined this crystal field quenching model in some detail

by considering the effect of the twelve nearest neighbour transition metal ions at a distance of $0.4146a_o$, and the four rare earth ions at a distance of $0.433a_o$. The transition metal ions, while not being in a cubic array, do give rise to a cubic potential, while the four lanthanon ions form a regular tetrahedron. Bleaney then calculated the interaction energy of these neighbours with the 4f electrons of the ion under consideration, and worked out the splitting of the energy levels which would result.

The results obtained by Bleaney for the RCo_2 compounds are shown in Table 2, where M_s^1 is the maximum moment allowed for the lanthanon ion in a cubic crystal field where the exchange interaction energy between lanthanon and cobalt ions is large compared with the individual splittings of the low-lying energy states, but is not large compared with the overall splitting. M_s^1 then induces a moment on the transition metal ion through an indirect exchange interaction proportional to $(g_J-1)\frac{M_s^1}{g_J}$. The estimated moment for the transition metal shown in the table is obtained by Bleaney using this expression and scaling from the moment of -2.6 magnetons ascribed to a pair of cobalt ions in $GdCo_2$. The resultant moment is compared with the moments observed by Skrabek and Wallace. As can be seen, agreement between calculated and observed resultant moments is quite good.

The work of Farrell and Wallace (ref 1.39) on the magnetic properties of RNi_2 and RCo_2 compounds tends to discount Bleaney's crystal field effect explanation for these compounds. If Bleaney's estimates of the strength of the crystal field are correct, there ought to be significant departures at low temperatures from the Curie-Weiss behaviour exhibited by the com-

COMPOUND	"MAXIMUM MOMENT" (LANTHANON) M's	ESTIMATED MOMENT FOR Co_2	RESULTANT MOMENT	OBSERVED MOMENT
Pr Co_2	2.07	+0.39	2.5	2.48
Nd Co_2	3.25	+0.90	4.1	3.46
Sm Co_2	0.71	+1.33	2.0	1.26
Gd Co_2	7.0	−2.6	4.4	4.31
Tb Co_2	5.62	−1.4	4.2	4.38
Dy Co_2	8.02	−1.5	6.5	6.72
Ho Co_2	10	−1.5	8.5	7.19
Er Co_2	6.07	−0.77	5.3	5.87
Tm Co_2	4.37	−0.46	3.9	3.96

TABLE 2. SHOWING MOMENTS CALCULATED BY BLEANEY FOR RCo_2 COMPOUNDS USING A CRYSTAL FIELD APPROACH.

pounds. Farrell and Wallace set out to detect any such deviations. Their results tend to show that in the RNi_2 compounds the nickel carries no moment, although the ferromagnetic moments of the compounds are well below the moments of the respective free tripositive rare earth ions.

All of the RNi_2 compounds, except $SmNi_2$ and the Pauli paramagnets $CeNi_2$ and YNi_2 follow the Curie-Weiss law, and exhibit effective magnetic moments, in the paramagnetic region, which agree well with the free ion values. The anomalous behaviour of $SmNi_2$ is ascribed by Farrell and Wallace to a contribution from the first excited state of tripositive samarium, with $J = 7/2$. The authors observe no departure from Curie-Weiss behaviour in those RNi_2 compounds, namely $PrNi_2$ and $TmNi_2$, which from Bleaney's calculations might be expected to show the largest deviations. For example, a deviation of 70% from the Curie-Weiss law is predicted for $PrNi_2$ at $15^{\circ}K$, whereas the measured deviation is zero. The authors state that the crystal field interaction in the RNi_2 compounds is much weaker than anticipated by Bleaney, and is without effect in the paramagnetic regions above $15^{\circ}K$. Their results show an appreciable quenching at $4.2^{\circ}K$, however, and they conclude that the onset of quenching must take place between $4.2^{\circ}K$ and $15^{\circ}K$. They do not consider the possibility that some entirely different mechanism may be the cause of the low moments in the ferromagnetic region.

Farrell and Wallace explain the results they obtain for the RCo_2 compounds of the heavy rare earth by assigning the full moment of the free tripositive ion to the rare earth component, and say that this is aligned antiparallel to cobalt moments of about $1\mu_B$ per cobalt atom. This inter-

pretation is in good agreement with the neutron diffraction results published by Moon et al (ref 4.1), and is consistent with an indirect exchange interaction, via the conduction electrons in the materials. The authors explain the fact that the rare earth moments in the RCo_2 compounds are higher than those in the RNi_2 compounds by concluding that the crystal field quenching is much smaller in the RCo_2 compounds. This is said to be due in part to a strengthening of the molecular fields, resulting in a more complete mixture of crystal field states, caused basically by the presence of localised moments at the cobalt sites. In addition to this effect, the interatomic distances in the RCo_2 compounds are greater than in the RNi_2, and this, taken in conjunction with the shielded Coulomb potential created by the conductivity of the materials, might greatly diminish the effect of the crystal field on the orbital moments of the rare earth ions.

From the results of Farrell and Wallace, it seems reasonable to say that their work suggests that the treatment of Bleaney can, at best, give no more than a small correction term to the final lanthanide moment in the cobalt compounds. However, the problem of the magnitude of the moment carried by the Co ion itself is still open to question. The experimental values obtained by neutron diffraction are probably no more accurate than $\pm 0.2\mu_B$, and hence the proposal of Wallace and his coworkers concerning electron transfer from the lanthanon to the cobalt ion, thus reducing the moment on the latter by $\sim 0.5\mu_B$ must remain open to doubt.

In the series of compounds which we have examined both the gadolinium and yttrium ions are S state ions (no orbital moment), and consequently the

quenching model is not applicable. It is therefore reasonable to assume that the saturation moment per ion on the Gd/Y sublattice may be taken to decrease linearly from $\sim 7\mu_B$ at $GdCo_2$ to zero at YCo_2. The unknown behaviour of the cobalt sublattice is then the predominant factor in examining any model to account for their behaviour.

4.5 Canted Spin Arrangements

If one adopts the Yafet, Kittel and Lotgering (YKL) (ref 1.40 and 4.5) theory of triangular spin arrangements mentioned in Chapter One, magnetisation versus temperature curves of the type shown in this thesis for $X > 0.33$ are to be expected for a spin system in which a triangular arrangement of moments as shown in figure 4.4 exists as a ground state at low temperatures, and changes to an antiparallel arrangement above some characteristic temperature θ_s. However, the field dependence of $\frac{\sigma_1 - \sigma_2}{\sigma_1}$ shown in figure 4.5 for $Gd_{0.6}Y_{0.4}Co_2$ indicates that at zero applied field there is no anomalous step in the magnetisation versus temperature curve, and therefore an antiparallel spin arrangement exists down to zero temperature when the applied field is below a critical value. It appears, then, that if a triangular state is to occur at all it must be induced by the external field, and will be favoured by an antiferromagnetic coupling between the two cobalt sublattices. That such a coup ling does in fact exist is suggested by the magnetisation versus temperature results for YCo_2 (ref Fig 3.15), which shows a very definite maximum in magnetisation at $190^{\circ}K$. It must be remembered, however, that this is the only measurement which does show YCo_2 as being antiferromagnetic, so that it would be wise to treat it with some reserve.

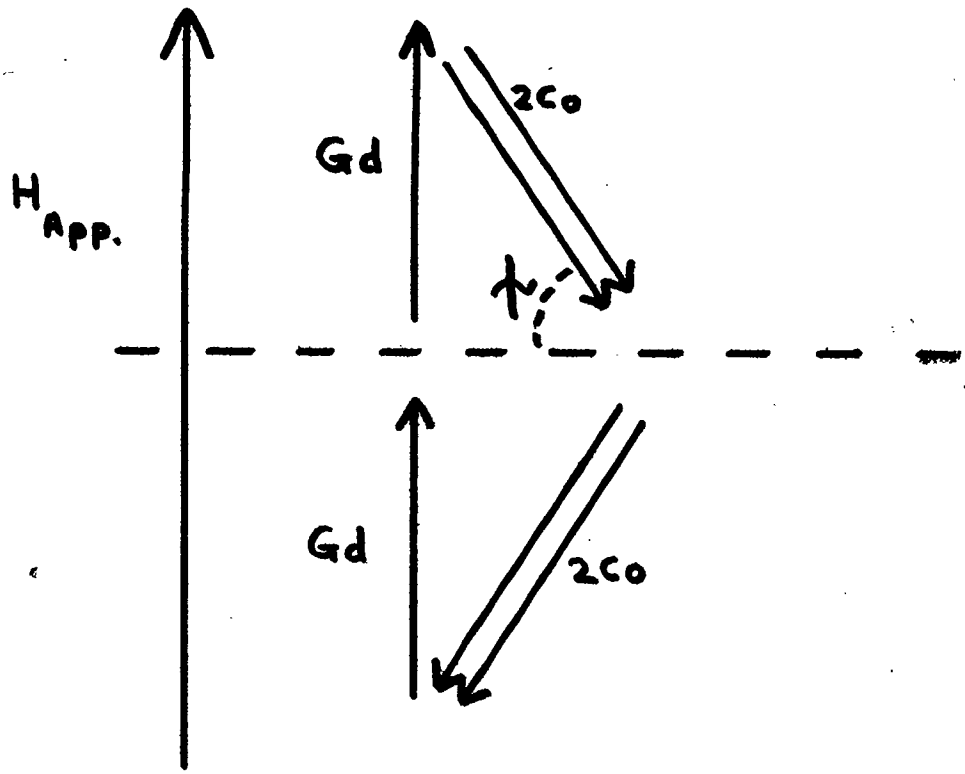

FIG. 4.4.

TRIANGULAR SPIN ARRANGEMENT.

FIG. 4.5

DATA TAKEN FROM

$Gd_{0.6}Y_{0.4}Co_2$ AT 80°K

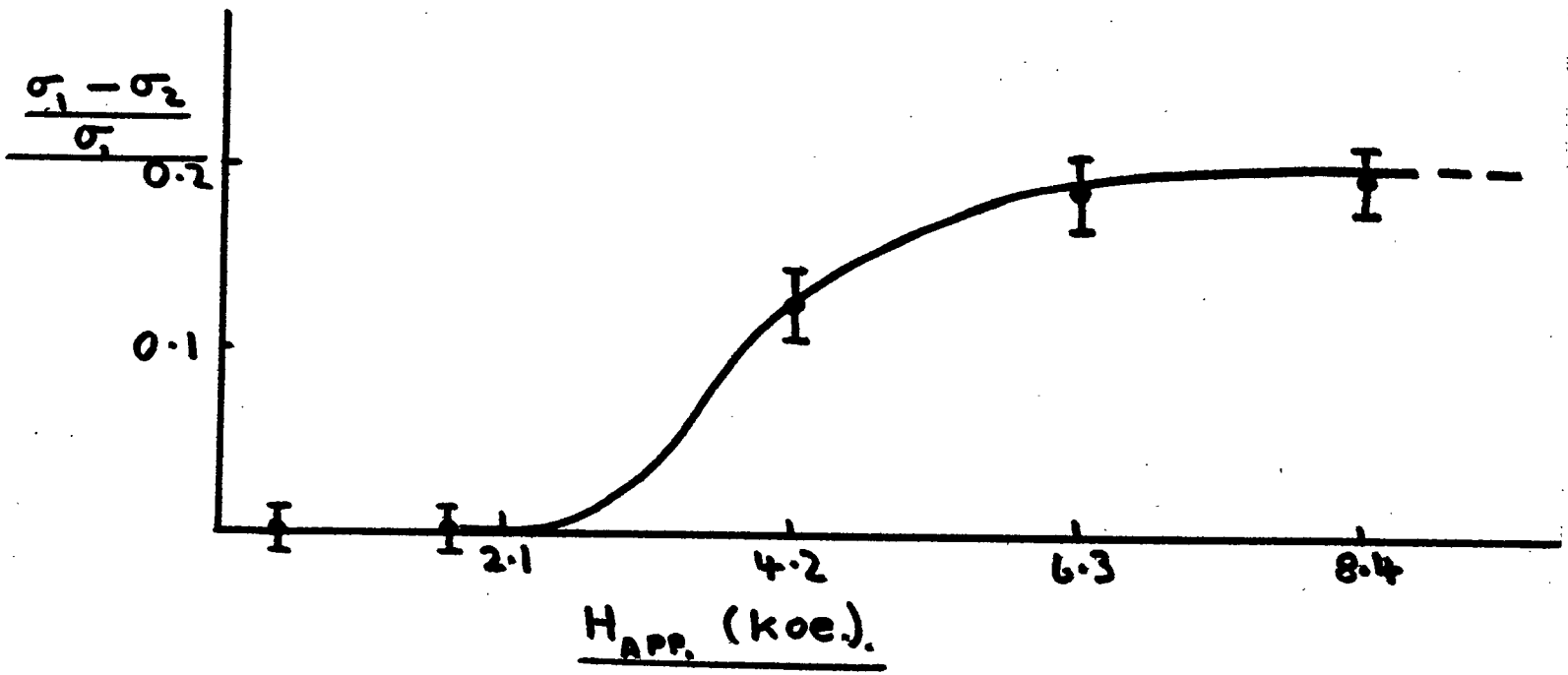

That a critical field (H_c), above which a triangular spin arrangement is stable, can exist may be shown by writing down the expression for the internal field at a cobalt site (say the Co_1 site,) the cobalt being divided into two sublattices:

$$\underline{h}_{B1} = -n\left[-\tfrac{1}{2}\beta\underline{b}_1 + \underline{A} + \beta\underline{B}\right] + \underline{H} \quad \text{---} \quad (1)$$

where $\underline{h}_{B1}$ is the field at the Co_1 site

n is the molecular field coefficient for the Gd-Co interaction

$n\beta$ is the molecular field coefficient for the Co-Co interaction

$\underline{b}_1$ is the magnetisation vector of the Co_1 sublattice

$\underline{H}$ is the applied magnetic field

$\underline{A} = \Sigma \underline{a}_i$ = resultant magnetisation of the lanthanon sublattice

$\underline{B} = \Sigma \underline{b}_i$ = resultant magnetisation of B_1 and B_2 (transition metal) sublattices

$\underline{h}_{B1}$ must be parallel to $\underline{b}_1$, and therefore $-\underline{A} + \beta\underline{B} + \underline{H}$ must be either parallel or antiparallel to $\underline{b}_1$. Similarly, if we write down the equation for the internal field on the second Co sublattice

$$\underline{h}_{B2} = -n\left[-\tfrac{1}{2}\beta\underline{b}_2 + \underline{A} + \beta\underline{B}\right] + \underline{H} \quad \text{---} \quad (2)$$

it follows that $\underline{h}_{B2}$ must be parallel to $\underline{b}_2$, and therefore $-\underline{A} + \beta\underline{B} + \underline{H}$ must be either parallel or antiparallel to $\underline{b}_2$. Thus, when $\underline{b}_1$ and $\underline{b}_2$ are not parallel, then $-n\underline{A} - n\beta\underline{B} + \underline{H} = 0$ .. .. (3)

If we use the notation shown in figure 4.4, where $\phi = 90^\circ$ represents the case of antiparallel alignment, then

$$\underline{B} = -4b \sin\phi$$

and $\underline{A} = 2a$

so that in scalar form, equation (3) becomes

$$-2na + 4n\beta b \sin\phi + H = 0$$

and therefore $\sin\phi = \frac{2a - H/n}{4\beta b}$ - - - - (4)

Since we have already built in a situation where there is non-alignment of the two cobalt sublattices, then $\sin\phi < 1$.

Thus the critical field, H_c, will be given by

$$\frac{2na - H_c}{4n\beta b} = 1$$

and therefore $H_c = 2n\ (a - 2\beta b)$ .. .. (5)

This solution bears all the qualitative properties observed in the behaviour of the compounds. For example from equation (4), as H increases $\sin\phi$ decreases, therefore experimentally, σ_1 increases, as is observed experimentally. This solution also theoretically predicts the existence of a critical field, which is observed experimentally in figure 4.5. As the applied field H is increased, $\sin\phi$ must decrease, and therefore $\frac{\sigma_1 - \sigma_2}{\sigma_1}$ must increase, as is observed experimentally (ref fig 4.5). At even higher fields one would expect $\sin\phi = 0$ (at a field $H = 2na$), at which point the magnetic moment in the direction of the applied field should be that of the free lanthanide moment. It is interesting that, for $GdCo_2$, the value of σ_2 corresponds to $3.8\mu_B$ per molecule at 8.4 Koe, which is the value to be expected for a straightforward antiparallel spin arrangement, with the

cobalt and gadolinium ions carrying the full value of their moment. The observed magnetisation for $GdCo_2$ (σ_1) corresponds to a moment of $4.8\mu_B$, which would be the moment observed for a triangular spin arrangement in which ψ was approximately 45°, all ions carrying their full moment.

It is also of interest to note that θ_s is not dependent upon the strength of the applied magnetic field, for any given compound. One might expect that the value of θ_s would increase with increasing magnetic field. One possible explanation is that any one compound is in fact a mixture of compounds, and that θ_s is the Curie temperature of one compound which has a very high saturation magnetisation (giving the strong field dependence), so that the observed curve is actually the addition of the magnetisation curves of two or more separate compounds. This is unlikely, however, since firstly, X-ray analysis of the compounds, though showing slight traces of cobalt and gadolinium, shows no traces of other simple compounds. Secondly, θ_s is strongly dependent on X, which means that for this proposition to be true, each specimen must contain at least one compound which is not contained in any other specimen.

It is convenient at this point to note that one other possible explanation is that θ_s is actually the Curie temperature of a Gd-Gd exchange interaction. It is of interest to note that there appears to be a relationship between θ_s and X of the form $\theta_s \simeq KX^{\frac{1}{2}}$, where K is a constant. It follows that the kink temperature is proportional to $d^{-3/2}$, where d is the average distance between gadolinium atoms. If we assume that thermal energy $= k\theta$, we arrive at the conclusion that the energy of exchange between the

gadolinium atoms in these compounds is proportional to $d^{-\frac{3}{2}}$.

4.5.1 Magnetic Moment Determination

It is possible to obtain an expression using the YKL approach for the magnetic moment at absolute zero in the following manner. The observed magnetisation at absolute zero, σ_1, may be written as

$$\sigma_1 = M_A - 2M_B \sin\psi$$

where M_A and M_B are the scalar magnetisations of the rare earth and cobalt sublattices respectively.

Then

$$\sigma_1 = M_A - 2M_B\left(\frac{2a - H/n}{4\beta b}\right)$$

$$= M_A - 4b\left(\frac{M_A - H/n}{4\beta b}\right)$$

since $M_A = 2a$ and $M_B = 4b$, in scalar quantities.

Therefore

$$\sigma_1 = M_A\left(1 - \frac{1}{\beta}\right) + \frac{H}{n\beta}$$

Hence the observed magnetic moment per molecule (m_o) is given by

$$m_o = 2j_A\left(1 - \frac{1}{\beta}\right) + \frac{H}{n\beta}$$

where j_A is the effective number of Bohr magnetons associated with the gadolinium ion, taking into account the concentration of Gd in any given compound. Since both m_o and H_c can be obtained for those compounds, where $X > 0.33$, it is possible to evaluate n and β. In the case of $X = 0.6$, the results give $n \simeq 1500$, and $\beta \simeq 0.5$. It must be emphasised that these figures can only be taken as an order of magnitude calculation, because

of the large possible errors involved. However the value of H_c obtained by substituting numbers for n and β in equation 5 certainly give something like the right order of magnitudes.

It appears that the theory of triangular spin configurations, as proposed by Yafet and Kittel (ref 4.5) and Lotgering (ref 1.40) provides a very reasonable explanation for the magnetic phenomena observed in the $Gd_xY_{1-x}Co_2$ compounds. Moon et al (ref 4.1) have however found no trace of triangular spin configurations in the unsubstituted RCo_2 compounds in their neutron diffraction work. This is not, of course, surprising, since it has been shown in this thesis that such a configuration is only set up if the applied magnetic field is above a certain level. There is no evidence to indicate that the neutron diffraction measurements carried out on the RCo_2 compounds involved the application of an external magnetic field to the specimens under investigations.

4.6 Collective Electron Theory

In a paper yet to be published, Piercy and Taylor (ref 4.6) discuss the results they obtain for the compounds $Dy_xY_{1-x}Fe_2$ in terms of a collective electron model for the s-d electrons associated with the iron ion. Their results show that a minimum occurs in the infinite field, 0^oK magnetic moment per molecule versus dysprosium concentration curve at a value for X of approximately 0.28. The coercivity also has a maximum value in this region, and has a value in excess of 10 Koe at X = 0.35 at 4.2^oK. Piercy and Taylor show that the iron moment must change in a non-linear manner through the series. They suggest that a collective electron model readily explains the required variation of the iron moment, which must have

a constant value of about 1.4 μ_B for $0.3 > X > 0$, and then increases more or less linearly to a value of about 2.2 μ_B at $X = 1$. They suggest that the constant iron moment at low X values occurs because the Fermi level is locked at a minimum of the density of states curve. With increasing dysprosium concentration the exchange energy increases, and causes the Fermi level to move through the minimum, so that the iron moment increases. The results which they obtain respond quite well to this treatment, as do previously published results on RFe_2 compounds. This would suggest that the results presented in this thesis for the $Gd_xY_{1-x}Co_2$ compounds might respond well to a similar model, but such a model must await the development of a theoretical treatment of the exchange between the localised rare earth moment and the collective electron transition metal moment.

For any such model to work, however, there must be an exchange interaction in the materials between the lanthanon and the cobalt electrons. Consequently, any splitting of the cobalt Fermi levels must be proportional to the strength of the exchange interaction, which in turn is proportional to the Curie temperature. Thus, the magnetic moment of the cobalt in these compounds must be dependent upon the Curie temperature, and figure 4.6 shows μ_{Co}, the estimated magnetic moment of the cobalt at $0^{\circ}K$, plotted against the paramagnetic Curie temperature.

I am indebted to Messrs. Piercy and Taylor for bringing their work to my notice prior to publication.

4.7 Recent Publication

Since the completion of this work, Lemaire and Schweizer (ref 4.7) have published their magnetic measurements on $Gd_xY_{1-x}Co_2$ compounds. Their

FIG. 4.6. MAGNETIC MOMENT OF COBALT AT 0°K VERSUS CURIE TEMPERATURE.

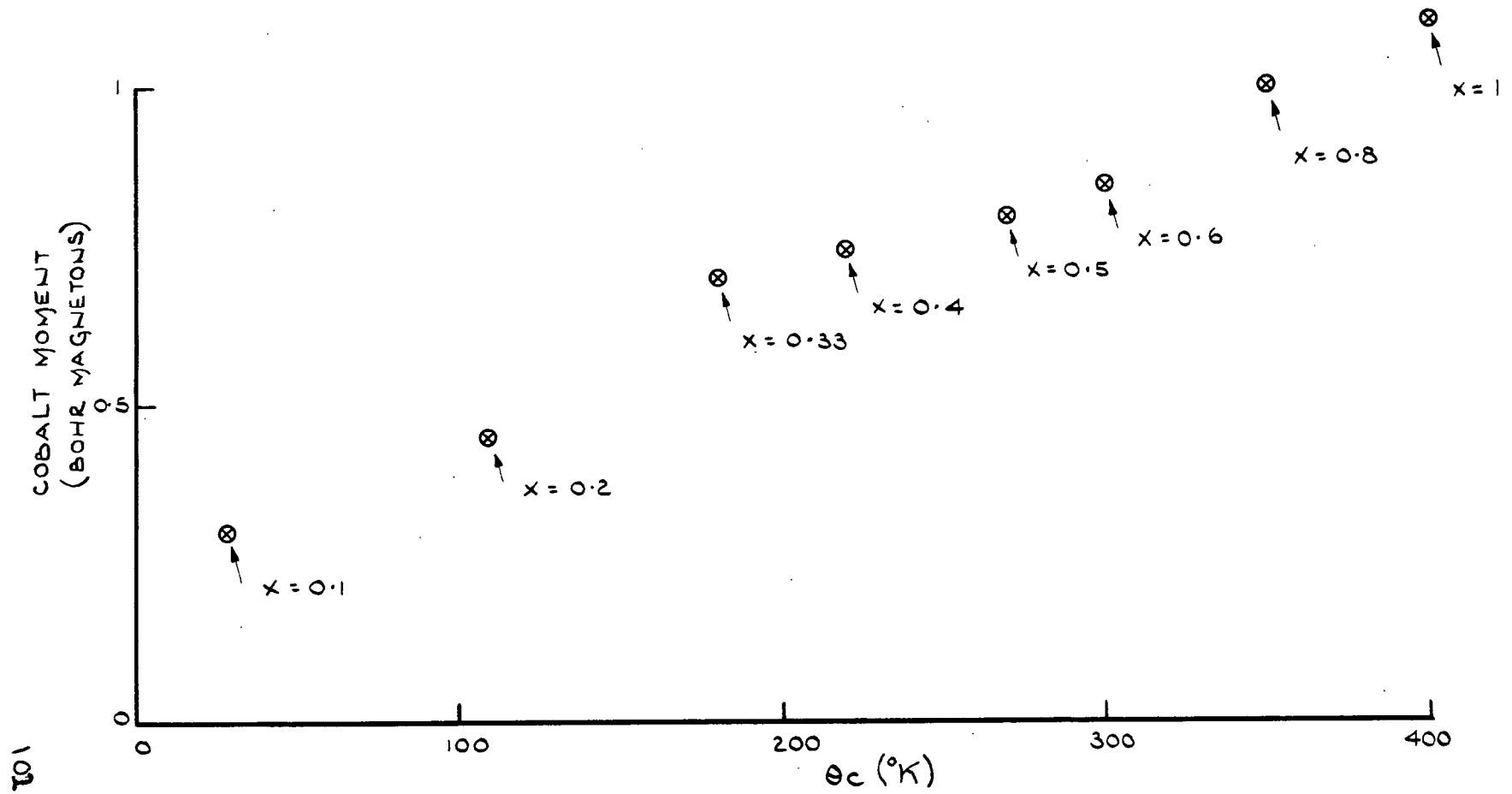

101

results show that YCo_2 is paramagnetic, and this might suggest that not only the antiferromagnetism of YCo_2 reported in this thesis, but also the anomaly in the magnetisation versus temperature curves may be due to the presence of gadolinium or cobalt metal particles as an impurity, or possibly that the effect is enhanced by impurities. Since the results agree so closely at $0^{o}K$, however, it is surprising that the effect appears to be to lower the magnetisation temporarily at θ_s, the effect disappearing quite quickly at either side of this temperature.

Lemaire and Schweizer's results do show the presence of an anomaly in the high gadolinium concentration alloys, however, but they are much less noticeable than in the present work. The presence of the anomaly is amply borne out by the previously mentioned results of Ross and Crangle and Farrell and Wallace, however, so there is little doubt that it does in fact exist.

Lemaire and Schweizer conclude that the magnetic structure of the $Gd_xY_{1-x}Co_2$ compounds is one of antiparallel alignment between the gadolinium and cobalt moments, and that the cobalt moment values depend on the strength of the interaction with the gadolinium moments, and on the concentration of gadolinium.

Though Lemaire and Schweizer's results tend to show that the cobalt moment is reduced in these compounds, it must be pointed out that this reduction would not of itself preclude the existence of triangular spin configurations, with a smaller deviation from true antiparallelism.

CHAPTER FIVE

SUMMARY

CHAPTER 5

SUMMARY

The magnetic properties of the substituted compounds of the form $Gd_xY_{1-x}Co_2$ have been shown in this thesis to have an anomalous feature, which takes the form of a kink in the magnetisation versus temperature graphs, at least for those compounds for which X is greater than 0.33. The results have been examined in the light of models which have been proposed by previous workers to explain the magnetic properties of similar unsubstituted compounds. A model due to Bleaney which takes into account the effects of crystal fields on the orbital moments of the lanthanide ions has been shown to have, in all probability, little effect on the moments of these compounds. Secondly, a model due to Piercy and Taylor which suggests that the magnetic phenomena observed in this type of compound might be explained in terms of an exchange between the lanthanon moment and a collective electron band of the cobalt has been briefly mentioned. Though this model has not been applied as yet to these compounds, it seems possible that such a theory might explain the observed phenomena.

The final model, adapted from work by Yafet, Kittel and Lotgering, seems to provide a very reasonable basis for explaining all the magnetic properties of these compounds presented in this thesis, including:

a) The decrease of low temperature magnetic moment with decreasing gadolinium content.

b) The presence of a kink anomaly in the magnetisation versus temperature curves for those compounds with $X > 0.33$.

c) The fact that the kink anomaly only occurs when the applied field is above a certain critical value.

d) The antiferromagnetic behaviour of YCo_2.

This model (YKL model) predicts a ferrimagnetic behaviour from the ordering temperature down to a characteristic critical temperature, followed by the setting up of a triangular spin arrangement, provided the applied field is above a critical value, in which the moment of the gadolinium sublattice is parallel to the applied field, and two cobalt sublattices are antiparallel, but tilted at an angle, thus forming a triangular arrangement.

The resolution of the arrangement of the moments in the RCo_2 and RFe_2 compounds, as well as the arrangements in the $Gd_xY_{1-x}Co_2$ compounds, must await future work, which should follow three main lines of inquiry. Firstly, high field measurements should be carried out to obtain a more nearly true saturation. Secondly, neutron diffraction work involving the application of variable magnetic fields to the single crystals should be carried out to determine the spin arrangements. Finally, single crystal magnetic measurements must be carried out to determine the anisotropy constants of these materials.

No mention has been made in this work of the apparent anomalies which exist in the elevated temperature regions of the magnetisation versus temperature curves, at low magnetisation values, since it is felt that these anomalies are almost certainly due to the presence of impurities, and as such, should be totally disregarded.

ACKNOWLEDGEMENTS.

I would like to express my grateful thanks to Professor G. D. Rochester, head of the Physics Department, to my supervisor, Dr. K. N. R. Taylor, and to the workshop and other staff of the Physics Department, Durham University, for their help to me during my three years of research work at Durham. Thanks are especially due to Dr. Taylor and Mr. Piercy, of Durham, for bringing to my notice their work on $Dy_x Y_{1-x} Fe_2$ compounds.

I am grateful to Dr. J. Crangle, of the Physics Department, Sheffield University, not only for making available to me an argon arc furnace, but for preparing the specimens used in this work.

Mrs. H. Chapman and Mrs. E. Cleminson typed the script of this work, for which I am extremely grateful.

This work was carried out during my tenure of a research grant from the Department of Scientific and Industrial Research, as it then was.

REFERENCES

1.1 Hund, Z. Physik, 33, 855, (1925)

1.2 Van Vleck and Frank, Phys. Rev. 34, 1494, 1625, (1929)

1.3 Ruderman and Kittel, Phys. Rev. 96, 1, 99, (1954)

1.4 Yosida, Phys. Rev. 106, 893, (1957)

1.5 Kasuya, Prog. Theor. Phys. 16, 58, (1956)

1.6 De Gennes, J. Phys. Rad. 23, (1962)

1.7 Anderson, Phys. Rev. 124, 41, (1961)

1.8 Yoshimori, J. Phys. Soc. Japan 14, 807, (1959)

1.9 Villain, Chem. Phys. Solids 11, 303, (1959)

1.10 Kaplan, Phys. Rev. 116, 888, (1959)

1.11 Miwa and Yosida, Prog. Theor. Phys. 26, 693, (1961)

1.12 Dekker, J. Appl. Phys. 36, 906, (1965)

1.13 Elliott and Wedgwood, Proc. Phys. Soc. 81, 846, (1963)

1.14 Freeman and Watson, Phys. Rev. Letts 14, 695, (1965)

1.15 Overhauser and Sterns, Phys. Rev. Letts 13, 316, (1964)

1.16 Yosida and Watabe, Prog. Theor. Phys. 28, 361, (1962)

1.17 De Gennes and St James, Solid State Commun. 1, 62, (1963)

1.18 Overhauser, J. Appl. Phys. Suppl 34, 1019, (1963); Phys Rev 128, 1437, (1962)

1.19 Mackintosh, Phys. Rev. Letts 9, 90, (1962)

1.20 Miwa, Prog. Theor. Phys. 28, 208, (1962)

1.21 Elliott and Wedgwood, Proc-Phys. Soc. 81, 846, (1963); 84, 63, (1964)

1.22 Miwa, Proc. Inter. Conf. Magnetism, Nottingham, 1964.

1.23 Darby and Taylor, J. Appl. Phys. 37, 1442, (1966)

1.24 Gschneidner, "Rare Earth Alloy". Van Nostrand (1961)

1.25 Spedding and Daane, "The Rare Earths". Wiley (1961)

1.26 Bozorth, J. Appl. Phys. 38, 3, 1366, (1967)

1.27 Koehler, J. Appl. Phys. 36, 1078, (1965)

1.28 De Gennes, Compt. Rend. 247, 1836, (1958)

1.29 Wilkinson et al, J. Phys. Soc. Japan 17, Suppl. BIII, 32, (1962)
Wilkinson et al, J. Appl. Phys. 31, 3585, (1960)

1.30 Pauthenet, Compt. Rend. 243, 1737, (1956)

1.31 Matthias, Bozorth and Van Vleck, Phys. Rev. Letts 7, 160, (1961)

1.32 Shirane and Pickart, J. Appl. Phys 37, 1032, (1966)

1.33 Nesbitt et al, J. Appl. Phys. 33, 5, 1674, (1962); 30, 365, (1959)

1.34 Bleaney, Proc. Roy. Soc. 276A, 19 and 28, (1963)
Bleaney, Proc. Roy. Soc. 82, 469, (1963)

1.35 Abrahams et al, J. Phys. Chem. Solids, 25, 1069, (1964)

1.36 Skrabek and Wallace, J. Appl. Phys. 34, 1356, (1963)

1.37 Bozorth et al, Phys. Rev. 115, 1599, (1959)

1.38 Ross and Crangle, Phys. Rev. 133, A509, (1964)
Crangle and Ross, Proc. International Conference on Magnetism, 240, (1964)

1.39 Farrell and Wallace, Inorg. Chem. 5, 105, (1966)

1.40 Lotgering, Phillips Res. Repts. 11, 190, 337, (1956)

1.41 Wallace and Skrabek, "Rare Earth Research", Vol II, Gordon and Breach, New York, 1964, page 431 et seq.

1.42 Bleaney, "Rare Earth Research", page 499 et seq.

2.1 Foner, Rev. Sci. Inst. 30, 7, 548, (1959)

2.2 Hutchinson, Ph. D. Thesis, Durham University, 1958

2.3 See, for example, "Ferromagnetism" by Bozorth. Van Nostrand, (1951)

2.4 "Physical and Chemical Constants." Longmans, Green and Co.

2.5 Schuster, Rev. Sci. Inst. 22, 254, (1951)

3.1 Wernick and Geller, Trans. AIME 218, 806, (1960)

3.2 Weiss and Forrer, Ann. Phys. (Paris), 12, 297, (1929)

4.1 Moon et al J. Appl. Phys. 36, 978, (1965)

4.2 Peter, J. Appl. Phys. 32, 338S, (1961)

4.3 Jaccarino et al, Phys. Rev. Letts. 5, 251, (1960)

4.4 Jaccarino, ibid, 32, 102S, (1961)

4.5 Yafet and Kittel, Phys, Rev. 87, 290, (1952)

4.6 Piercy and Taylor, private communication, to be published.

4.7 Lemaire and Schweizer, Phys. Letts. 21, 4, 366, (1966)